

European Journal of Inorganic Chemistry

Supporting Information

Structural Elucidation, Aggregation, and Dynamic Behaviour of *N,N,N,N*-Copper(I) Schiff Base Complexes in Solid and in Solution: A Combined NMR, X-ray Spectroscopic and Crystallographic Investigation

Isabelle Gerz, Sergio Augusto Venturinelli Jannuzzi, Knut T. Hylland, Chiara Negri, David S. Wragg, Sigurd Øien-Ødegaard, Mats Tilset, Unni Olsbye, Serena DeBeer,* and Mohamed Amedjkouh*

Contents

General Considerations	3
Synthesis and Characterization of Compounds.....	5
Compound 1	5
Compound 1b	10
Compound 2	12
Compound 3	16
Compound 4	23
Compound 5	31
Compound 6	34
Synthesis of Ligands	37
L1	38
L2	39
L3	41
L4	43
L5	45
L6	46
¹ H- ¹⁵ N HMBC	47
Variable Temperature NMR Experiments	54
Compound 1	55
Compound 3	57
Compound 5	59
Decomposition During Longer NMR Experiments	61
Reduction of complex 1b with ascorbic acid to form complex 1	63
Ligand exchange NMR experiments	64
Diffusion Ordered Spectroscopy (DOSY)	67
Crystallographic Data.....	72
Compound 2	72
Compound 4	74
XAS.....	77
XES	79
DFT	80
MOF Incorporation	81
Synthetic procedure for UiO-67-(NH ₂) ₂ -10%.....	81
Synthetic procedure for UiO-67-1b.....	81
	1

NMR.....	83
Elemental Mapping	85
EDX.....	85
TGA.....	Error! Bookmark not defined.
Sources	87

General Considerations

All syntheses involving Cu(I) species were carried out in an Ar-filled UNIlab pro glovebox from MBraun. All solvents used with copper(I) species were degassed with the freeze-pump-thaw technique (3 cycles). CuOTf, CuOTf₂, the respective aldehydes, biphenyl-2,2'-diamine and biphenyl-2-amine were purchased from commercial sources and used as received. Dimethyl 2-aminobiphenyl-4,4'-dicarboxylate and dimethyl 2,2'-diaminobiphenyl-4,4'-dicarboxylate were synthesized according to literature.^{1,2} Yield ranges for the copper complexes were determined from triplets of each synthesis. Melting points, if measured, are uncorrected and were measured on a Stuart SMP10 instrument. NMR spectra were recorded on the following Bruker instruments: DPX300, AVIII400, DRX500, AVI600, AVII600, AVIIHD800. ¹H and ¹³C NMR spectra are referenced to residual solvent signals. ¹⁵N NMR signals are referenced to an external nitromethane standard. ¹⁹F NMR signals are referenced to an internal C₆F₆ standard. For the DOSY measurement, the calibration of the Z-gradient probe was verified for the HDO peak in D₂O. All NMR spectra were recorded at ambient temperature, unless specified. The NMR samples of compounds containing copper were prepared in the glovebox in commercial 9 inch NMR tubes. The samples were transferred out of the glovebox with the adapter depicted in **Figure S1**. The sample was connected to a vacuum line and the solvent was frozen with liquid nitrogen. The tube was flame sealed under vacuum.



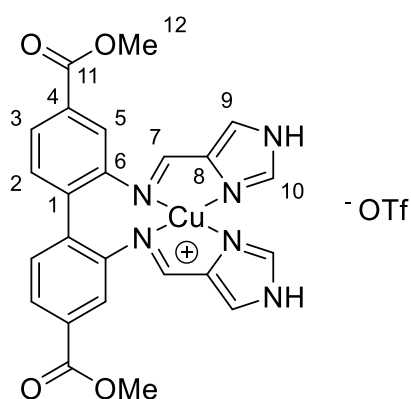
Figure S1. Reusable adapter to seal NMR tubes for samples in high boiling point solvents. This adapter has been developed by Elijah Aller.

MS (ESI) was recorded on a Bruker maXis II ETD spectrometer. Elemental analysis was performed by Mikroanalytisches Laboratorium Kolbe, Oberhausen, Germany. UV/Vis measurements were performed on a Specord 200 Plus instrument for solutions, and on a UV-3600 UV-Vis-NIR Spectrophotometer from Shimadzu for solids. Powder X-ray diffraction was performed with a Bruker D8 Discover diffractometer, using Cu K α_1 radiation selected by a Ge (111) Johanssen monochromator. Thermogravimetric analysis was conducted on a NETZSCH STA 449 F3 Jupiter, ramping from 30 to 900 °C with a 10 K/min ramping rate. The samples were under a stream of synthetic air, consisting of a 20 ml/min flowrate of N₂ and 5 mL/min flowrate of O₂. SEM images were taken on a Hitachi SU8230 Field Emission Scanning Electron Microscope (FE-SEM). Single crystal diffraction data were acquired on a Bruker D8 Venture equipped with a Photon 100 detector, and using Mo K α radiation ($\lambda = 0.71073 \text{ \AA}$) from an Incoatec i μ S microsource. Data reduction was performed with the Bruker Apex3 Suite, the structures were solved with ShelXT and refined with ShelXL.^{3,4} Olex2 was used as user interface.⁵ The cif files were edited with enCIFer v. 1.4.⁶ and molecular graphics were produced with Diamond v. 4.6.2.

Synthesis and Characterization of Compounds

Compound 1

A mixture of dimethyl 2,2'-diaminobiphenyl-4,4'-dicarboxylate (0.50 mmol, 150 mg), CuOTf (0.50 mmol, 106 mg, 1 equiv.) and 1*H*-imidazole-4-carbaldehyde (1.0 mmol, 96 mg, 2 equiv.) were stirred in acetonitrile (3 mL) overnight. The solid was collected through filtration and washed with 2 mL acetonitrile and 4 mL diethyl ether. Residual solvent was left to evaporate over night to yield **1** as an ochre solid. Yield: 77-82 %.



^1H NMR (d_6 -DMSO, 600 MHz): δ 13.35 (2H, s, NH), 8.37 (2H, s, H10), 8.31 (2H, s, H7), 7.89 (2H, s, H9), 7.81 (2H, dd, $^3J_{\text{H,H}} = 7.9$ Hz, $^4J_{\text{H,H}} = 1.5$ Hz, H3), 7.57 (2H, d, $^3J_{\text{H,H}} = 7.9$ Hz, H2), 7.49 (2H, d, $^4J_{\text{H,H}} = 1.2$ Hz, H5), 3.83 (6H, s, H12). ^{13}C NMR (d_6 -DMSO, 150 MHz): δ 165.5 (C11), 154.5 (C7), 147.6 (C6), 138.7 (C10), 137.7 (C8), 133.7 (C1), 132.3 (C2), 130.0 (C4), 125.3 (C3), 123.0 (C9), 120.7 (q, $^1J_{\text{C-F}} = 322$ Hz, CF_3), 120.3 (C5), 52.3 (C12). $^{15}\text{N}\{^1\text{H}\}$ NMR (800 MHz, d_6 -DMSO): δ -83.2 (N_{imine}), -173.4 (N_{IM}), -203.7 (N_{AZ}). ESI-MS: m/z 519.083 (100 %, $[\text{CuL}]^+$), 521.082 (46 %, $[\text{CuL}]^+$). HRMS m/z $[\text{CuL}]^+$ ($\text{C}_{24}\text{H}_{20}\text{CuN}_6\text{O}_4^+$): Calcd: 519.0837 Found: 519.0833. Anal. Calcd: C, 44.88; H, 3.01; N, 12.56 Found: C, 44.57; H, 3.06; N, 12.44.

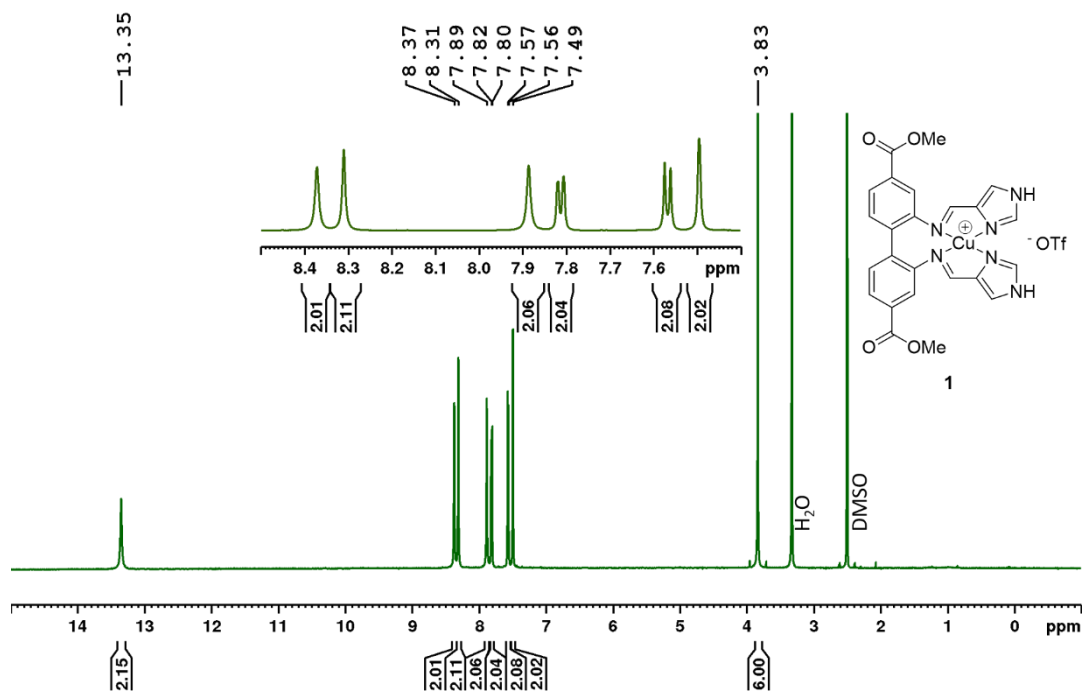


Figure S2. ¹H NMR (600 MHz, *d*₆-DMSO) of **1**.

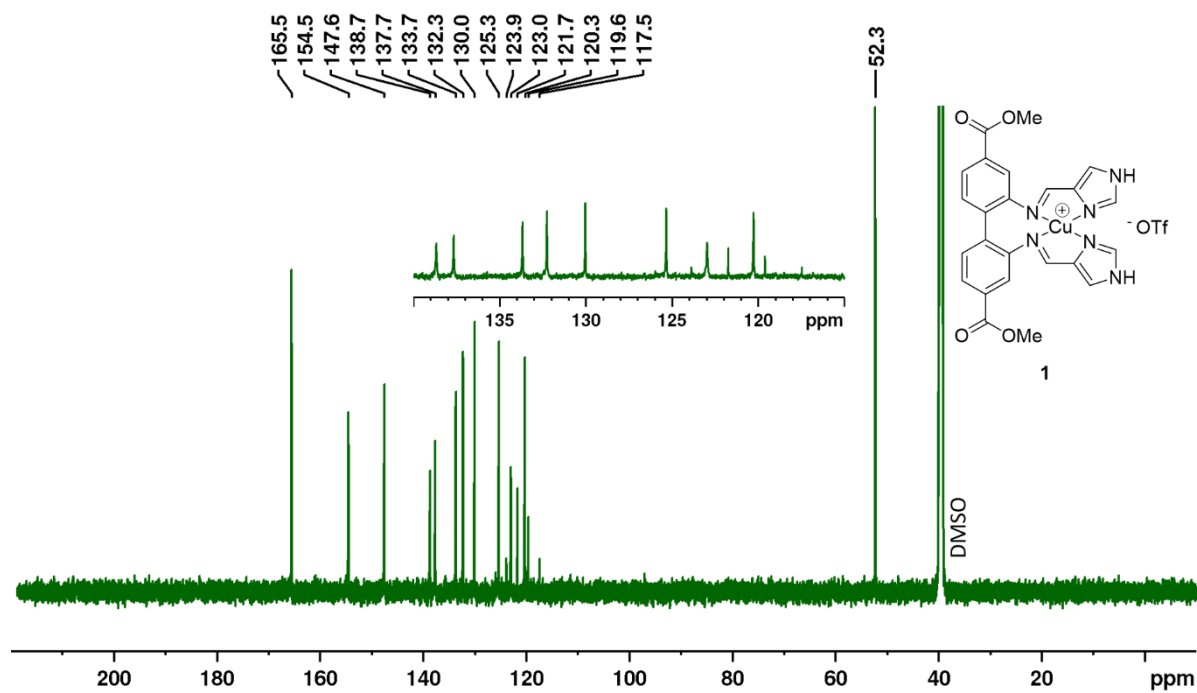


Figure S3. ¹³C NMR (150 MHz, *d*₆-DMSO) of **1**.

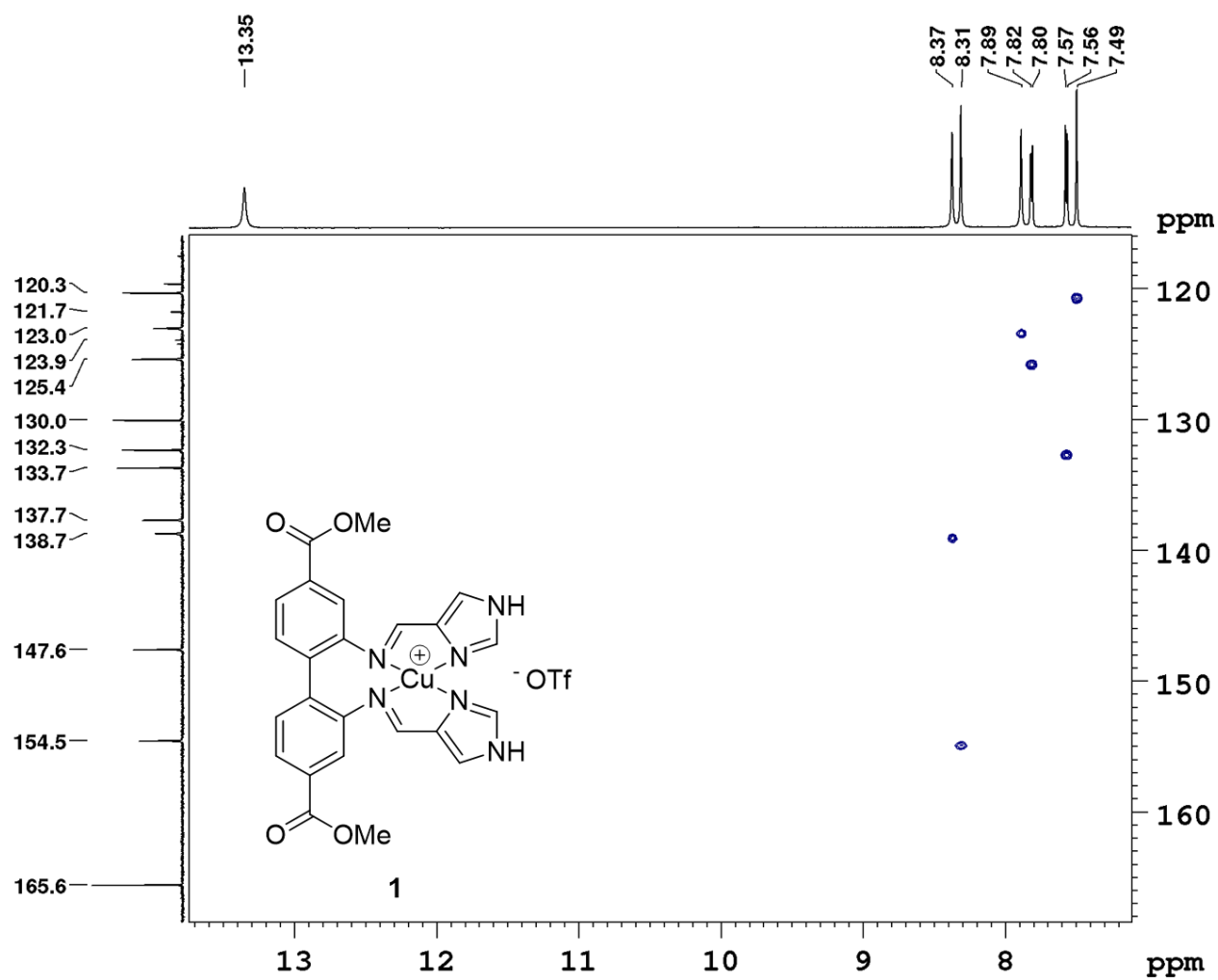


Figure S4. HSQC spectrum (600 MHz, d_6 -DMSO) of **1**.

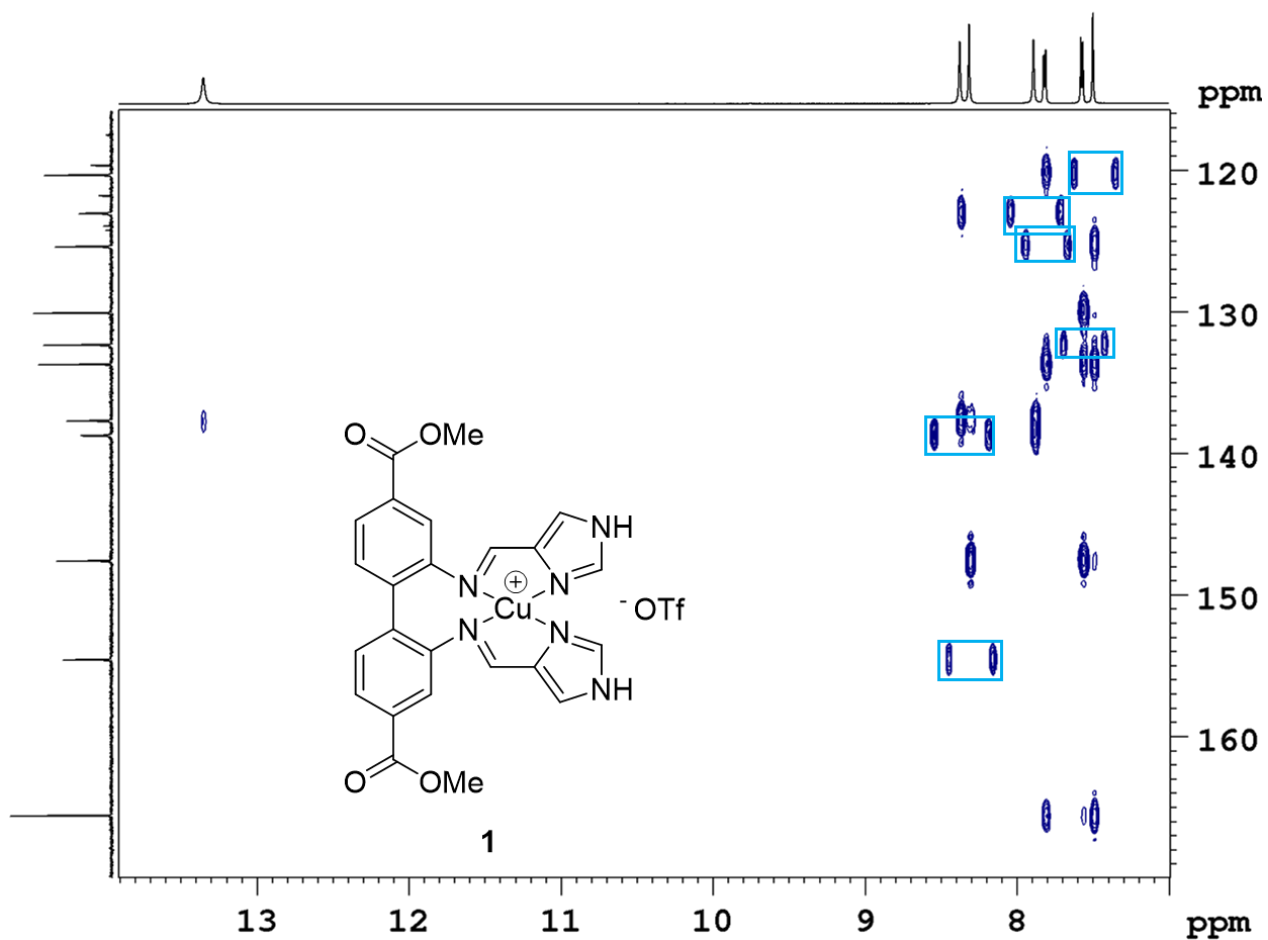


Figure S5. HMBC spectrum (600 MHz, d_6 -DMSO) of **1**. Doublets originating from HSQC correlations are framed for clarity.

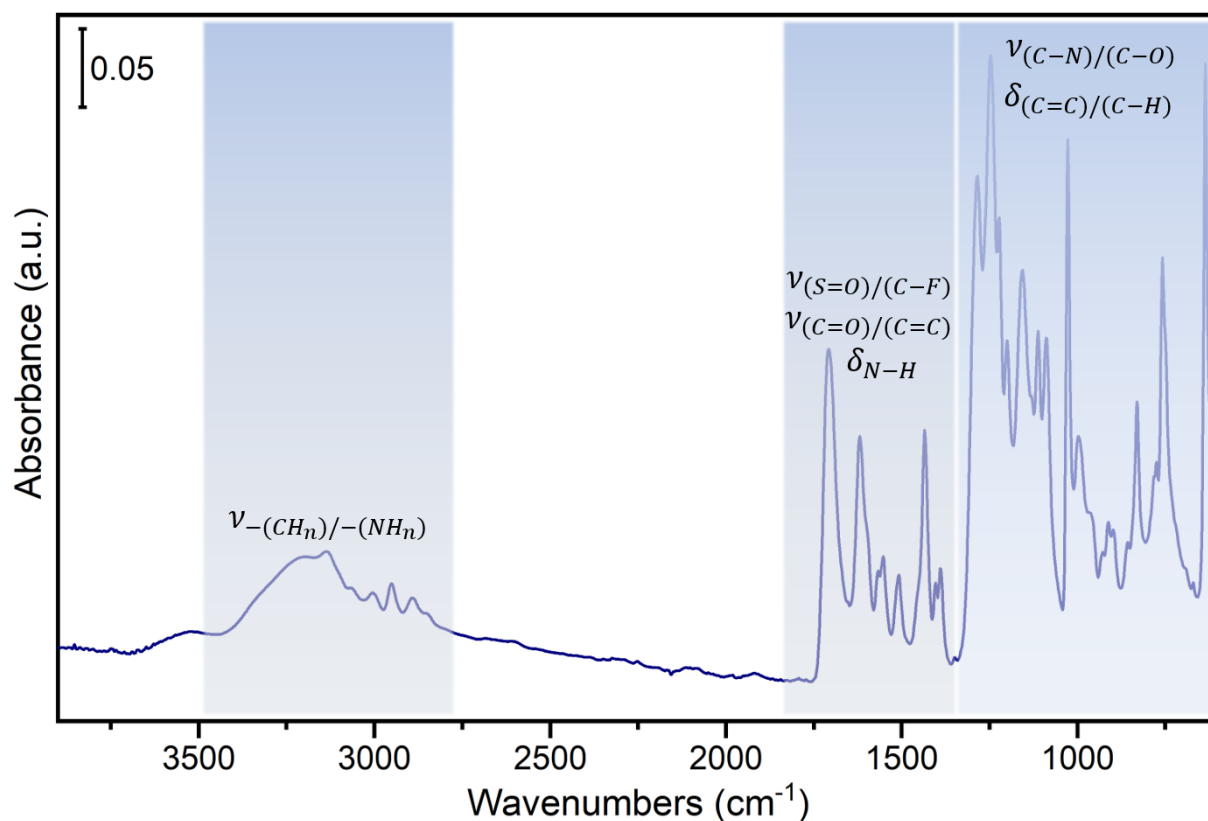
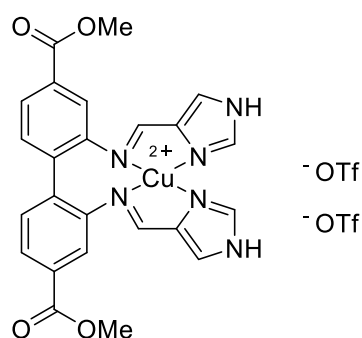


Figure S6. ATR spectrum of **1**, with reported range for the frequencies of the main functional groups.

Figure S6 reports the ATR spectrum for complex **1**. The spectrum shows the frequencies for the main functional groups present in the molecule. In the high frequencies region we can observe the contribution from the stretching modes of $-CH$ and $-NH$ groups, while in the 1700-1300 cm⁻¹ region we can identify the frequencies of the stretching modes of carboxylic $C=O$ and of the $C=C$ bonds. Those signals are superimposed with the contribution from $S=O$ and $C-F$ stretching modes from the triflate group and with the bending modes of $-NH$ groups. In the low frequencies region fall the bands related to the stretching modes of $C-N$ and $C-O$, as well as those of the bending modes of $C=C$ and $C-H$. Due to the structure of complex **1**, the peaks expected on the basis of the functional groups present are significantly overlapped in the entire spectral range, not allowing for a peak-to-peak assignment. The characteristic frequencies for the $Cu-N$ stretching modes are expected to be in the Far-Infrared region (and consequently not accessible).

Compound 1b

A mixture of dimethyl 2,2'-diaminobiphenyl-4,4'-dicarboxylate (1.00 mmol, 300 mg), Cu(OTf)₂ (1.00 mmol, 362 mg, 1 equiv.) and 1*H*-imidazole-4-carbaldehyde (2.00 mmol, 192 mg, 2 equiv.) were stirred in MeOH (3 mL) overnight. The solvent was removed under reduced pressure. After drying in a vacuum oven at 50 °C overnight, **1b** was obtained as a dark green solid. Yield: 94-97 %.



M.p. 206 °C. HRMS m/z [CuL²⁺] (C₂₄H₂₀CuN₆O₄²⁺): Calcd: 259.5416 Found: 259.5418. Anal.

Calcd: C, 38.17; H, 2.46; N, 10.27 Found: C, 37.65; H, 2.51; N, 10.01. UV/Vis (MeCN):

$\epsilon_{670\text{ nm}} = 104\text{ L}\cdot\text{mol}^{-1}\text{cm}^{-1}$

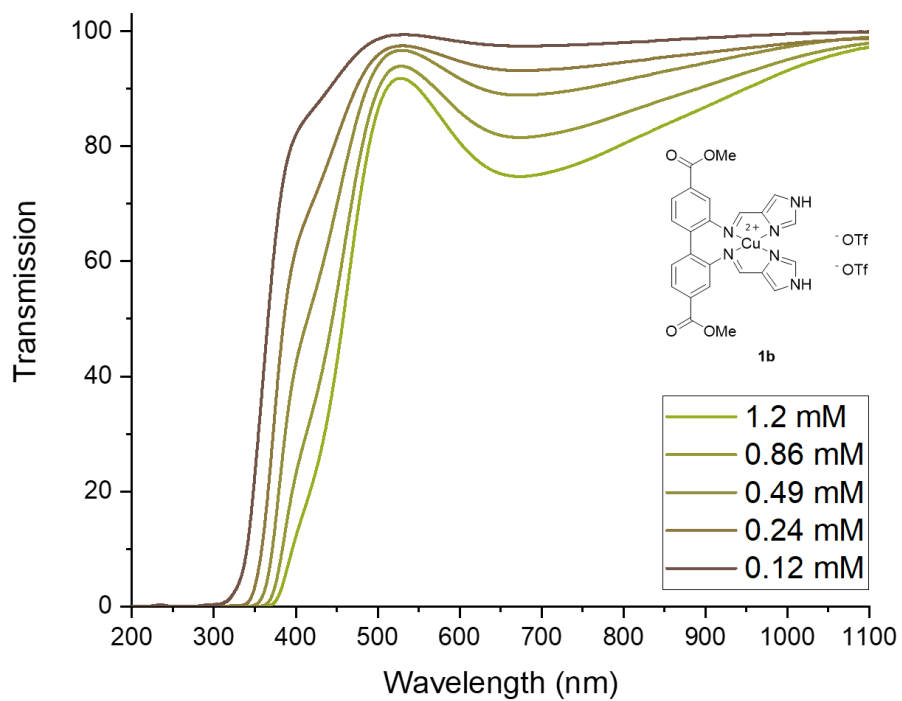
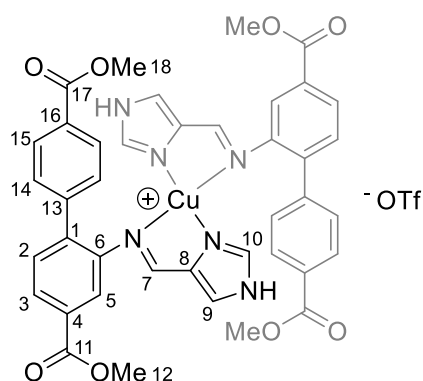


Figure S7. UV/Vis spectra of **1b** measured in MeCN.

Compound 2

A mixture of CuOTf (0.18 mmol, 37 mg, 1 equiv.), dimethyl 2-aminobiphenyl-4,4'-dicarboxylate (0.35 mmol, 100 mg, 2 equiv.) and 1*H*-imidazole-4-carbaldehyde (0.35 mmol, 37 mg, 2 equiv.) were stirred in acetonitrile (3 mL) overnight. Diethyl ether (4 mL) was added, and the precipitated solid was collected through filtration and washed with diethyl ether (2 mL). Residual solvent was left to evaporate over night to yield **2** as a brown solid. Yield: 71-80 %.



^1H NMR (600 MHz, CD_3CN): δ 10.80 (2H, s, NH), 8.38 (2H, s, H7), 7.71 (2H, d, $^3J_{\text{H,H}} = 7.0$ Hz, H3), 7.56 (6H, m, overlap H imidazole and H phenyl), 7.37 (2H, d, $^3J_{\text{H,H}} = 6.4$ Hz, H2), 7.28 (2H, s, H imidazole) 7.16 (4H, s, H phenyl), 6.98 (2H, s, H5), 3.93 (6H, s, CO_2CH_3), 3.91 (6H, s, CO_2CH_3). ^1H NMR (600 MHz, d_6 -DMSO): δ 13.07 (2H, s, NH), 8.49 (2H, s, H7), 7.82 (2H, s, H9), 7.66 (2H, d, $^3J_{\text{H,H}} = 7.1$ Hz, H3), 7.53 (6H, m, overlap H10 and H15), 7.39 (2H, d, $^3J_{\text{H,H}} = 7.3$ Hz, H2), 7.13 (4H, s, H14), 6.86 (2H, s, H5), 3.90 (6H, s, CO_2CH_3), 3.88 (6H, s, CO_2CH_3). ^{13}C NMR (150 MHz, CD_3CN): δ 167.3 (C17), 166.6 (C11), 154.1 (C7), 147.6 (C6), 142.9 (C13), 139.5 (C1), 139.4 (*br*, C8) 137.9 (*br*, CH imidazole), 131.5 (C4), 130.9 (C2), 130.8 (CH phenyl), 129.9 (C16), 129.1 (CH phenyl), 127.9 (C3), 122.5 (*br*, CH imidazole), 122.2 (*m**, $^1J = 321$ Hz, CF_3), 121.3 (C5), 52.9 (CO_2CH_3), 52.8 (CO_2CH_3). ^{19}F NMR (376 MHz, CD_3CN): δ -79.8 (CF_3). $^{15}\text{N}\{^1\text{H}\}$ NMR (800 MHz, d_6 -DMSO): δ -86.0 (N_{imine}), -171.7 (N_{IM}), -205.6 (N_{AZ}). ESI-MS: m/z 386.111 (38 %, $[\text{L}+\text{Na}]^+$), 426.051 (78 %, $[\text{CuL}]^+$), 428.049

(34 %, [^{65}CuL] $^+$), 789.173 (100 %, [$^{63}\text{CuL}_2$] $^+$), 791.172 (51 %, [$^{65}\text{CuL}_2$] $^+$). HRMS m/z [$^{63}\text{CuL}_2$] $^{2+}$ ($\text{C}_{40}\text{H}_{34}\text{CuN}_6\text{O}_8^+$): Calcd: 789.1734 Found: 789.1726. Anal. Calcd: C, 52.42; H, 3.65; N, 8.95 Found: C, 52.05; H, 3.77; N, 8.84. * d visible, expected q

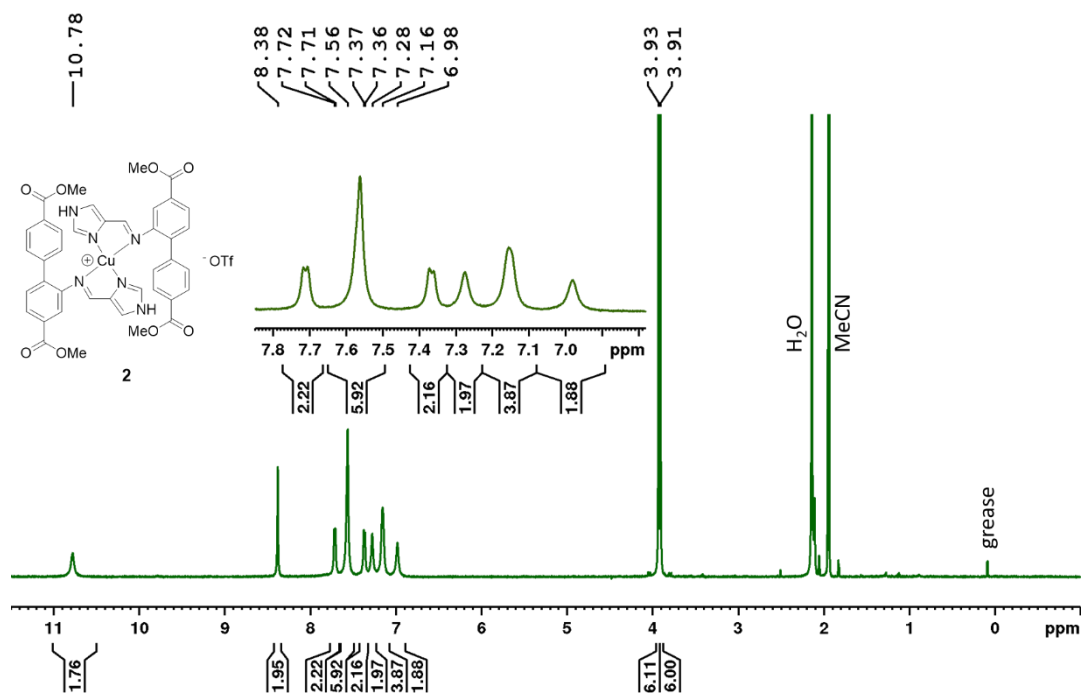


Figure S8. ^1H NMR (600 MHz, CD_3CN) of **2**.

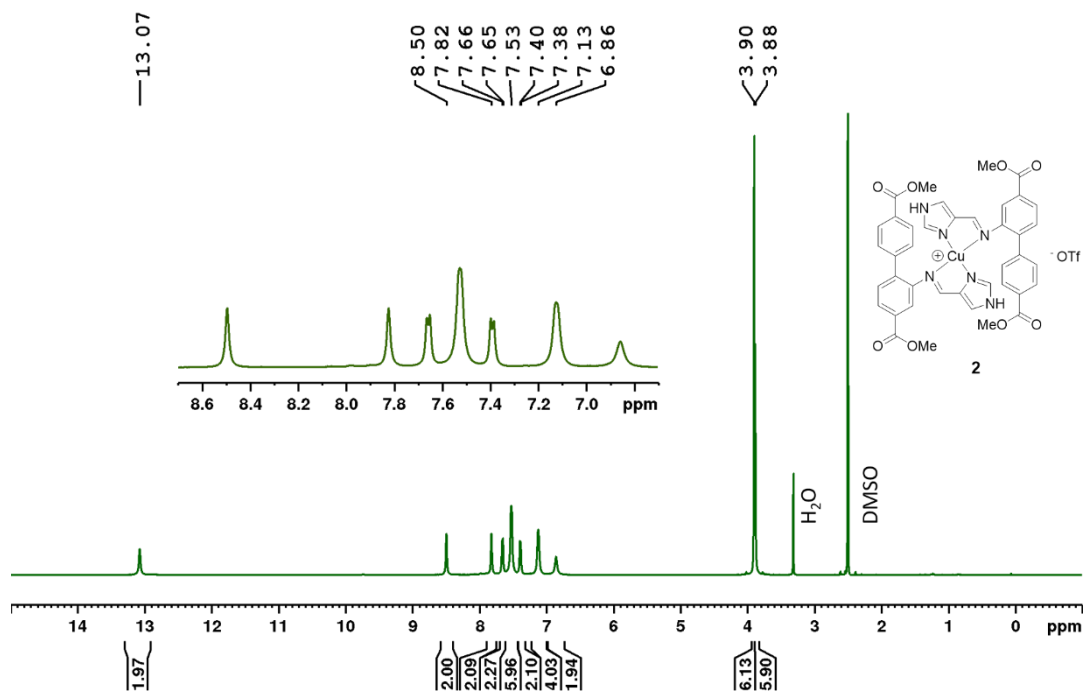


Figure S9. ¹H NMR (600 MHz, *d*₆-DMSO) of **2**.

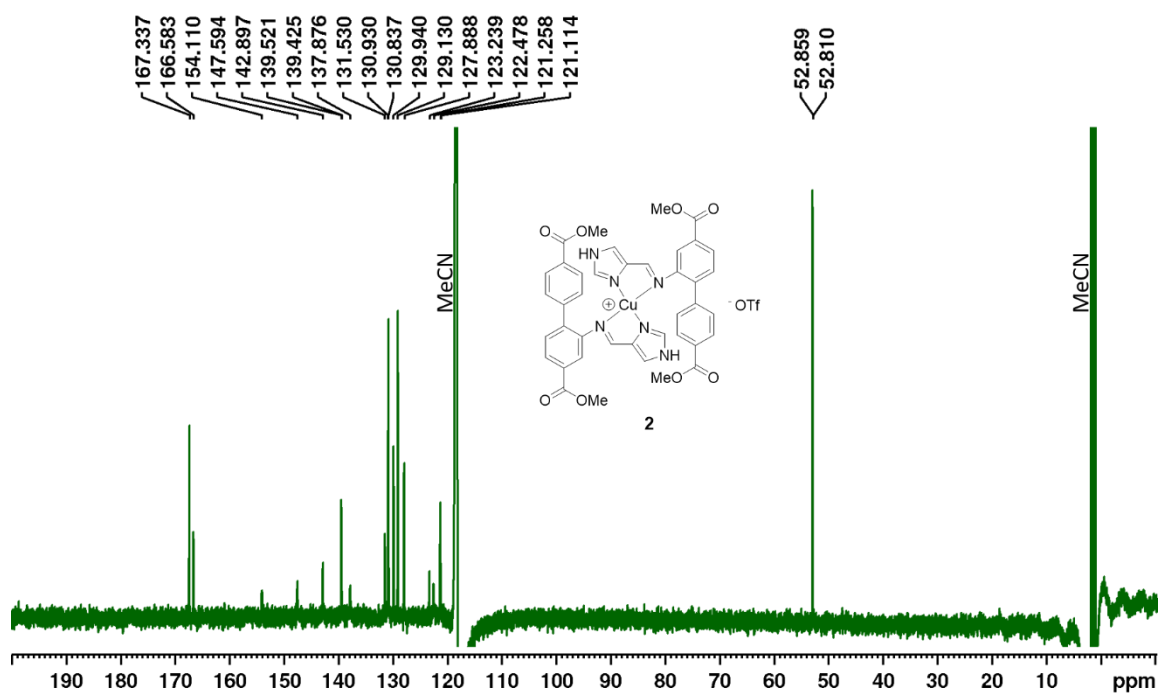


Figure S10. ¹³C NMR (150 MHz, CD₃CN) of **2** (15360 scans, d1= 8 s).

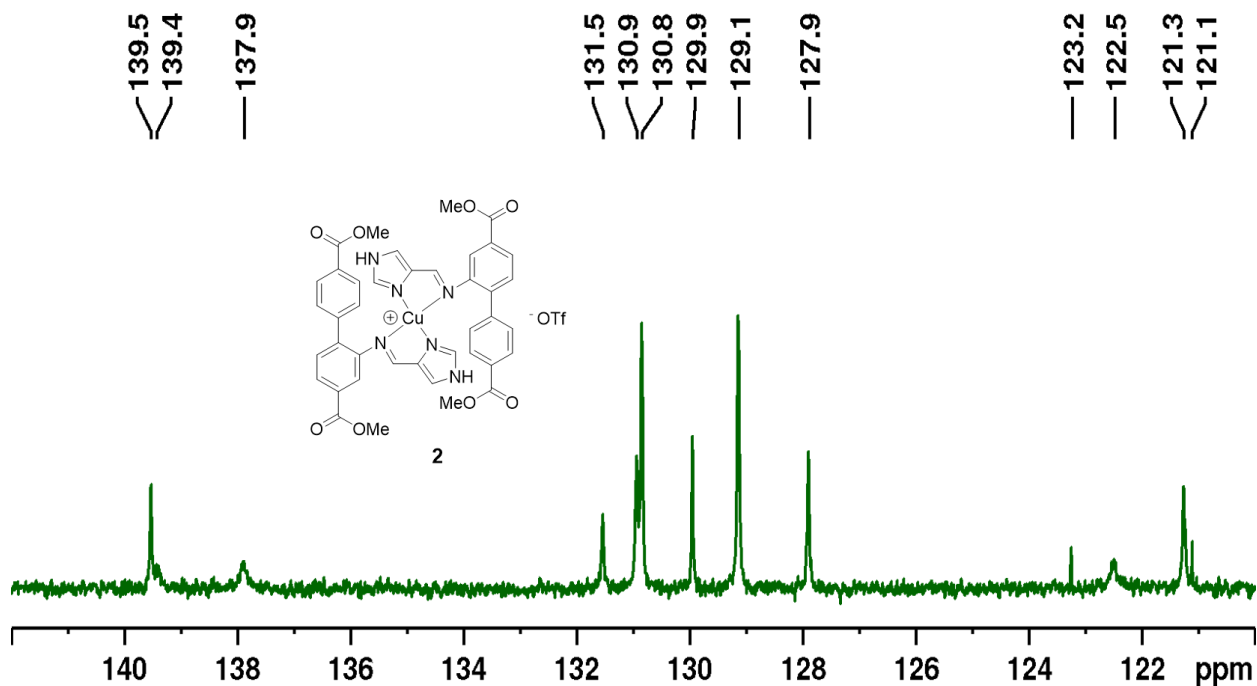


Figure S11. Detail of the ^{13}C NMR spectrum of **2**. The relatively sharp peaks at 123.2 ppm and 121.1 ppm are most likely originating from the counter ion (SO_3CF_3^-). A low intensity quartet (with a 1:3:3:1 intensity ratio) can appear as a doublet, with only the inner peaks distinguished from the baseline.

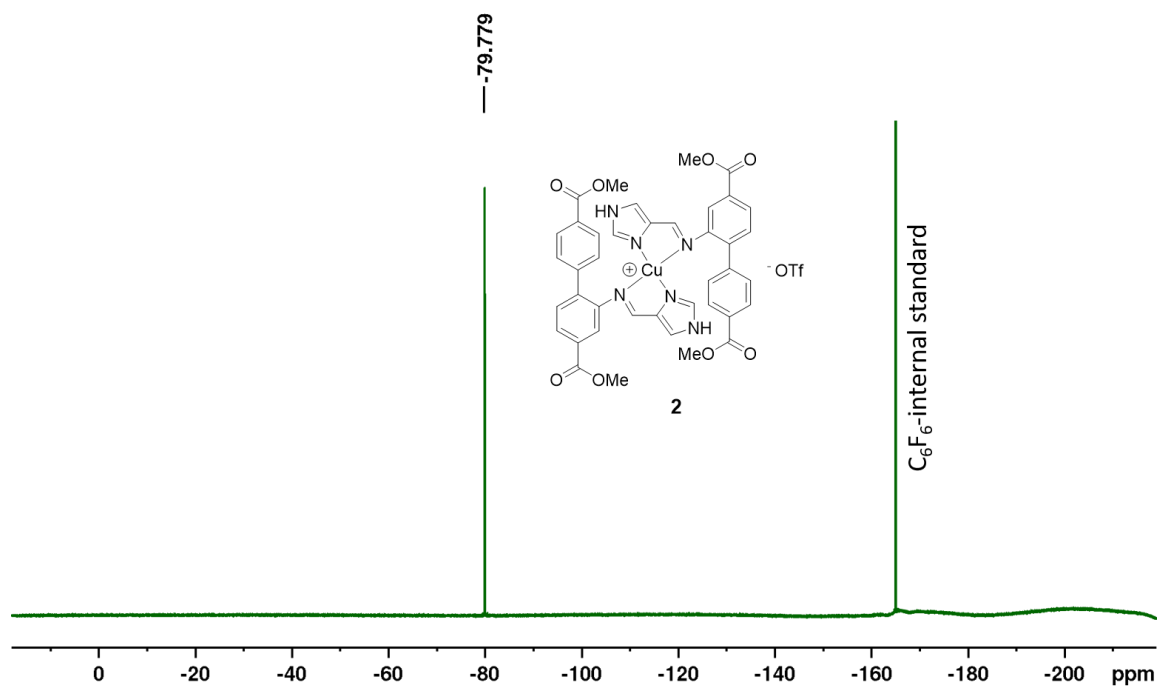
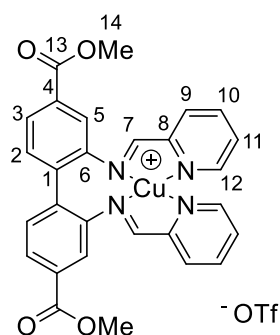


Figure S12. ^{19}F NMR (376 MHz, CD_3CN) of **2** with hexafluorobenzene as internal standard.

Compound 3

A mixture of dimethyl 2,2'-diaminobiphenyl-4,4'-dicarboxylate (0.33 mmol, 100 mg), CuOTf (0.33 mmol, 70 mg, 1 equiv.) and picolinaldehyde (0.66 mmol, 72 mg, 64 μ L, 2 equiv.) were stirred in MeCN (3 mL) overnight. Et₂O (4 mL) were added. The solid was collected through filtration and washed with Et₂O (2 mL). Residual solvent was left to evaporate overnight to yield **3** as a dark green solid. Yield: 63-85 %.

HRMS m/z [⁶³CuL⁺] (C₂₈H₂₂CuN₄O₄⁺): Calcd: 541.0932 Found: 541.0932 Anal. Calcd: C, 50.40; H, 3.21; N, 8.11 Found: C, 50.14; H, 3.22; N, 8.09.



The presence of multiple species (**3-M**, **3-D**, **3-A**) at room temperature impeded the assignment of resonances by classical NMR full characterization techniques (Figure S13-S18). At higher temperatures, only **3-M** and **3-D** were present, which facilitated structure elucidation. For the assignments of the major (**3-M**) and minor (**3-D**) species observed in the ¹H NMR spectrum of complex **3** in *d*₆-DMSO at room temperature, spectra collected at other temperatures were consulted (25 °C to 92 °C). The assigned NMR resonances belonging to each species (**3-M** and **3-D**) are listed separately below. NMR data for **3-A** are not listed.

NMR Data for **3-M**

^1H NMR (800 MHz, d_6 -DMSO): δ 8.94 (2H, s, H7), 8.90 (2H, s, H12), 8.26 (2H, s, H10), 8.08-8.09 (2H, m, H9), 7.90-7.92 (4H, m, H3 and H11), 7.83 (2H, s, H5), 7.61 (2H, s, H2), 3.87 (6H, s, H14). All resonances were significantly broadened at 55 °C, and no fine structure could be detected. ^{13}C NMR (200 MHz, d_6 -DMSO): δ 165.1 (C13), 162.4 (C7), 150.1 (C12), 149.8 (C8), 146.0 (C6), 138.7 (C10), 132.9 (C2), 130.5 (C4), 129.2 (C11), 128.8 (C9), 126.1 (C3), 120.6 (C5), 52.1 (C14). The resonance corresponding to C1 was not observed. $^{15}\text{N}\{^1\text{H}\}$ NMR (800 MHz, d_6 -DMSO): δ -89.6 (N_{imine}), -128.6 ($\text{N}_{\text{pyridine}}$).

NMR Data for **3-D**

^1H NMR (800 MHz, d_6 -DMSO): δ 9.19 (4H, s, H7), 8.10 (4H, m, H10), 8.06 (4H, d, $^3J_{\text{H,H}} = 7.7$ Hz, H9), 7.88 (4H, s, H5), 7.50-7.51 (4H, m, H11), 7.44 (4H, d, $^3J_{\text{H,H}} = 4.4$ Hz, H12), 7.27 (4H, dd, $^3J_{\text{H,H}} = 7.8$ Hz, $^4J_{\text{H,H}} = 1.0$ Hz, H3), 7.15 (4H, d, $^3J_{\text{H,H}} = 7.8$ Hz, H2), 3.77 (12H, s, H14). For some of the resonances, specifically those corresponding to H10 and H5, the integrals are less accurate because of overlap with resonances corresponding to **3-A**. ^{13}C NMR (200 MHz, d_6 -DMSO): δ 164.2 (C13), 163.9 (C7), 148.6 (C8), 147.7 (C12), 145.6 (C6), 138.0 (C10), 137.0 (C1), 132.3 (C2), 130.2 (C4), 128.3 (C11), 128.2 (C9), 127.8 (C3), 121.4 (C5), 51.9 (C14). $^{15}\text{N}\{^1\text{H}\}$ NMR (800 MHz, d_6 -DMSO): δ -105.3 ($\text{N}_{\text{pyridine}}$), -107.7 (N_{imine}).

In addition, one resonance corresponding to the triflate anion was observed at δ 120.5 (d, q expected, $^1J_{\text{C,F}} = 322$ Hz) in the ^{13}C NMR spectrum of **3**.

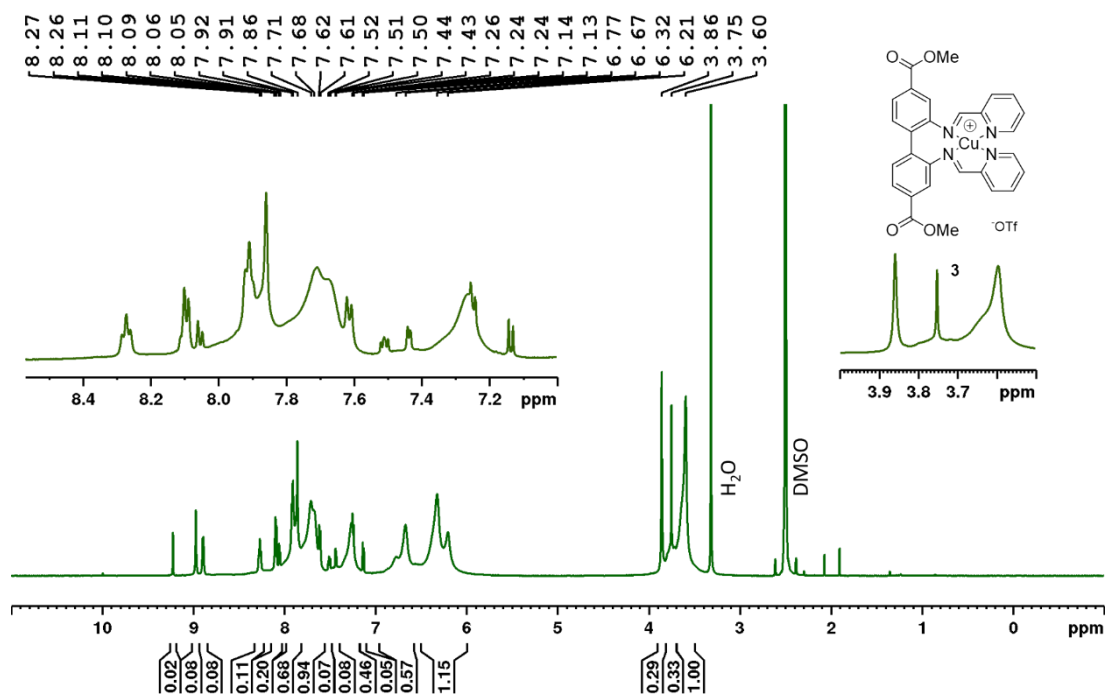


Figure S13. $^1\text{H NMR}$ (600 MHz, d_6 -DMSO) of 3.

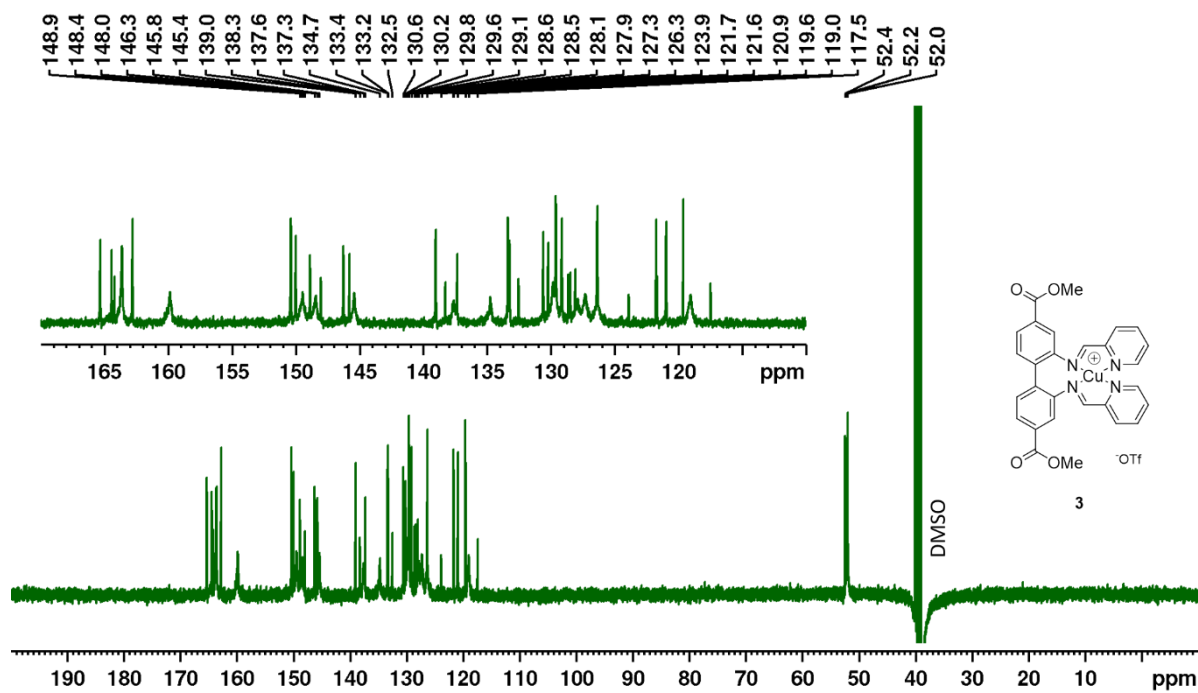


Figure S14. $^{13}\text{C NMR}$ (150 MHz, d_6 -DMSO) of 3.

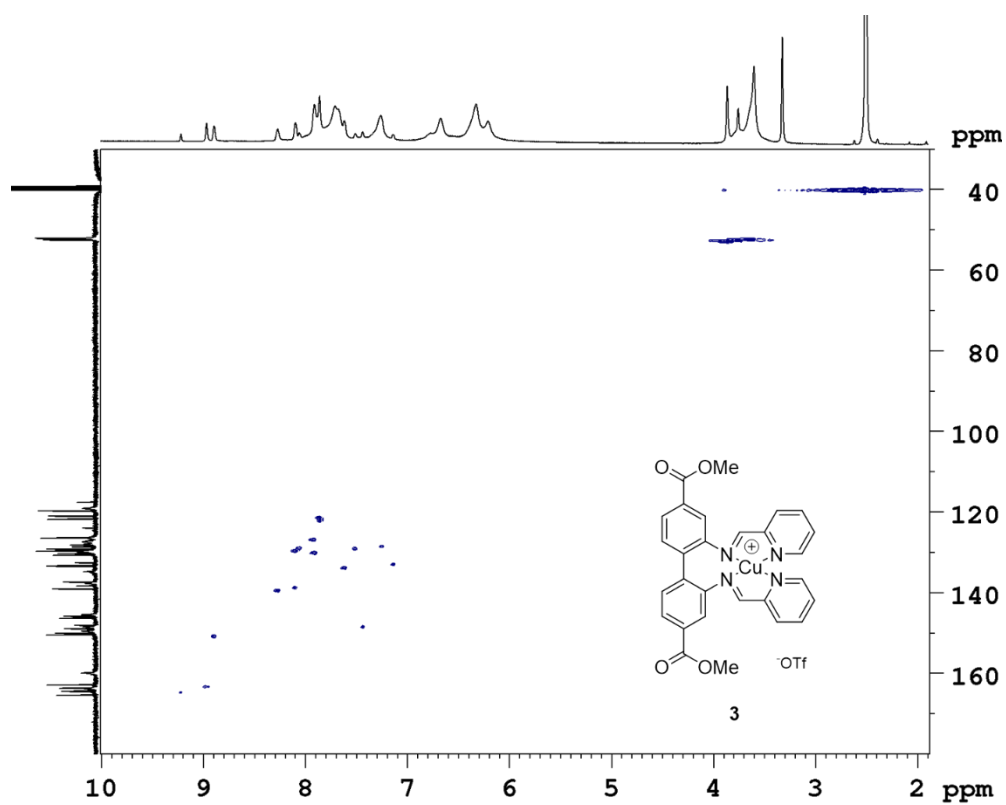


Figure S15. HSQC (600 MHz, d_6 -DMSO) of 3.

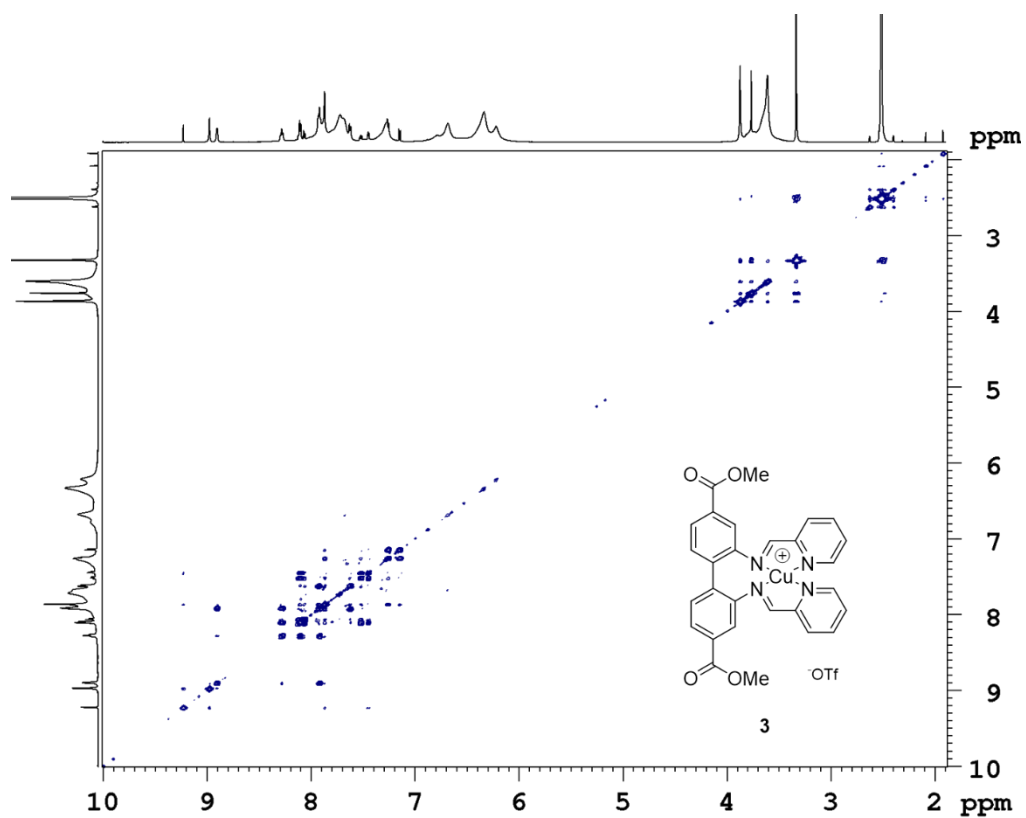


Figure S16. COSY (600 MHz, d_6 -DMSO) of 3.

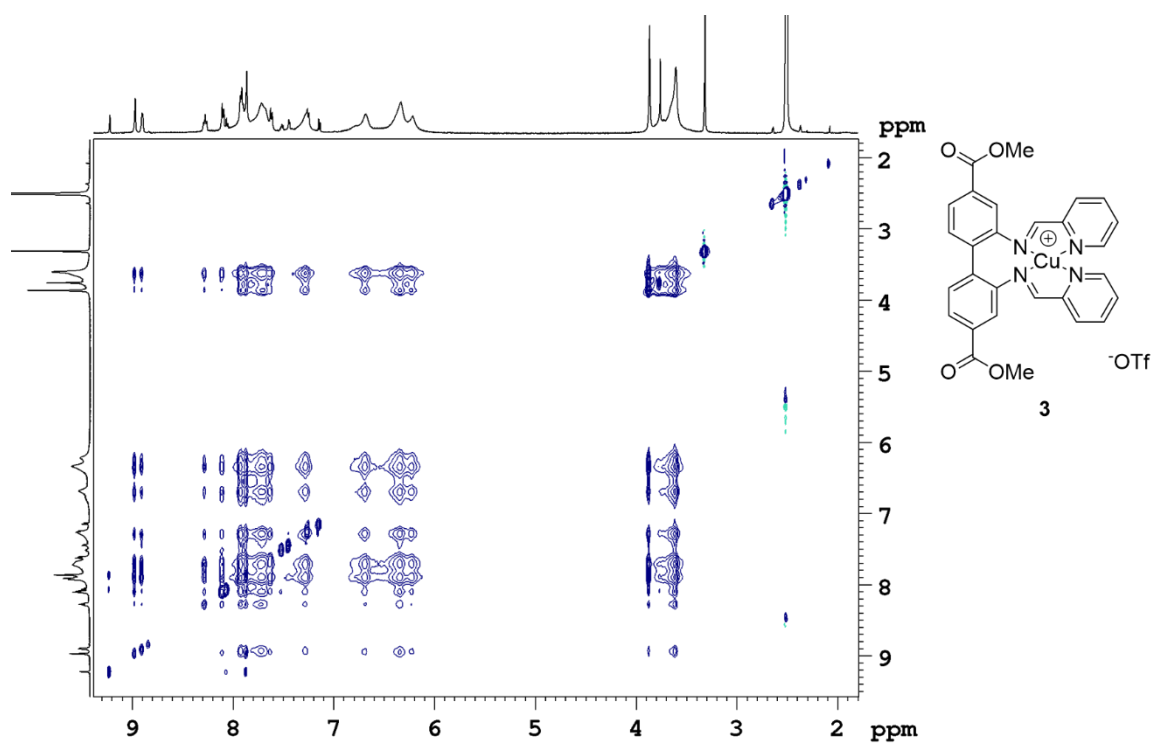


Figure S17. NOESY/EXSY (500 MHz, d_6 -DMSO) of **3**. No correlations that clearly indicate exchange between **3-M** and **3-D** could be identified, as opposed to the NOESY/EXSY spectrum collected at 92 °C (Figure S21).

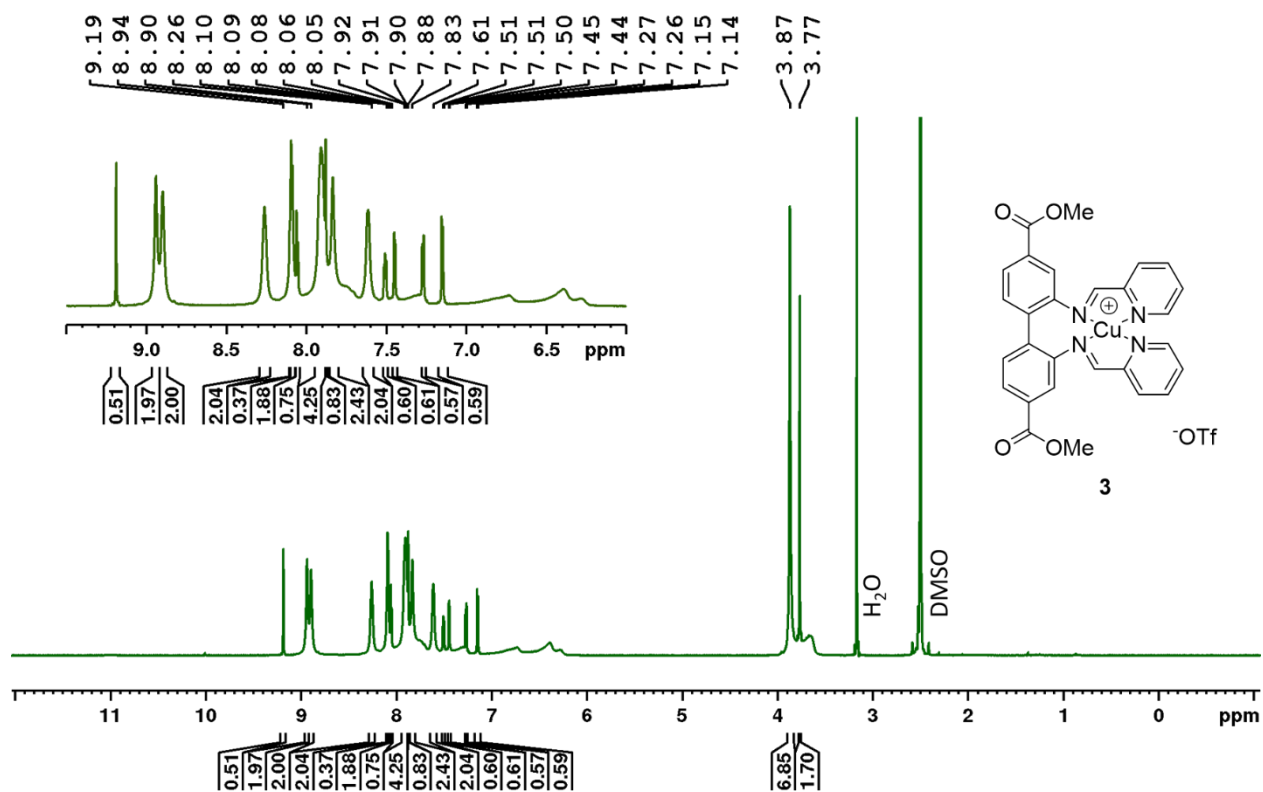


Figure S18. ¹H NMR (800 MHz, *d*₆-DMSO, 55 °C) of **3**.

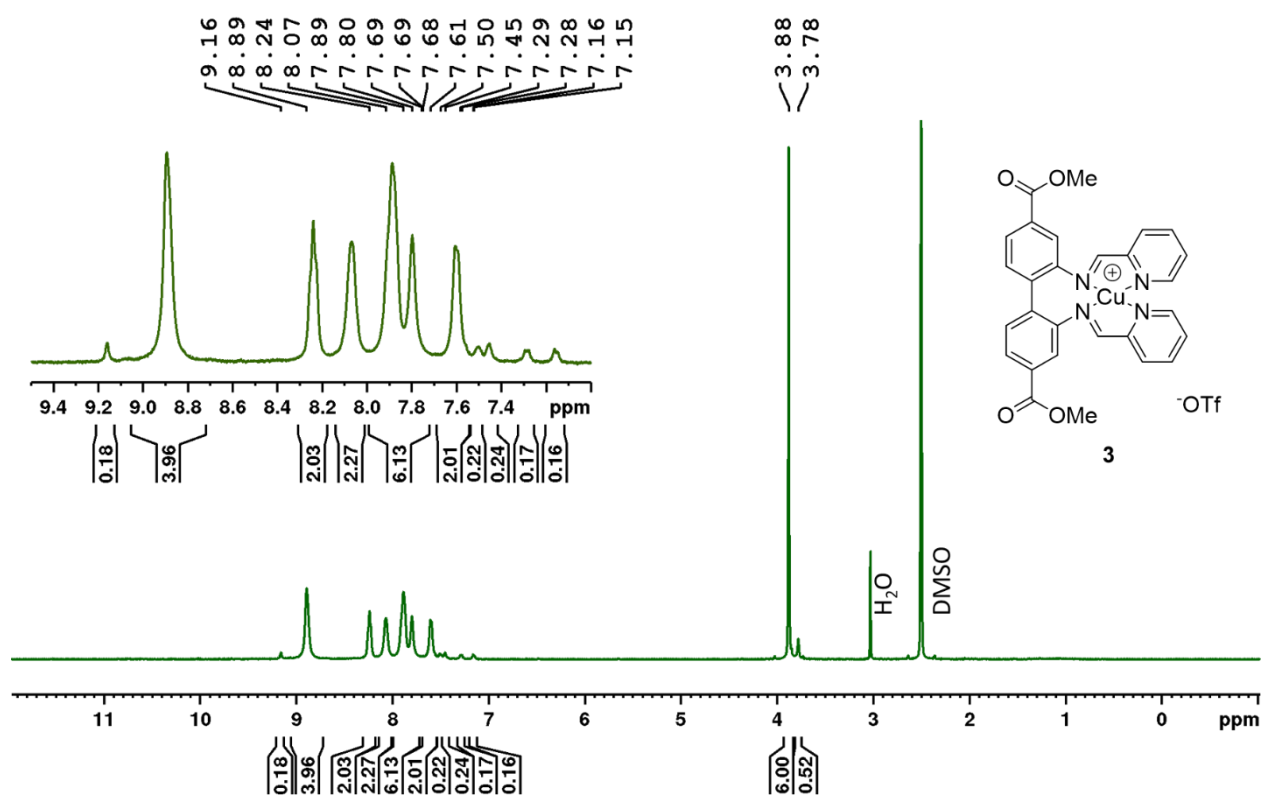


Figure S19. ¹H NMR (500 MHz, *d*₆-DMSO, 92 °C) of **3**.

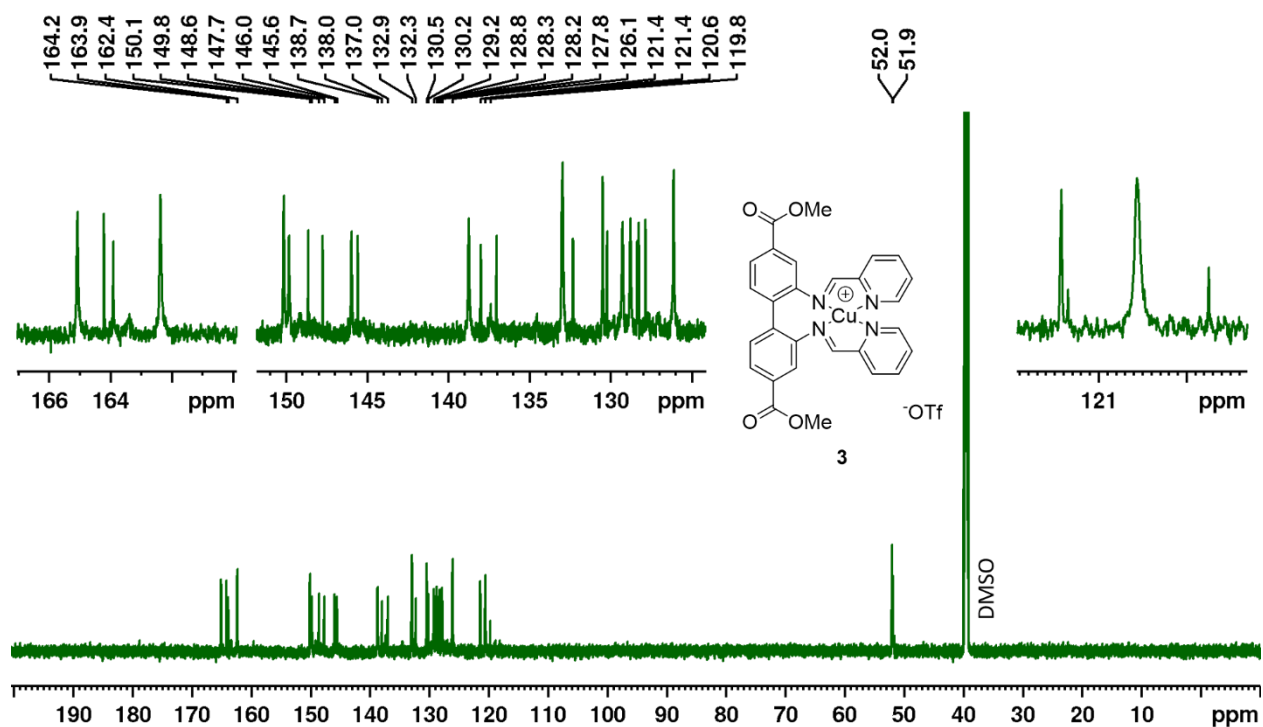


Figure S20. ^{13}C NMR (200 MHz, d_6 -DMSO, 55 °C) of **3**.

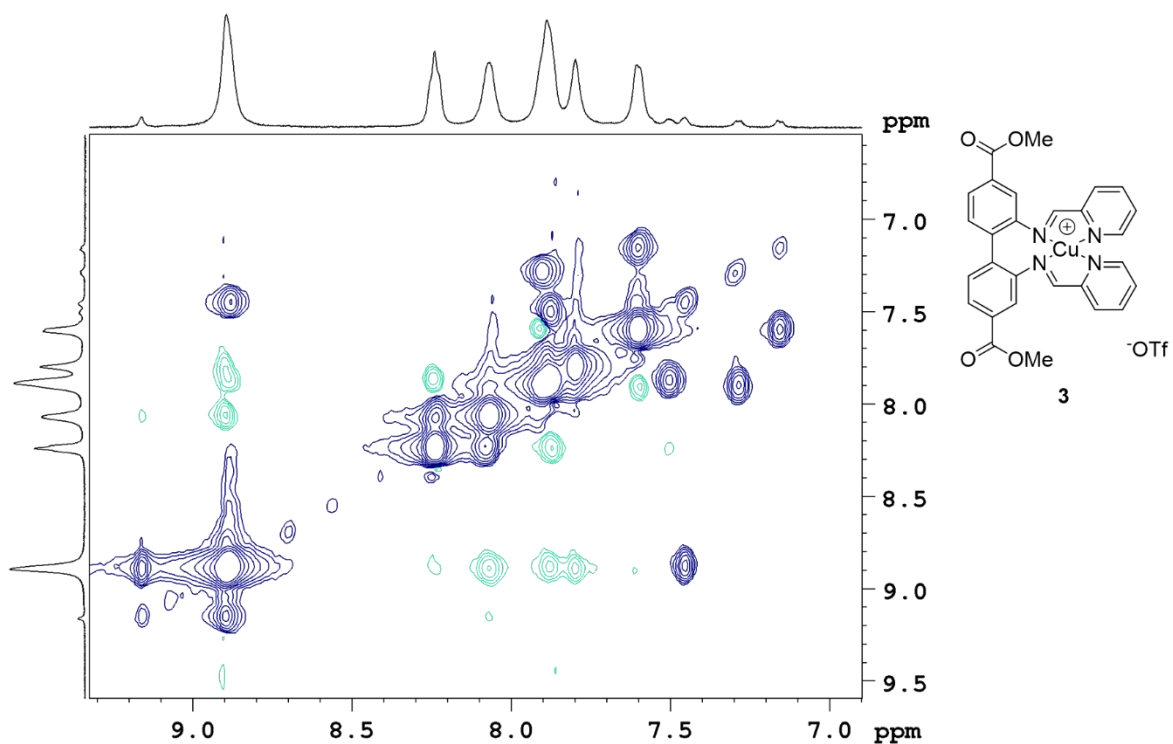
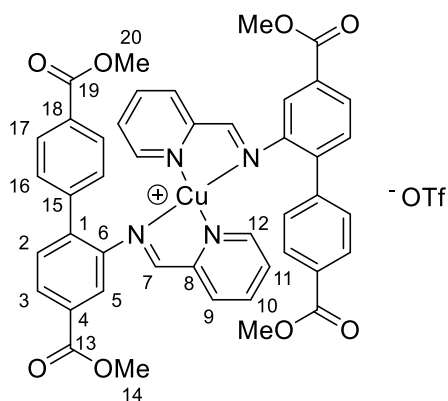


Figure S21. NOESY/EXSY (500 MHz, d_6 -DMSO, 92 °C) of **3**. The exchange peaks (black cross-peaks) between the major species (**3-M**) and the minor species (**3-D**) suggest the species are interconverting.

Compound 4

A mixture of CuOTf (0.175 mmol, 37 mg, 1 equiv.), dimethyl 2-aminobiphenyl-4,4'-dicarboxylate (0.350 mmol, 100 mg, 2 equiv.) and picolinaldehyde (0.350 mmol, 38 mg, 33 μ L, 2 equiv.) were stirred in 2 mL MeCN overnight. 6 mL of Et₂O were added. The precipitated solid was collected through filtration and washed with 2 mL Et₂O. Residual solvent was left to evaporate over night to yield **4** as a dark green solid. Yield: 67-87 %.

NMR Data for Compound **4** in CD₃CN



¹H NMR (600 MHz, CD₃CN): δ 8.77 (*br*, 1H, s, H7) 8.06 (*br*, 1H, s, H pyridine), 7.87 (*br*, 2H, s, H pyridine), 7.75 (1H, d, ³J_{H,H} = 5.6 Hz, H3), 7.46 (2H, s, H17), 7.41 (1H, d, ³J_{H,H} = 6.1 Hz, H2) 7.28 (1H, s, H5), 7.14 (2H, s, H16), 3.99 (6H, s, H14), 3.83 (6H, s, H20), missing: H pyridine. ¹³C NMR (150 MHz, CD₃CN): δ 166.8 (C19), 166.3 (C13), 161.6* (*br*, C7), 150.8* (*br*, C pyridine), 146.1 (C6), 141.9 (C15), 140.2 (C1), 138.7* (*br*, C pyridine) 138.6* (*br*, C pyridine), 131.9 (C4), 131.3 (C2), 130.8 (C16), 130.4 (C18), 129.39 (C17), 129.35 (C3), 122.35 (q, ¹J = 320 Hz, CF₃), 122.34 (C5), 53.0 (C14), 52.7 (C20). ESI-MS: *m/z* 375.134 (100 %, [L+H]⁺), 437.056 (40 %, [⁶³CuL]⁺), 439.055 (18 %, [⁶⁵CuL]⁺), 811.183 (26 %, [⁶³CuL₂]⁺), 813.183 (13 %, [⁶⁵CuL₂]⁺). HRMS *m/z* [⁶³CuL₂²⁺] (C₄₄H₃₆CuN₄O₈⁺): Calcd: 811.1824 Found: 811.1825 Anal. Calcd: C, 56.22; H, 3.77; N, 5.83 Found: C, 56.08; H, 3.68; N, 5.75. *=detected through HSQC.

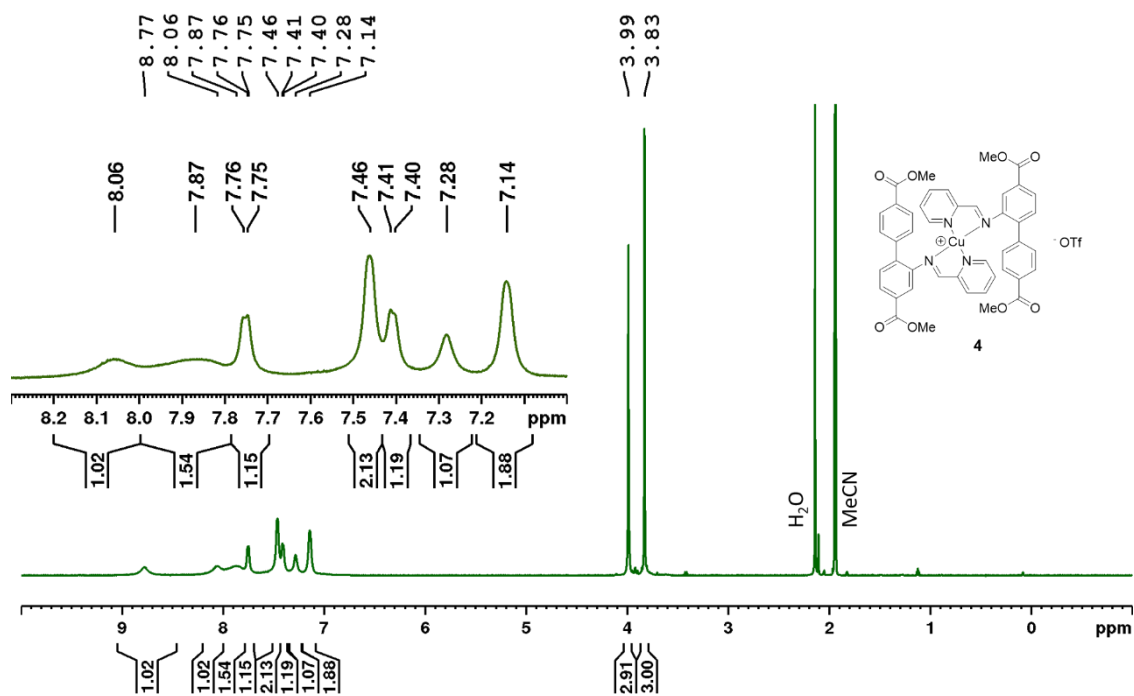


Figure S22. $^1\text{H NMR}$ (600 MHz, CD_3CN) of **4**.

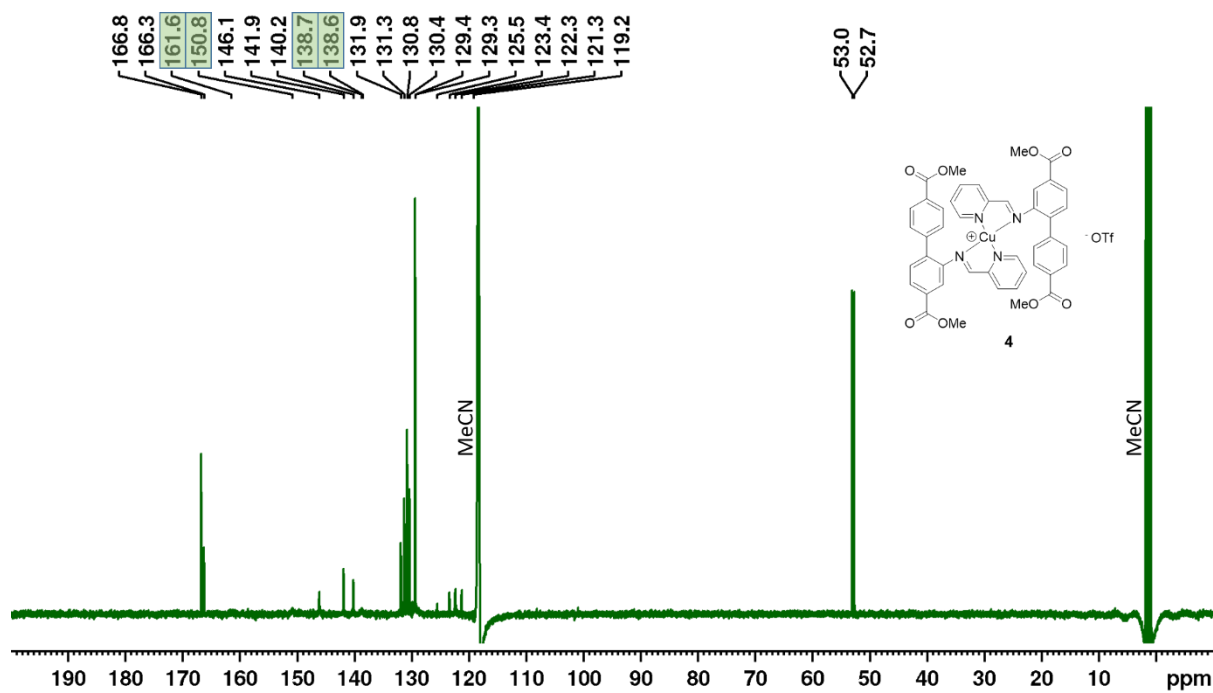


Figure S23. $^{13}\text{C NMR}$ (150 MHz, CD_3CN) of **4**. Peaks localized through HSQC are highlighted.

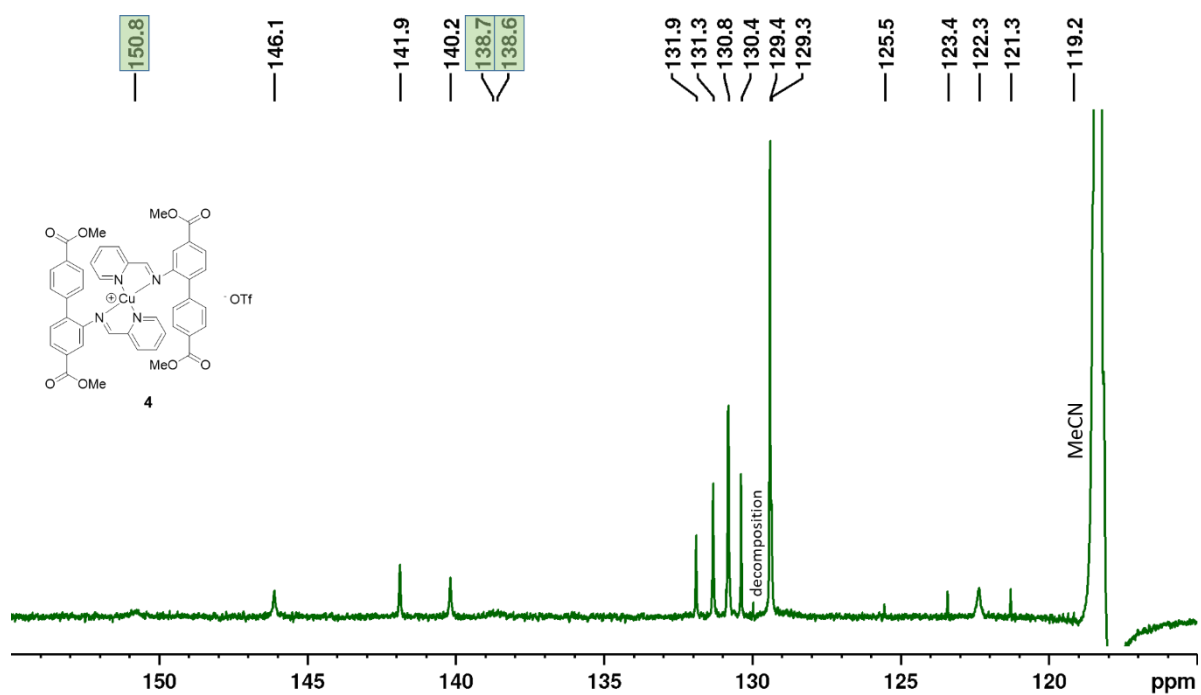


Figure S24. Detail of the ^{13}C NMR (150 MHz, CD_3CN) spectrum of **4**. Peaks localized through HSQC are highlighted.

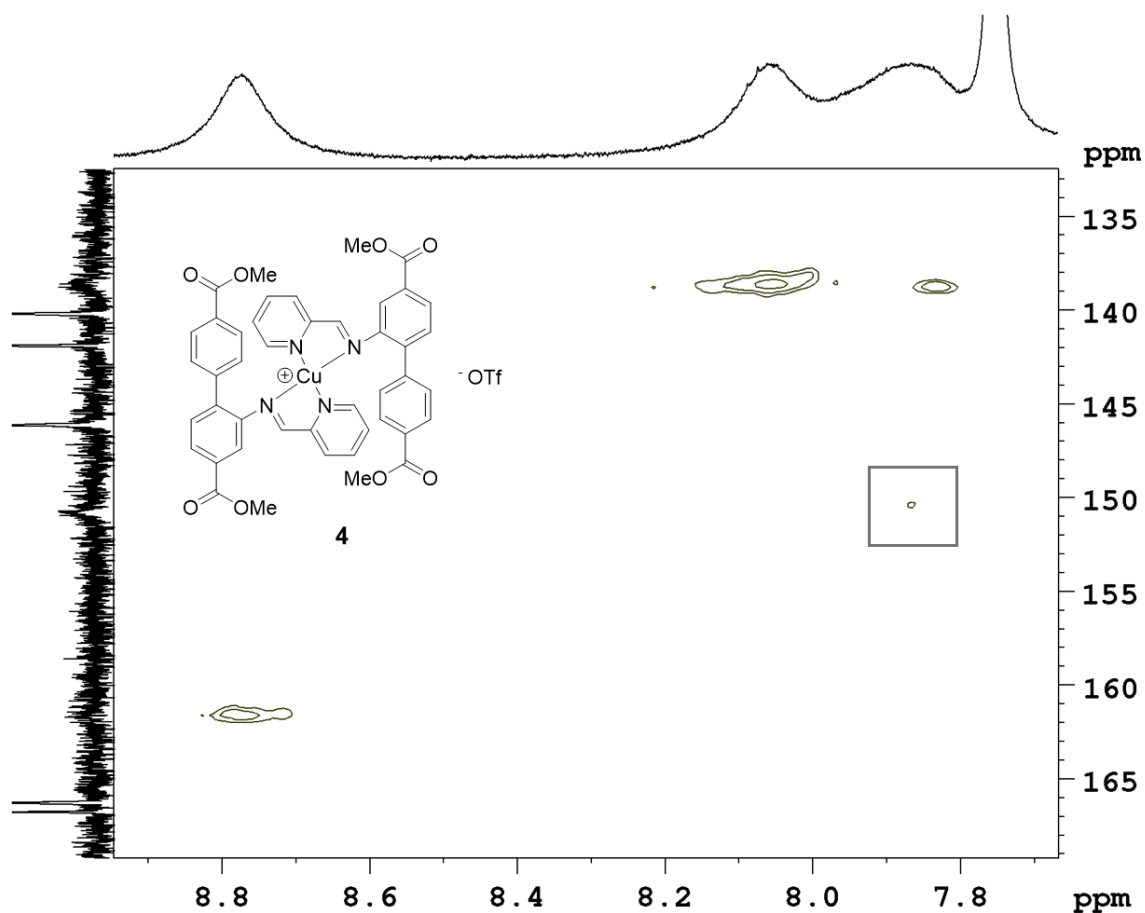


Figure S25. HSQC (600 MHz, CD₃CN) of **4** showing the carbons detected through HSQC.

Compound **4** showed minor species besides the main peaks in both, *d*₆-DMSO (at ambient temperature) and CD₃CN (at low temperatures). In order to see if the minor species and the major species interconvert, NOESY/EXSY experiments were conducted in both solvents (**Figure S26** and **Figure S30**). Both show correlations between the minor and the major species. In acetonitrile, the phase of the exchange peaks differs from the NOEs at room temperature. NOEs were only observed for the major species.

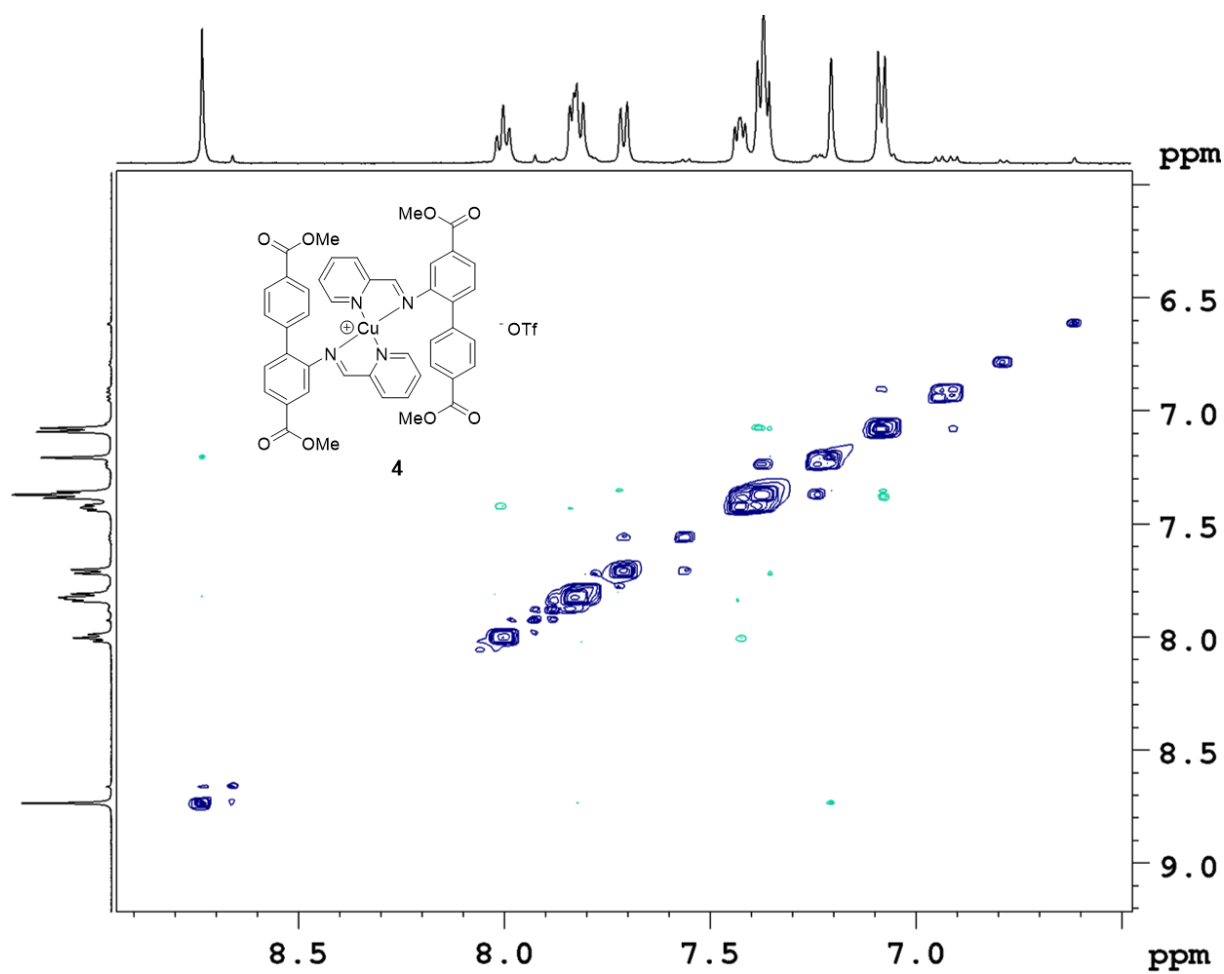
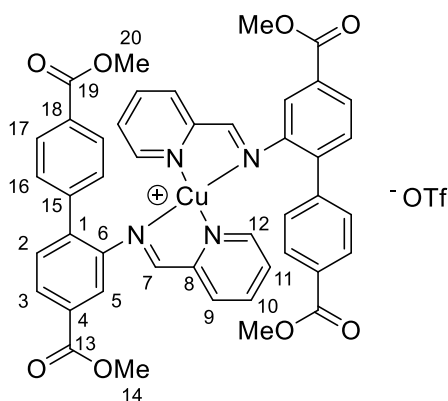


Figure S26. NOESY/EXSY (500 MHz, CD₃CN) of **4** at -34 °C showing chemical exchange (positive peaks off the diagonal) between the major species and the minor species. At higher temperatures, these peaks coalesced into a broadened peak.

NMR Data for Compound **4** in d_6 -DMSO



In the ^1H NMR spectrum of **4** in d_6 -DMSO, one or more minor species were observed in addition to the major species. Only NMR data for the major species are given below.

^1H NMR (600 MHz, d_6 -DMSO): δ 9.03 (2H, s, H7), 8.12-8.15 (2H, m, H10), 7.99 (2H, d, $^3J_{\text{H,H}} = 7.6$ Hz, H9), 7.89 (2H, d, $^3J_{\text{H,H}} = 4.4$ Hz, H12), 7.70 (2H, d, $^3J_{\text{H,H}} = 7.9$ Hz, H3), 7.51-7.53 (2H, m, H11), 7.43 (2H, d, $^3J_{\text{H,H}} = 7.9$ Hz, H2), 7.38 (4H, d, $^3J_{\text{H,H}} = 8.0$ Hz, H17), 7.19 (2H, s, H5), 7.12 (4H, d, $^3J_{\text{H,H}} = 8.0$ Hz, H16), 3.97 (6H, s, H14), 3.83 (6H, s, H20). ^{13}C NMR (150 MHz, d_6 -DMSO): δ 165.2 (C19), 164.8 (C13), 161.2 (C7), 149.5 (C8), 149.1 (C12), 144.7 (C6), 140.4 (C15), 138.6 (C1), 137.8 (C10), 130.1 (C2), 130.0 (C4), 129.5 (C16), 128.5 (C18), 128.2 (C9), 127.9 (C11 + C17), 127.8 (C3), 120.9 (C5), 120.6 (q, $^1J_{\text{C,F}} = 321$ Hz, CF_3), 52.2 (C14), 51.9 (C20). $^{15}\text{N}\{^1\text{H}\}$ NMR (600 MHz, d_6 -DMSO): δ -94.0 (N_{imine}), -126.8 ($\text{N}_{\text{pyridine}}$).

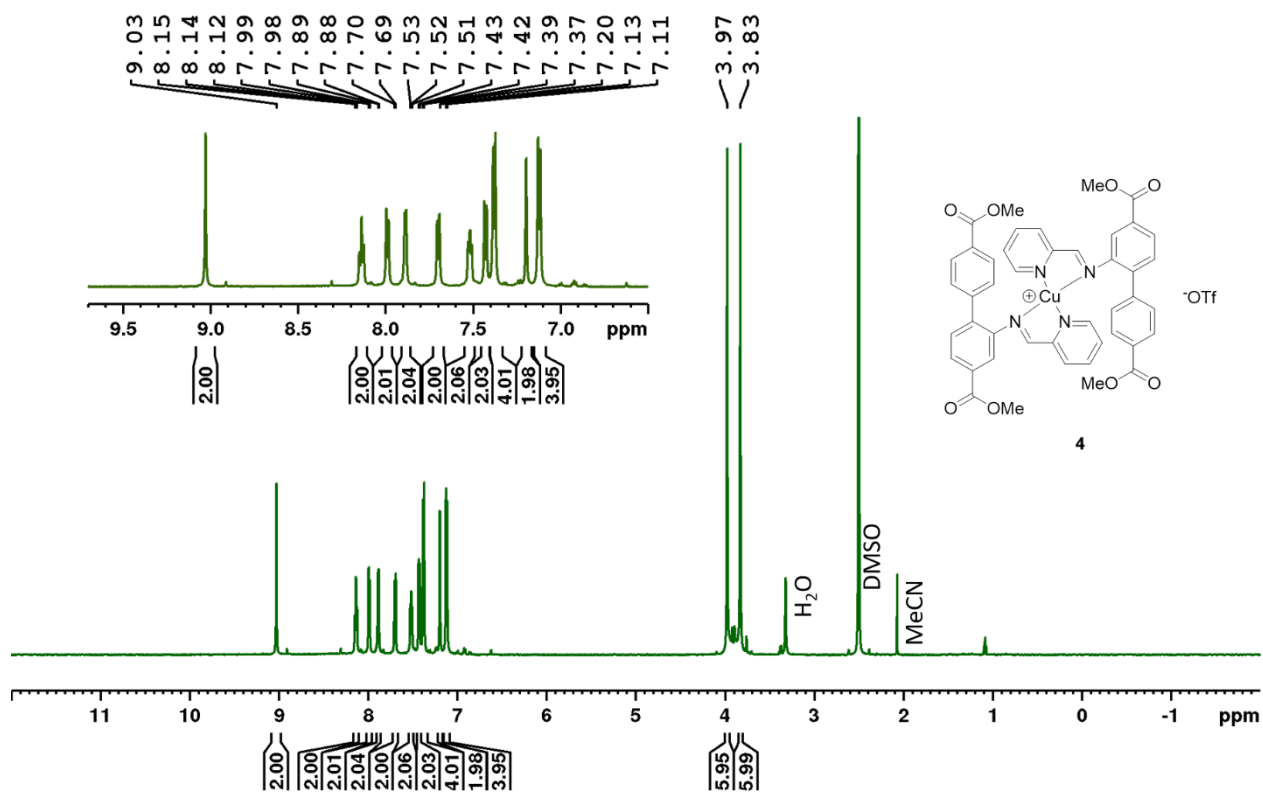


Figure S27. ^1H NMR (600 MHz, d_6 -DMSO) of 4.

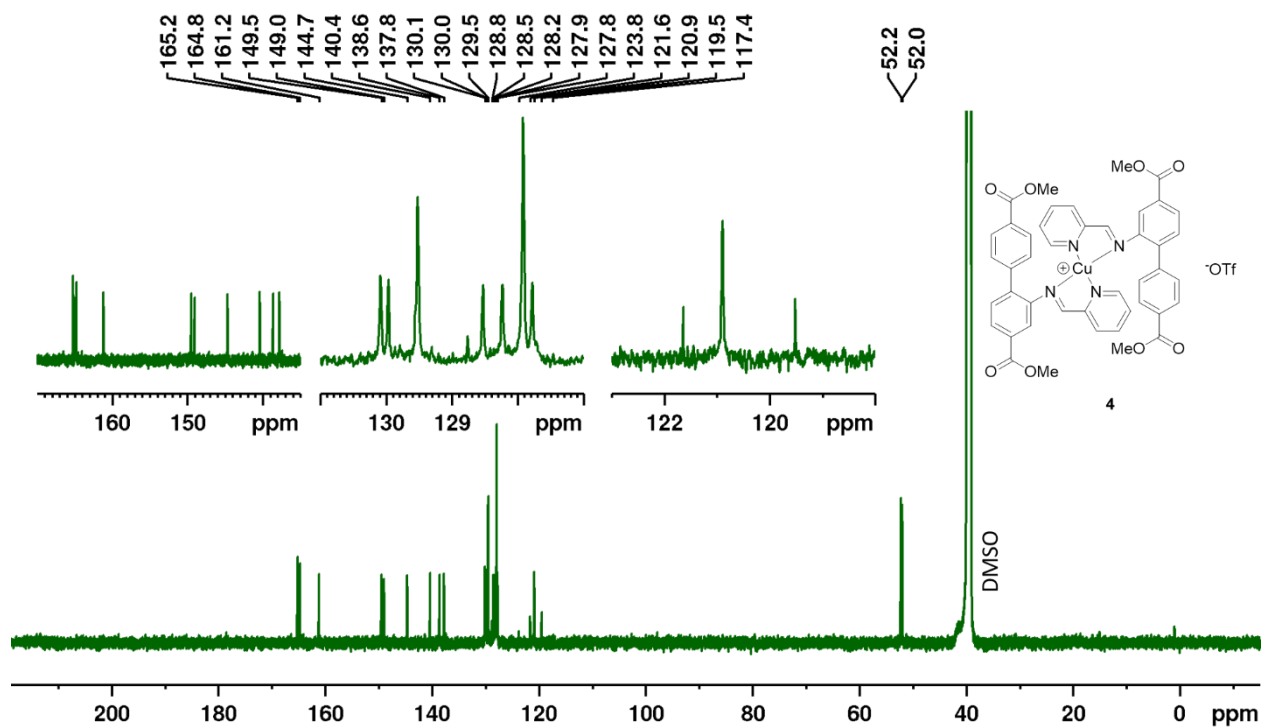


Figure S28. ^{13}C NMR (150 MHz, d_6 -DMSO) of 4.

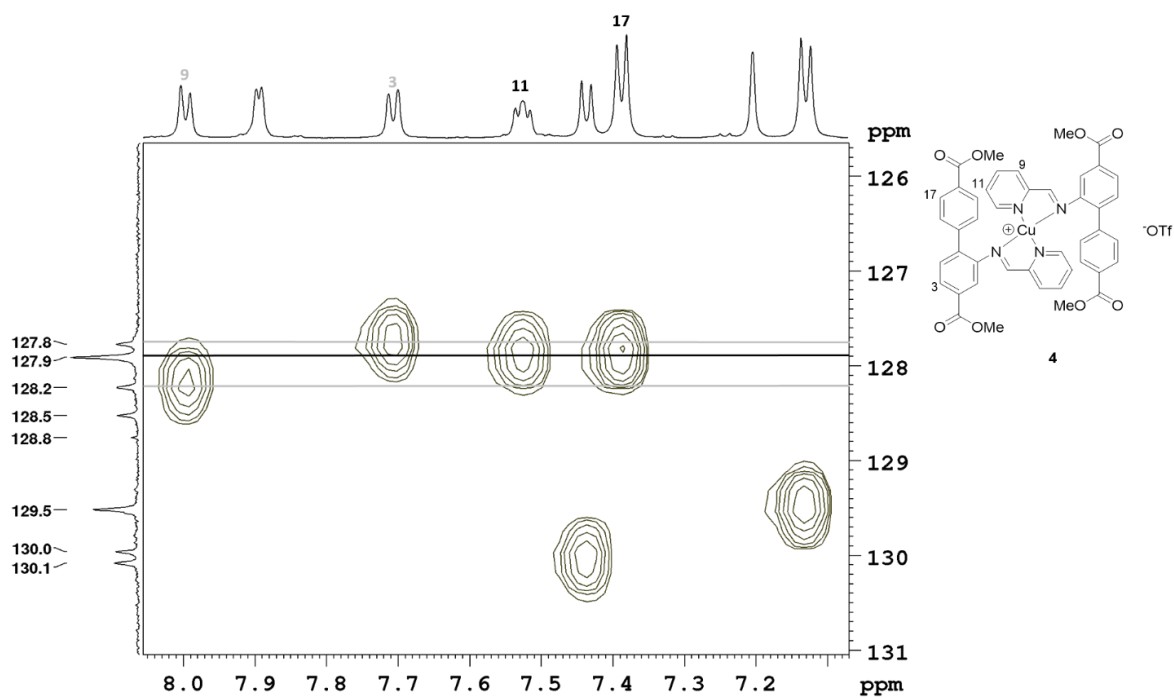


Figure S29. HSQC (600 MHz, d_6 -DMSO) of **4**. The resonances corresponding to H11 and H17 both show a correlation to the resonance at δ 127.9, suggesting overlapping ^{13}C resonances.

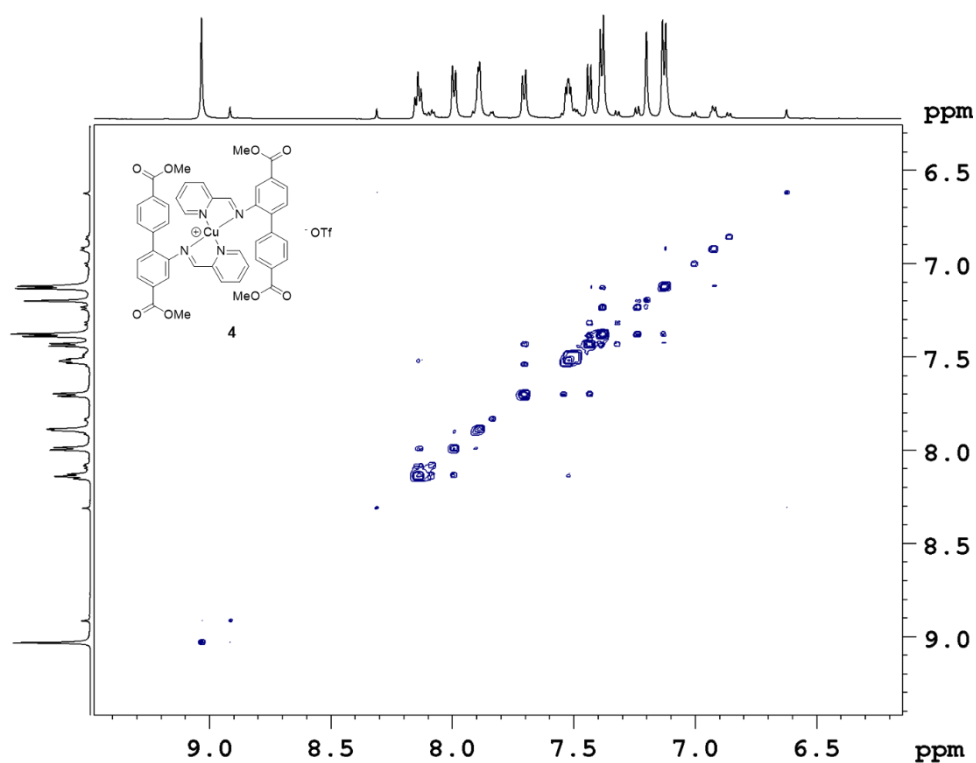
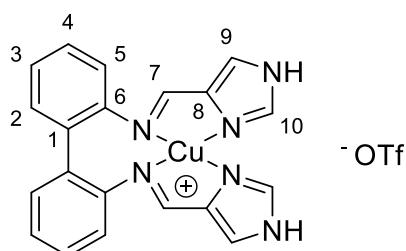


Figure S30. NOESY/EXSY (600 MHz, d_6 -DMSO) of **4** at ambient temperature, showing chemical exchange and NOEs in the same phase.

Compound 5

A mixture of biphenyl-2,2'-diamine (0.54 mmol, 100 mg), CuOTf (0.54 mmol, 115 mg, 1 equiv.) and 1*H*-imidazole-4-carbaldehyde (1.08 mmol, 104 mg, 2 equiv.) were stirred in MeCN (3 mL) overnight. Et₂O (4 mL) was added and the solid was collected through filtration and washed (2x 1 mL Et₂O). Residual solvent was left to evaporate over night to yield **5** as a brown solid. Yield: 60-69 %.



¹H NMR (600 MHz, CD₃CN): δ 11.01 (2H, NH), 8.13 (2H, H7), 7.97 (2H, H10), 7.57 (2H, H9), 7.38 (2H, H2), 7.34 (2H, H4), 7.25 (2H, H3), 6.92 (2H, H5). ¹³C NMR (150 MHz, CD₃CN): δ 154.1 (C7), 148.5 (C6), 139.3 (C8), 138.7 (C10), 133.0 (C2), 131.4 (C1), 129.5 (C4), 126.3 (C3), 122.2 (m*, ¹J_{C,F} = 325 Hz, CF₃), 122.1 (C9), 120.4 (C5). ¹⁵N{¹H} NMR (800 MHz, CD₃CN): δ -79.1 (N_{imine}), -170.5 (N_{IM}), -211.4 (N_{AZ}). HRMS *m/z* [⁶³CuL⁺] (C₂₀H₁₆CuN₆⁺): Calcd: 403.0727 Found: 403.0715 Anal. Calcd: C, 45.61; H, 2.92; N, 15.20 Found: C, 45.73; H, 2.92; N, 15.19.

* d visible, expected q

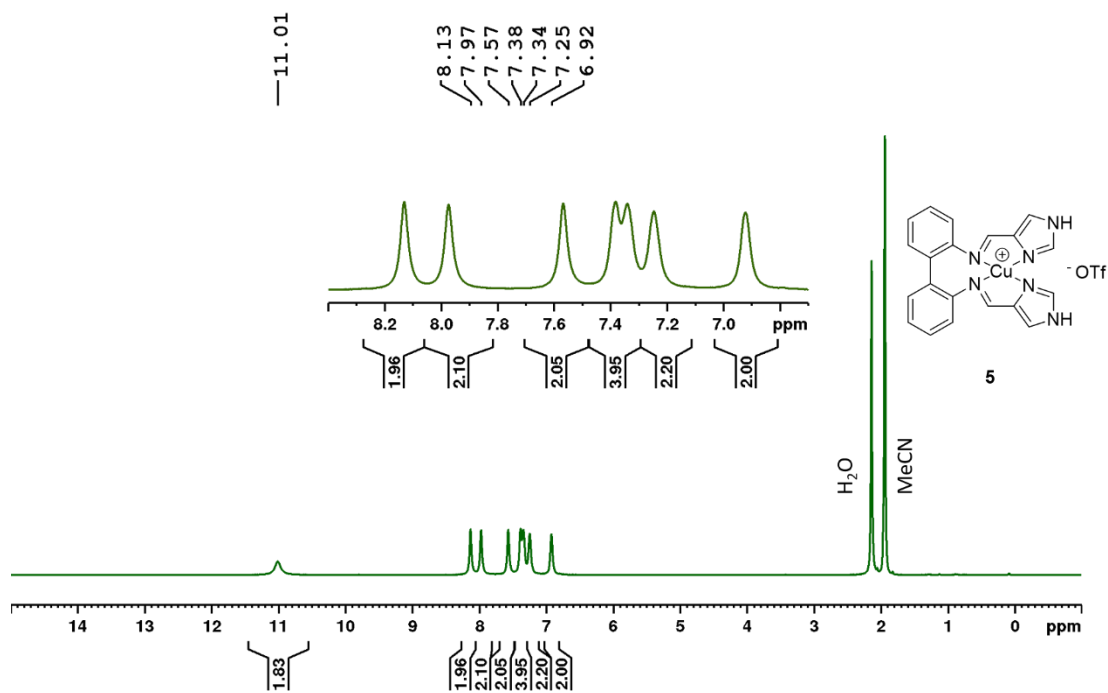


Figure S31. ^1H NMR (600 MHz, CD_3CN) of **5**.

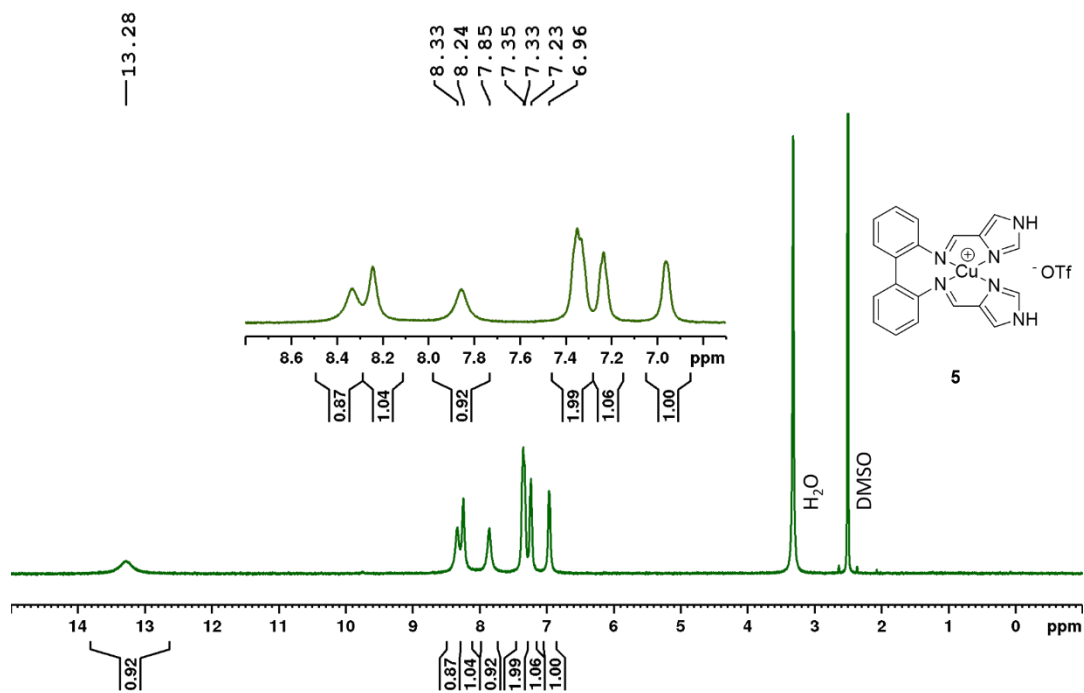


Figure S32. ^1H NMR (500 MHz, d_6 -DMSO) of **5**. The peaks are broader compared to the measurement in CD_3CN .

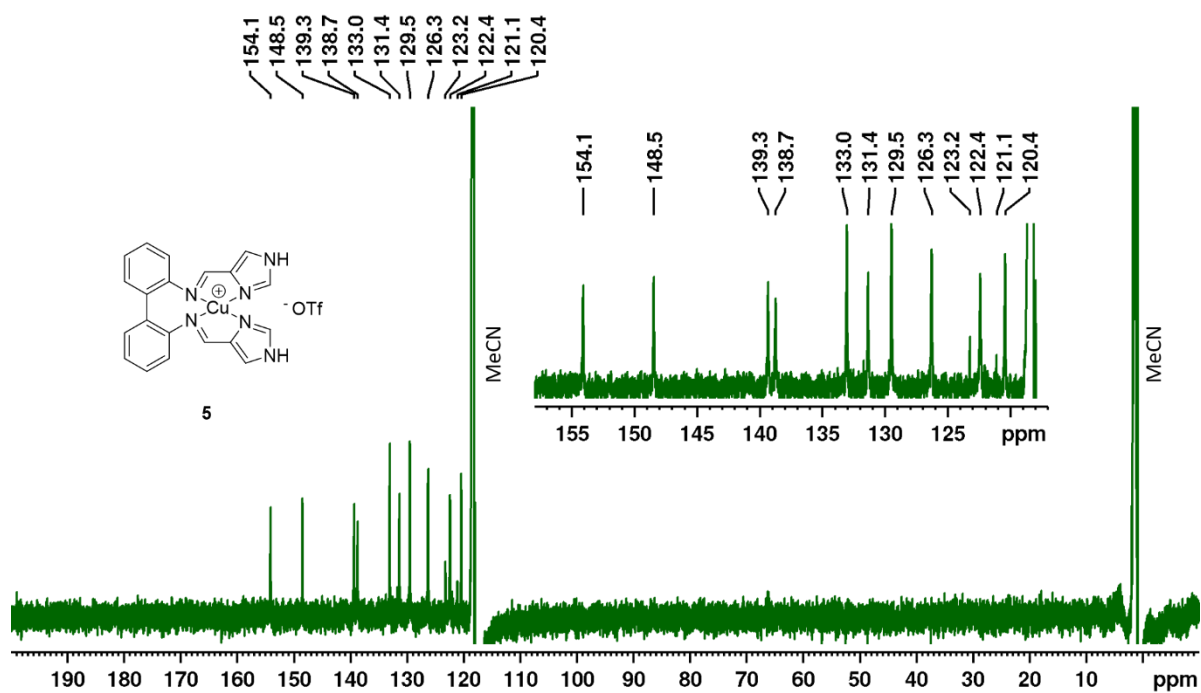


Figure S33. ¹³C NMR (150 MHz, CD₃CN) of 5.

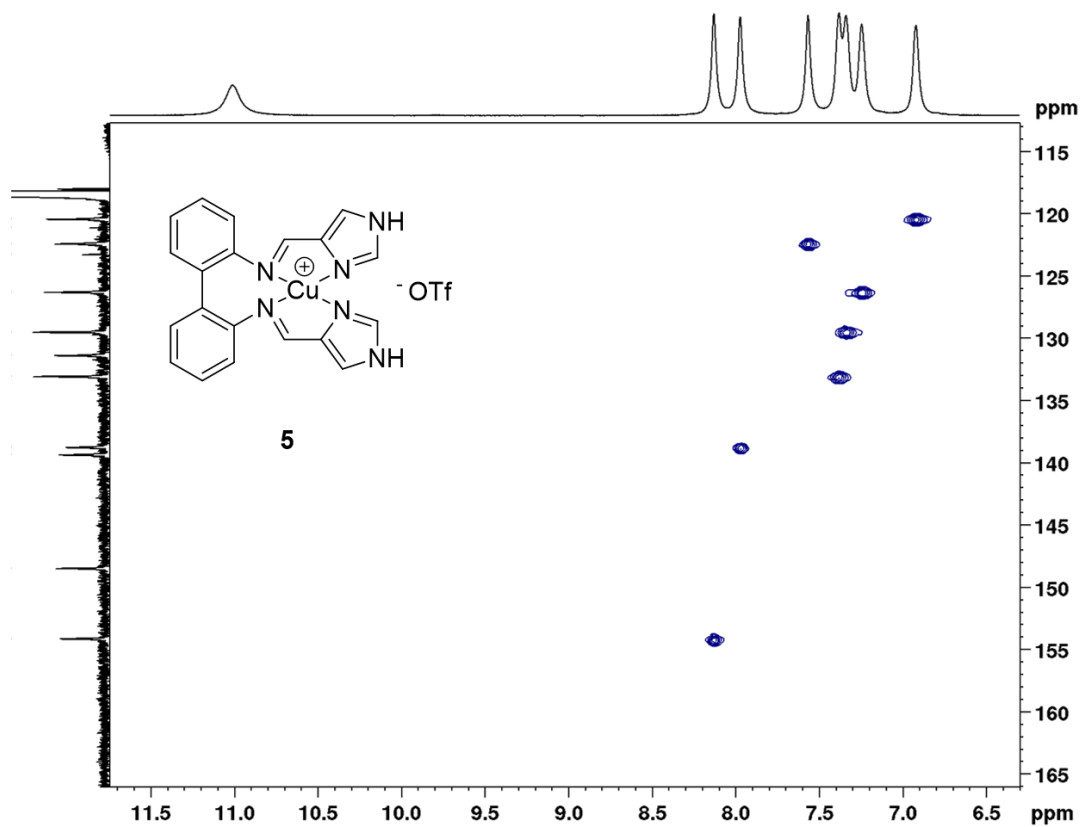
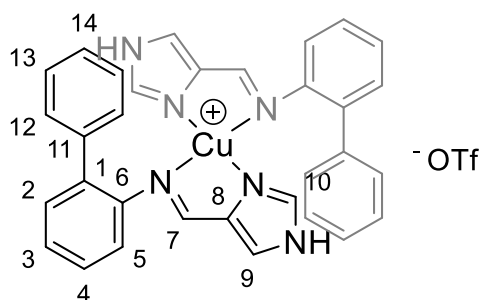


Figure S34. HSQC (600 MHz, CD₃CN) of complex 5.

Compound 6

A mixture of CuOTf (0.30 mmol, 63 mg, 1 equiv.), biphenyl-2-amine (0.59 mmol, 100 mg, 2 equiv.) and 1*H*-imidazole-4-carbaldehyde (0.59 mmol, 57 mg, 2 equiv.) were stirred in MeCN (2 mL) overnight. The formed solid was collected through filtration and washed with Et₂O (2 mL). Residual solvent was left to evaporate over night to yield **6** as an orange solid. Yield: 64-72 %.



¹H NMR (*d*₆-DMSO, 600 MHz): δ 13.03 (2H, s, NH), 8.32 (2H, s, H7), 7.79 (2H, s, H9), 7.64 (2H, s, H10), 7.25 (4H, m, H2, H3), 7.17 (2H, m, H4), 7.05 (10H, m, H12-14), 6.56 (2H, m, H5). ¹³C NMR (*d*₆-DMSO, 150 MHz): δ 153.7 (C7), 147.2 (C6), 138.3 (C11), 138.0 (C8), 137.4 (C10), 134.0 (C1), 130.0 (C2), 129.2 (CH phenyl), 128.2 (C4), 127.5 (CH phenyl), 126.5 (CH phenyl), 125.9 (C3), 121.9 (C9), 120.7 (q, ¹J_{C,F} = 322 Hz, CF₃), 120.6 (C5). ¹⁵N{¹H} NMR (800 MHz, *d*₆-DMSO): δ -86.1 (N_{imine}), -170.0 (N_{IM}), -206.1 (N_{AZ}). ESI-MS: *m/z* 248.118 (100 %, [L+H]⁺), 270.100 (63 %, [L+Na]⁺), 310.040 (11 %, [⁶³CuL]⁺), 312.038 (5 %, [⁶⁵CuL]⁺), 557.150 (9 %, [⁶³CuL₂]⁺), 559.149 (4 %, [⁶⁵CuL₂]⁺). HRMS *m/z* [⁶³CuL₂²⁺] (C₃₂H₂₆CuN₆⁺): Calcd: 557.1509 Found: 557.1499. Anal. Calcd: C, 56.05; H, 3.71; N, 11.88 Found: C, 55.88; H, 3.69; N, 11.78.

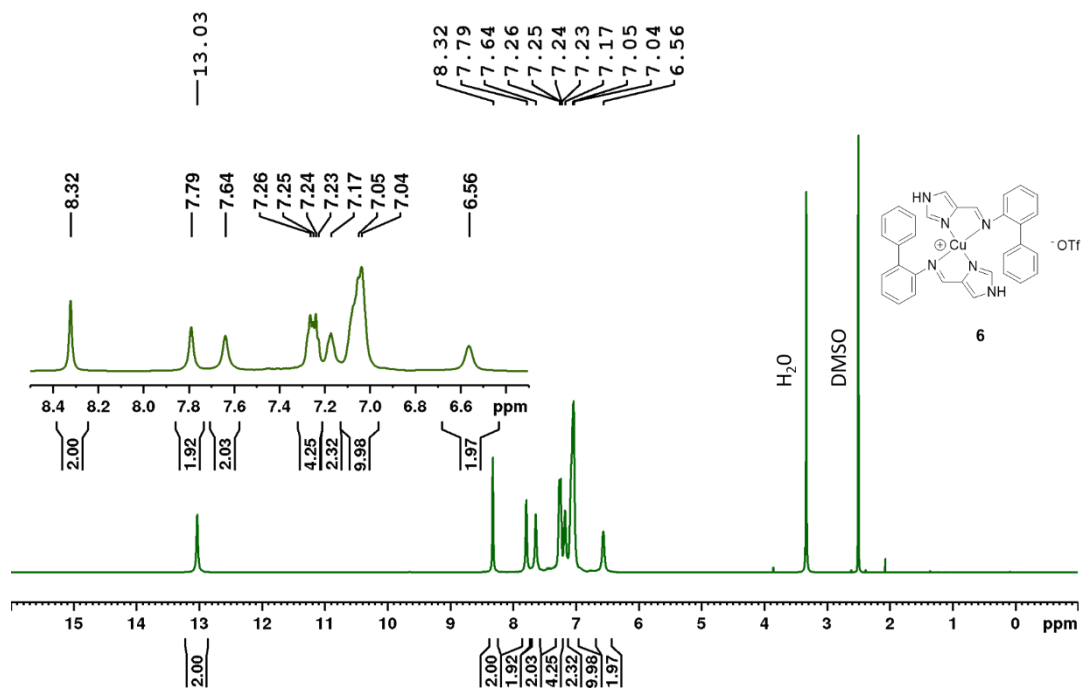


Figure S35. $^1\text{H NMR}$ (600 MHz, d_6 -DMSO) of **6**.

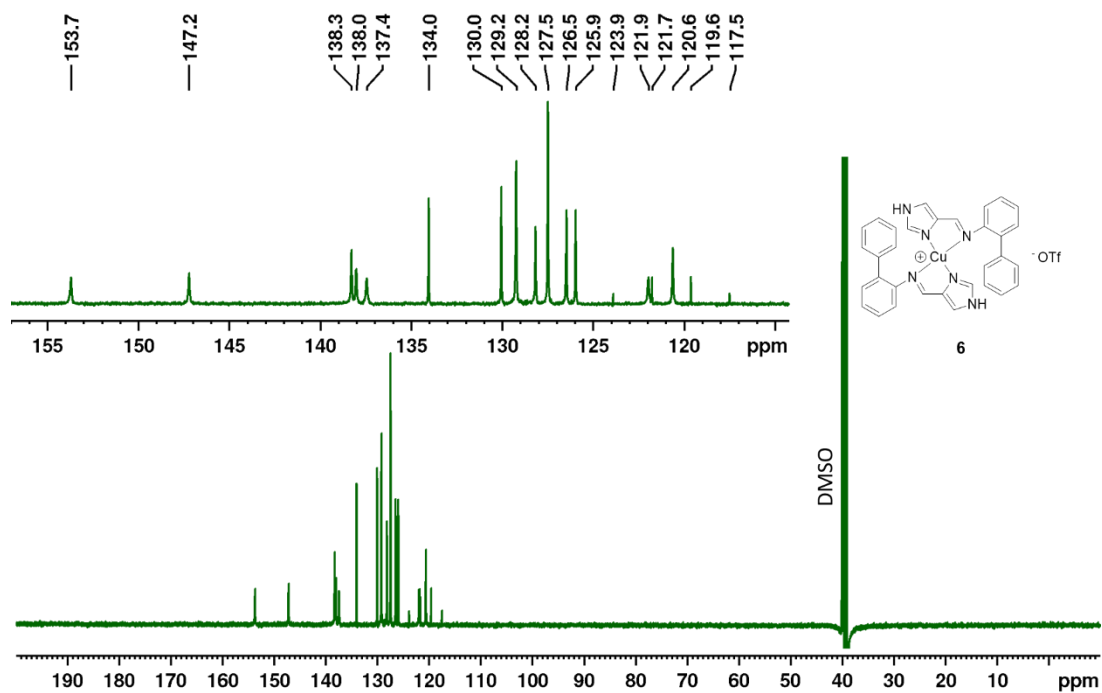


Figure S36. $^{13}\text{C NMR}$ (150 MHz, d_6 -DMSO) of **6**.

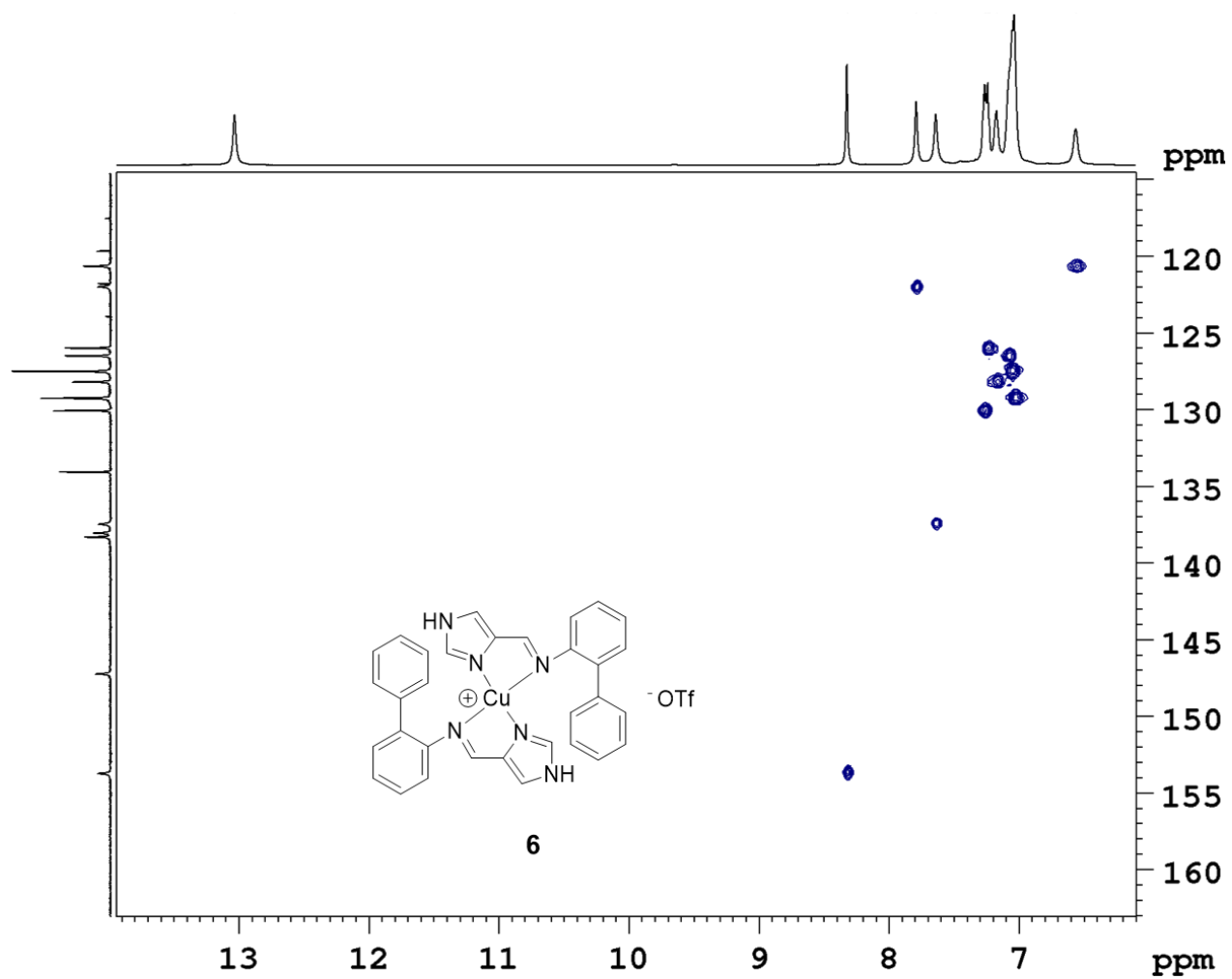


Figure S37. HSQC (600 MHz, d_6 -DMSO) of 6.

Synthesis of Ligands

The synthesis of ligands **L1-L6** was adapted from previously reported procedures for Schiff base ligands.¹

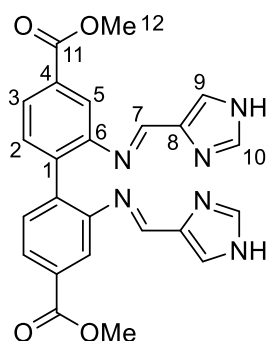
[A]: The diamine (1.00 mmol) and the respective aldehyde (2.20 mmol, 2.2 equiv.) were suspended in dry EtOH. 3 drops of formic acid were added. The mixture was stirred for 20 h and the precipitated product was collected through filtration. The product was washed with dry EtOH and dried in a vacuum oven at 70 °C over night.

[B]: The amine (1.00 mmol) and the respective aldehyde (1.05 mmol, 1.05 equiv.) were suspended in dry EtOH. 3 drops of formic acid were added. The mixture was stirred for 20 h and the precipitated product was collected through filtration. The product was washed with dry EtOH and dried in a vacuum oven at 70 °C over night.

The ligands bearing imidazole moieties (**L1, L2, L5, L6**) showed concentration-dependent NMR spectra. In order to minimize the line-broadening, the spectra were recorded at low concentrations (ca. 0.5-1 mg in 0.6 mL of *d*₆-DMSO). Incomplete carbon spectra were obtained for these compounds, even after prolonged experiment time on high-field instruments. In HSQC, two correlations were observed for some protons (H7, H9 and H10), indicating conformational changes and/or intermolecular hydrogen bonding associated with the imine and imidazole groups in the molecules. The broadened resonances observed for **L1, L2, L5** and **L6** are in accordance with NMR data for imidazole Schiff bases found in the literature.⁷⁻⁹ Therefore, only ¹H NMR spectra and ¹H-¹⁵N HMBC are reported.

L1

L1 was obtained as a colourless to pale yellow solid from ligand synthesis procedure A after recrystallization from acetonitrile (23% yield).



M.p. > 220 °C (decomposes). ^1H NMR (600 MHz, d_6 -DMSO): δ 12.48 (*br*, 2H, s, NH), 8.20 (2H, s, H7), 7.81 (2H, d, $^3J_{\text{H,H}} = 7.7$ Hz, H3), 7.72 (2H, s, H10), 7.51 (2H, s, H5), 7.5-7.1 (*br*, 2H, H9), 7.46 (2H, d, $^3J_{\text{H,H}} = 7.6$ Hz, H2). $^{15}\text{N}\{^1\text{H}\}$ NMR (800 MHz, d_6 -DMSO): δ -69.5 (N_{imine}), -116.1 (N_{IM}), -210.8 (N_{AZ}). HRMS (ESI) m/z ($\text{C}_{24}\text{H}_{20}\text{N}_6\text{O}_4 + \text{Na}^+$): Calcd: 479.1438 Found: 479.1438. Anal. Calcd: C, 63.15; H, 4.42; N, 18.41 Found: C, 62.87; H, 4.45; N, 18.38.

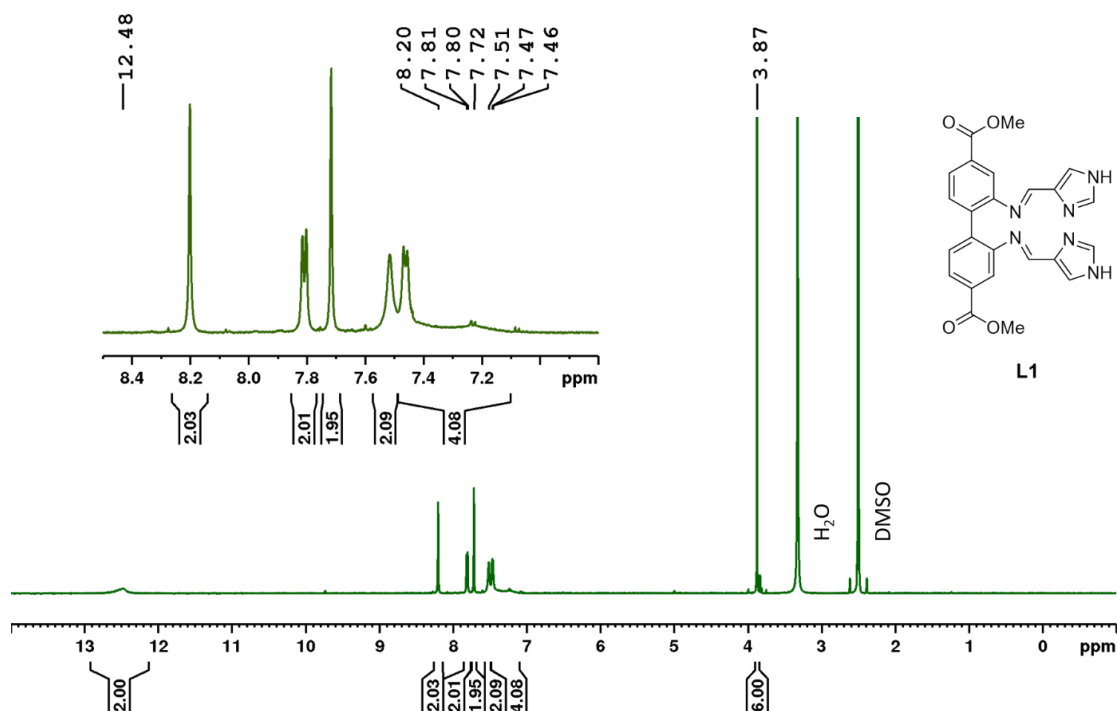
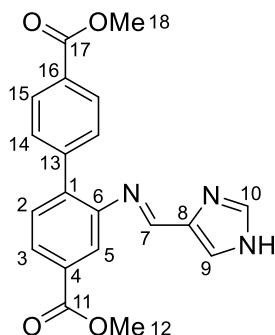


Figure S38. ^1H NMR (600 MHz, d_6 -DMSO) of L1.

L2

L2 was obtained as a colourless solid from ligand synthesis procedure B after two-fold recrystallization from toluene (33 % yield).



M.p. 191-193 °C (decomposes). ^1H NMR (600 MHz, d_6 -DMSO): δ 12.67 (*br*, 1H, s, **NH**), 8.49 (1H, s, H7), 7.98 (2H, d, $^3J_{\text{H,H}} = 8.4$ Hz, H15), 7.88 (1H, dd, $^3J_{\text{H,H}} = 8.0$ Hz, $^4J_{\text{H,H}} = 1.5$ Hz, H3), 7.81 (1H, s, H10), 7.7-7.6 (5H, overlapping m, H14, H2, H3, H9), 3.89 (3H, s, CO_2CH_3), 3.87 (3H, s, CO_2CH_3). $^{15}\text{N}\{^1\text{H}\}$ NMR (800 MHz, d_6 -DMSO): δ -69.9 (N_{imine}), -116.5 (N_{IM}). ^{15}N shifts originate from two separate HMBC experiments at different concentrations. N_{AZ} not found. HRMS (ESI) m/z ($\text{C}_{20}\text{H}_{17}\text{N}_3\text{O}_4 + \text{Na}^+$): Calcd: 386.1111 Found: 386.1111. Anal. Calcd: C, 66.11; H, 4.72; N, 11.56 Found: C, 65.95; H, 4.71; N, 11.48.

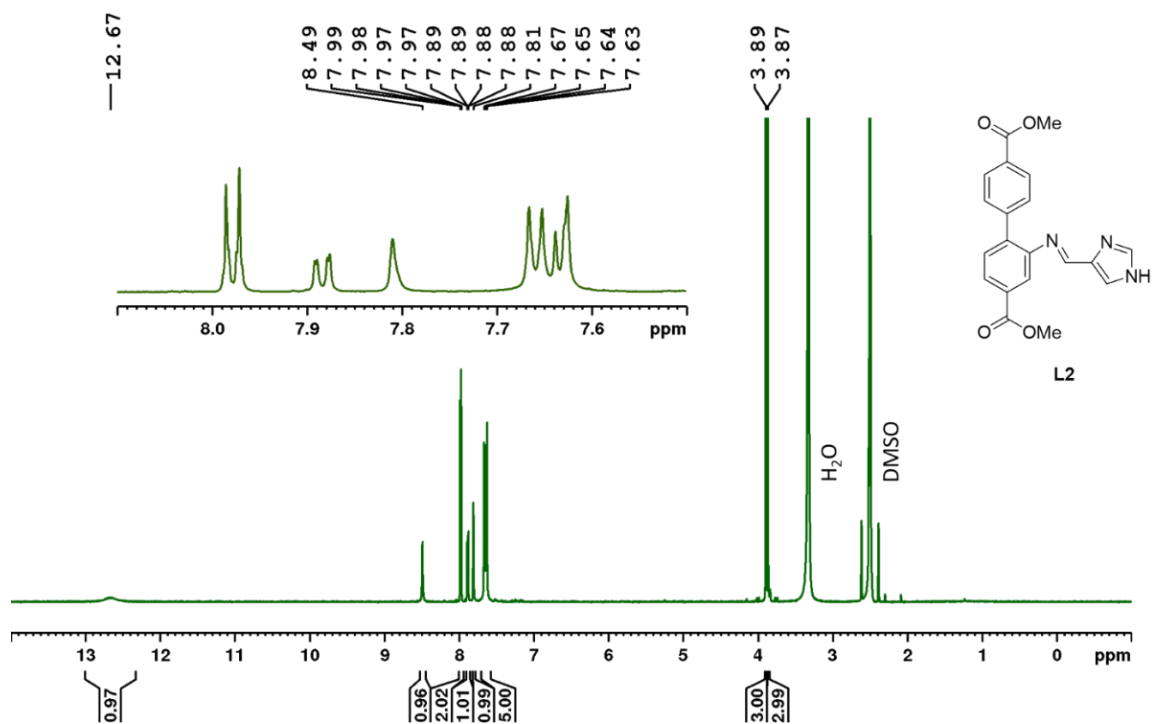
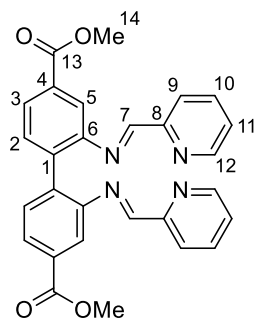


Figure S39. ¹H NMR (600 MHz, *d*₆-DMSO) of L2.

L3

L3 was synthesized according to ligand synthesis procedure A. After recrystallization from toluene, **L3** was obtained as pale yellow solid (82% yield).



M.p. 219-222 °C (decomposes). ^1H NMR (600 MHz, d_6 -DMSO): δ 8.55 (2H, ddd, $^3J_{\text{H,H}} = 4.8$ Hz, $^4J_{\text{H,H}} = 1.6$ Hz, $^5J_{\text{H,H}} = 0.9$ Hz, H12), 8.33 (2H, s, H7), 7.94 (2H, dd, $^3J_{\text{H,H}} = 7.9$ Hz, $^4J_{\text{H,H}} = 1.7$ Hz, H3), 7.83 (2H, ddd, $^3J_{\text{H,H}} = 7.7$ Hz, $^4J_{\text{H,H}} = 1.6$ Hz, H10), 7.73 (2H, d, $^4J_{\text{H,H}} = 1.6$ Hz, H5), 7.65 (2H, dd, $^3J_{\text{H,H}} = 8.0$ Hz, $J_{\text{H,H}} = 0.9$ Hz, H9), 7.60 (2H, d, $^3J_{\text{H,H}} = 7.9$ Hz, H2), 7.45 (2H, ddd, $^3J_{\text{H,H}} = 7.5$ Hz and 4.8 Hz, $^4J_{\text{H,H}} = 1.2$ Hz, H11), 3.90 (6H, s, H14). ^{13}C NMR (150 MHz, d_6 -DMSO): δ 165.8 (C13), 162.0 (C7), 153.4 (C8), 149.7 (C6), 149.5 (C12), 137.7 (C1), 137.0 (C10), 131.4 (C2), 130.6 (C4), 126.4 (C3), 125.7 (C11), 121.2 (C9), 118.8 (C5), 52.3 (C14). $^{15}\text{N}\{^1\text{H}\}$ NMR (800 MHz, d_6 -DMSO): δ -47.9 (N_{imine}), -61.6 ($\text{N}_{\text{pyridine}}$). HRMS (ESI) m/z ($\text{C}_{28}\text{H}_{22}\text{N}_4\text{O}_4 + \text{Na}^+$): Calcd: 501.1532 Found: 501.1533. Anal. Calcd: C, 70.28; H, 4.63; N, 11.71 Found: C, 69.92; H, 4.61; N, 11.64.

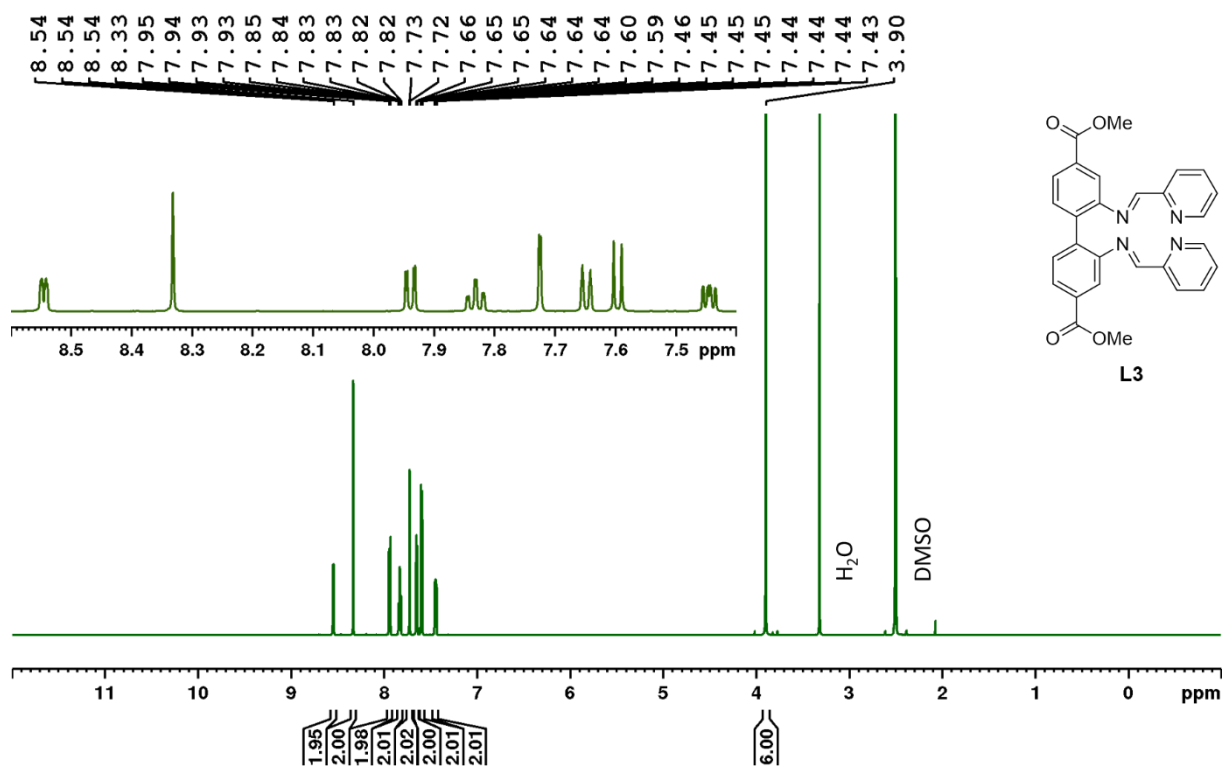


Figure S40. ^1H NMR (600 MHz, d_6 -DMSO) of L3.

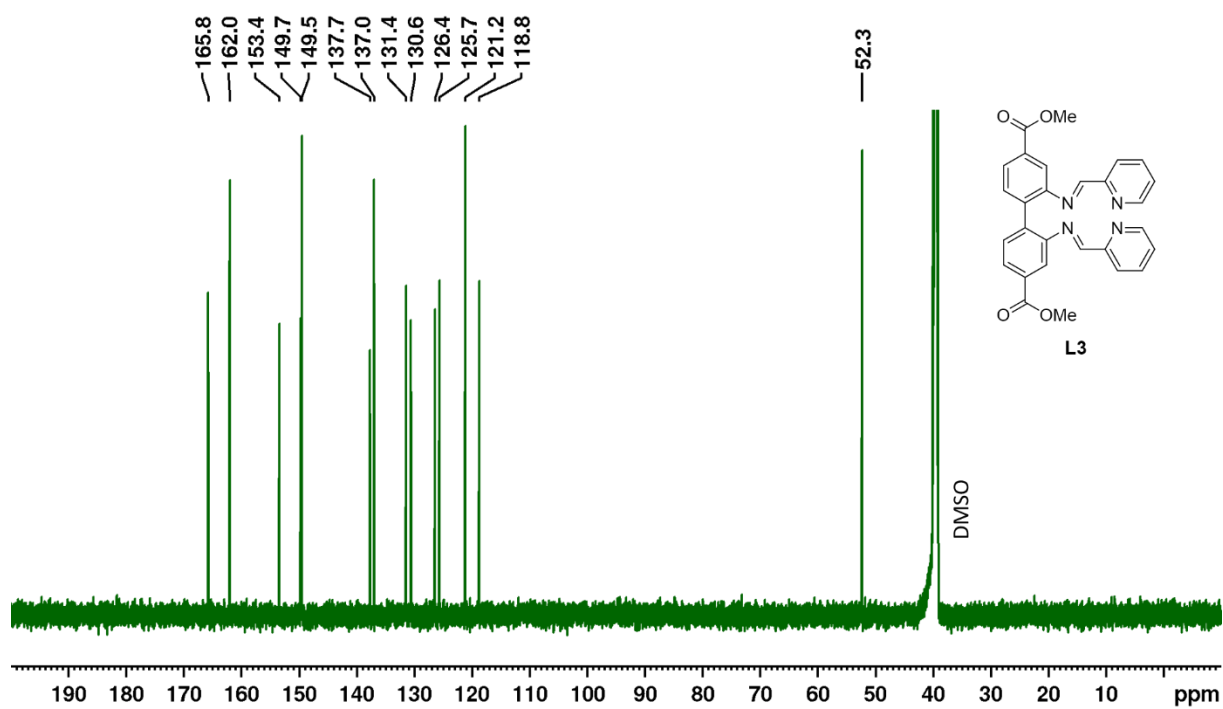
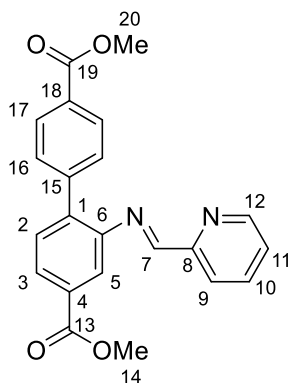


Figure S41. ^{13}C NMR (150 MHz, d_6 -DMSO) of L3.

L4

L4 was obtained from ligand synthesis procedure B as a colourless solid (77-84 % yield).



M.p. 176-178 °C. ^1H NMR (600 MHz, d_6 -DMSO): δ 8.73 (1H, m, H12), 8.67 (1H, s, H7), 8.00 (2H, d, $^3J_{\text{H,H}} = 8.4$ Hz, H17), 7.97 (1H, dd, $^3J_{\text{H,H}} = 8.0$ Hz, $^4J_{\text{H,H}} = 1.7$ Hz, H3), 7.94-7.89 (2H, overlapping m, H9 and H10), 7.73 (1H, d, $^4J_{\text{H,H}} = 1.6$ Hz, H5), 7.69 (1H, d, $^3J_{\text{H,H}} = 8.0$ Hz, H2), 7.67 (2H, d, $^3J_{\text{H,H}} = 8.5$ Hz, H16), 7.53 (1H, m, H11), 3.91 (3H, s, H14), 3.87 (3H, s, H20). ^{13}C NMR (150 MHz, d_6 -DMSO): δ 166.0 (C19), 165.6 (C13), 162.7 (C7), 153.7 (C8), 149.7 (C12), 148.6 (C6), 142.6 (C15), 138.2 (C1), 137.2 (C10), 130.6 (C2), 130.5 (C4), 130.3 (C16), 128.7 (C17), 127.1 (C3), 125.9 (C11), 121.5 (C9), 119.6 (C5), 52.4 (C14), 52.2 (C20), missing: C18. $^{15}\text{N}\{^1\text{H}\}$ NMR (600 MHz, d_6 -DMSO): δ -47.9 (N_{imine}), -62.5 ($\text{N}_{\text{pyridine}}$). HRMS (ESI) m/z ($\text{C}_{22}\text{H}_{18}\text{N}_2\text{O}_4 + \text{Na}^+$): Calcd: 397.1158 Found: 397.1159. Anal. Calcd: C, 70.58; H, 4.85; N, 7.48 Found: C, 70.51; H, 4.88; N, 7.46.

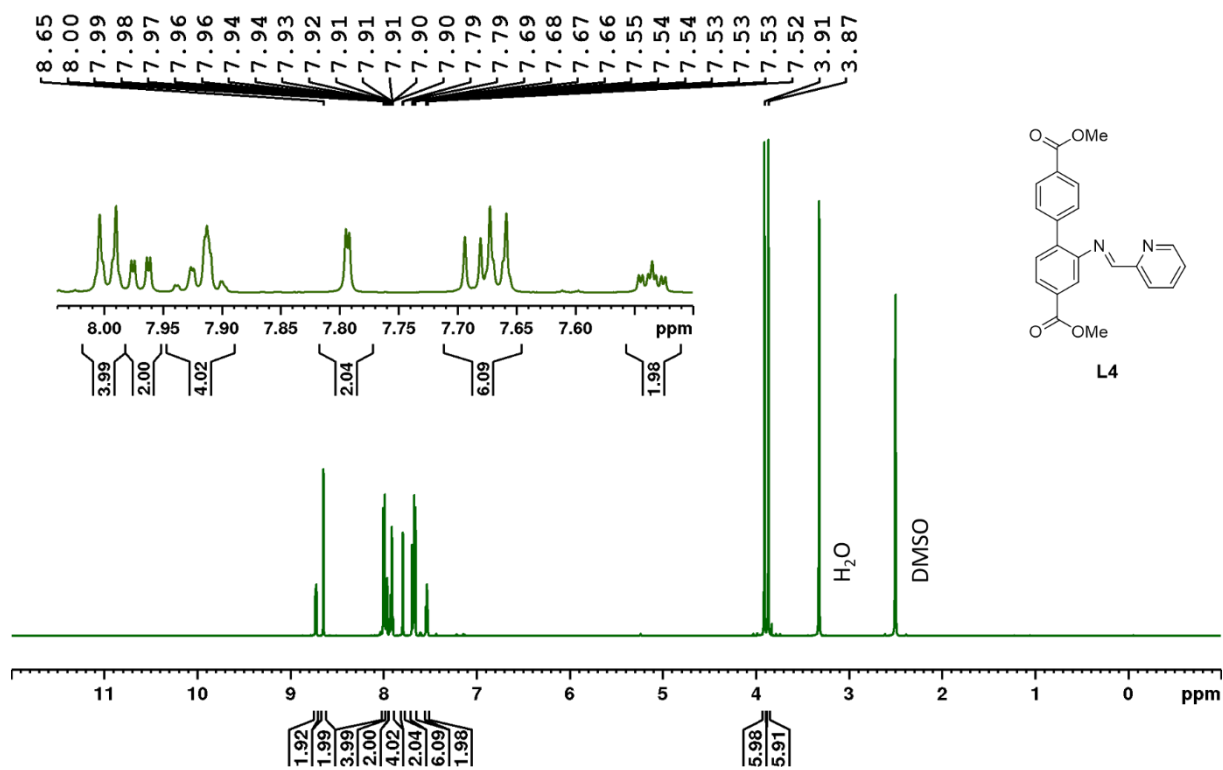


Figure S42. ¹H NMR (600 MHz, *d*₆-DMSO) of L4.

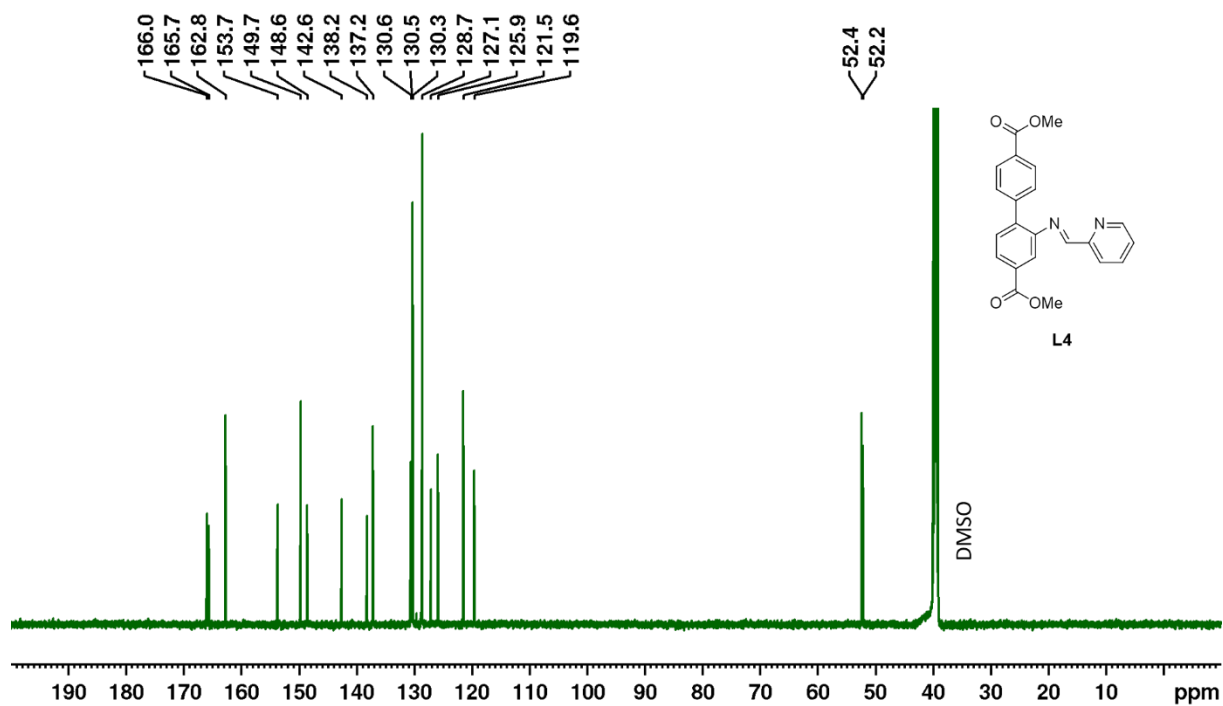
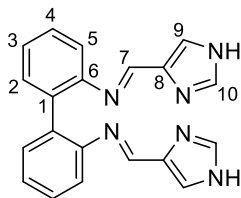


Figure S43. ¹³C NMR (150 MHz, *d*₆-DMSO) of L4.

L5

L5 was obtained from ligand synthesis procedure A as a colourless solid (79-91 % yield).



M.p. 230-231 °C (decomposes). ^1H NMR (600 MHz, d_6 -DMSO): δ 12.45 (*br*, 2H, NH), 8.09 (2H, s, H7), 7.69 (2H, s, H10), 7.4-7.1 (*br*, 2H, H9), 7.33 (2H, dd, $^3J_{\text{H,H}} = 7.5$ Hz, H3), 7.26 (2H, d, $^3J_{\text{H,H}} = 7.2$ Hz, H5), 7.19 (2H, dd, $^3J_{\text{H,H}} = 7.3$ Hz, H4), 6.92 (2H, d, $^3J_{\text{H,H}} = 7.7$ Hz, H2). $^{15}\text{N}\{^1\text{H}\}$ NMR (800 MHz, d_6 -DMSO): δ -63.4 (N_{imine}), -117.0 (N_{IM}). N_{AZ} not found. HRMS (ESI) m/z ($\text{C}_{20}\text{H}_{16}\text{N}_6 + \text{Na}^+$): Calcd: 363.1328 Found: 363.1329. Anal. Calcd: C, 70.57; H, 4.74; N, 24.69 Found: C, 70.41; H, 4.73; N, 24.61.

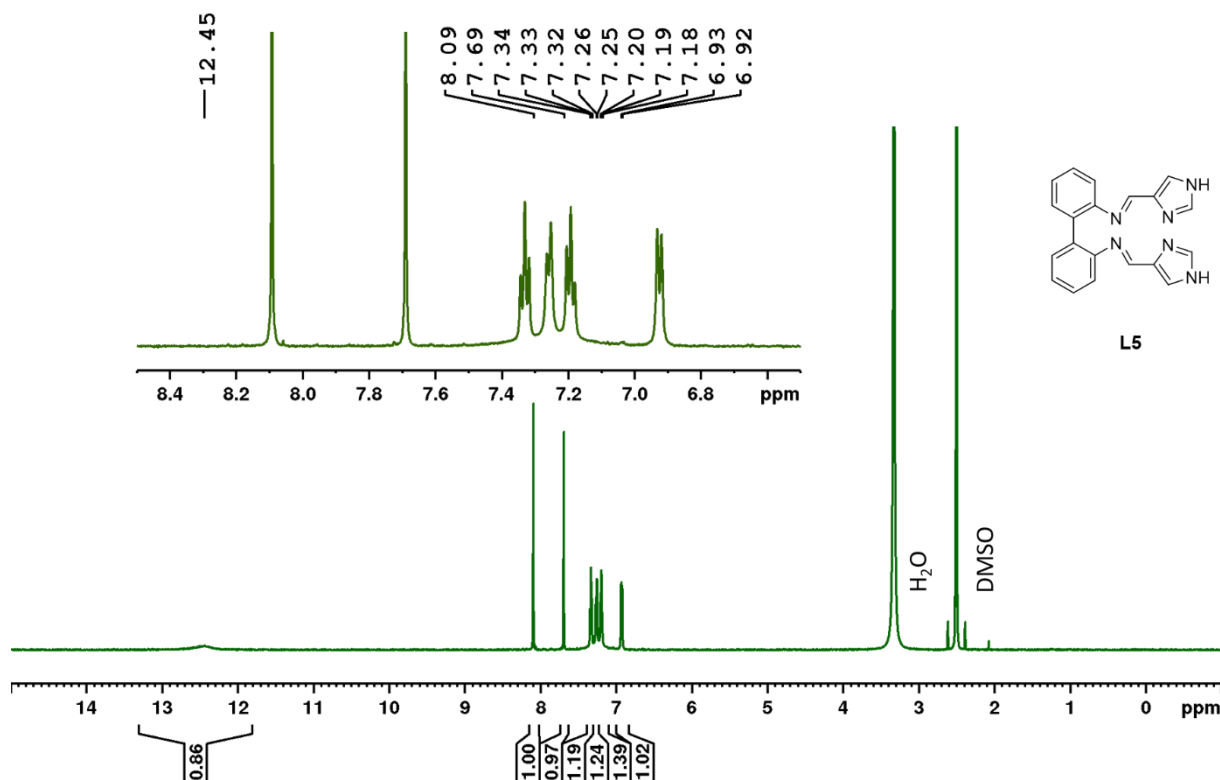
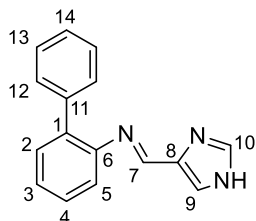


Figure S44. ^1H NMR (600 MHz, d_6 -DMSO) of **L5**.

L6

L6 was obtained from ligand synthesis procedure B as an off-white solid (34-41 % yield).



M.p. 189-190 °C (decomposes). ^1H NMR (600 MHz, d_6 -DMSO): δ 12.65 (*br*, 1H, s, NH), 8.39 (1H, s, H7), 7.77 (1H, s, H10), 7.57 (*br*, 1H, s, H9), 7.47-7.33 (6H, overlap of phenyl-H), 7.15-7.04 (6H, overlap of phenyl-H). $^{15}\text{N}\{^1\text{H}\}$ NMR (800 MHz, d_6 -DMSO): δ -65.0 (N_{imine}), -117.2 (N_{IM}), -209.6 (N_{AZ}). HRMS (ESI) m/z ($\text{C}_{16}\text{H}_{13}\text{N}_3 + \text{Na}^+$): Calcd: 270.1001 Found: 270.1002. Anal. Calcd: C, 77.71; H, 5.30; N, 16.99 Found: C, 77.25; H, 5.27; N, 16.91.

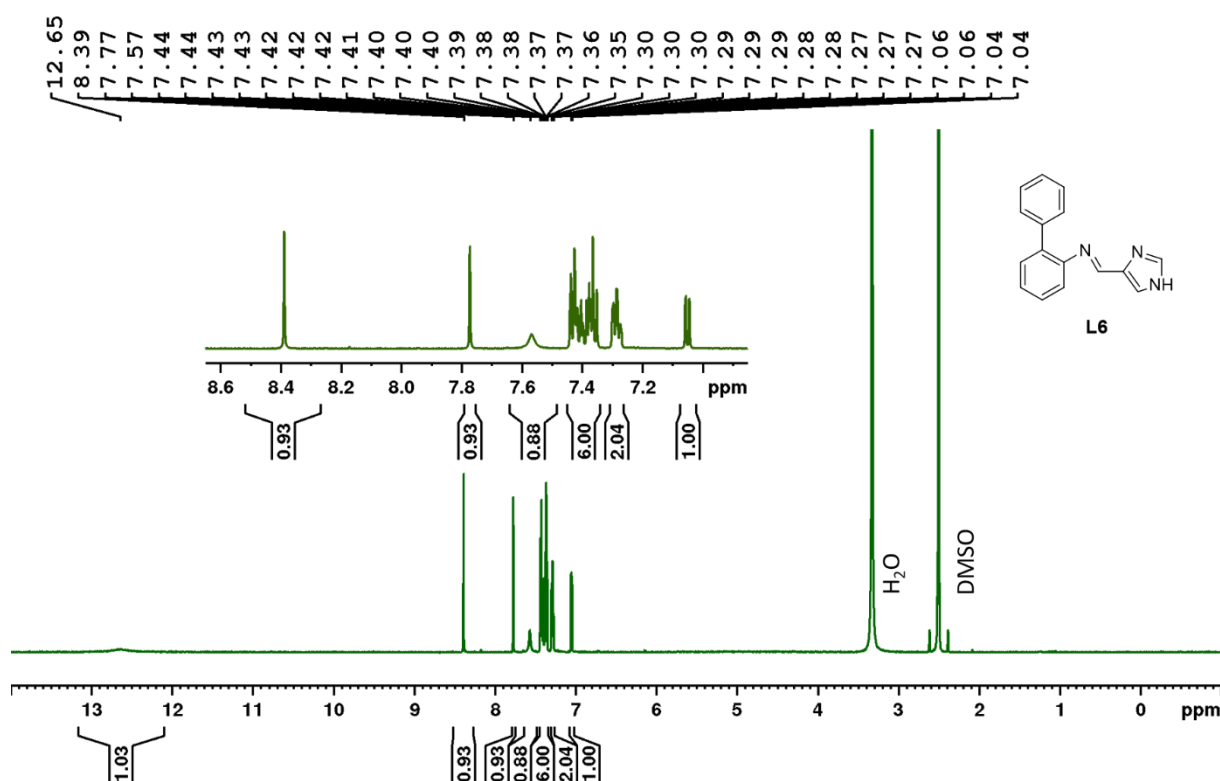


Figure S45. ^1H NMR (600 MHz, d_6 -DMSO) of **L6**.

^1H - ^{15}N HMBC

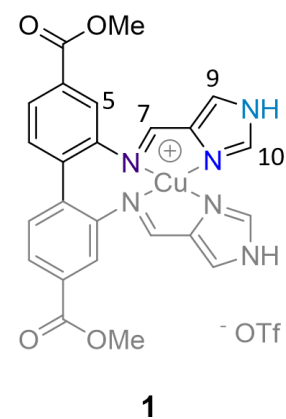
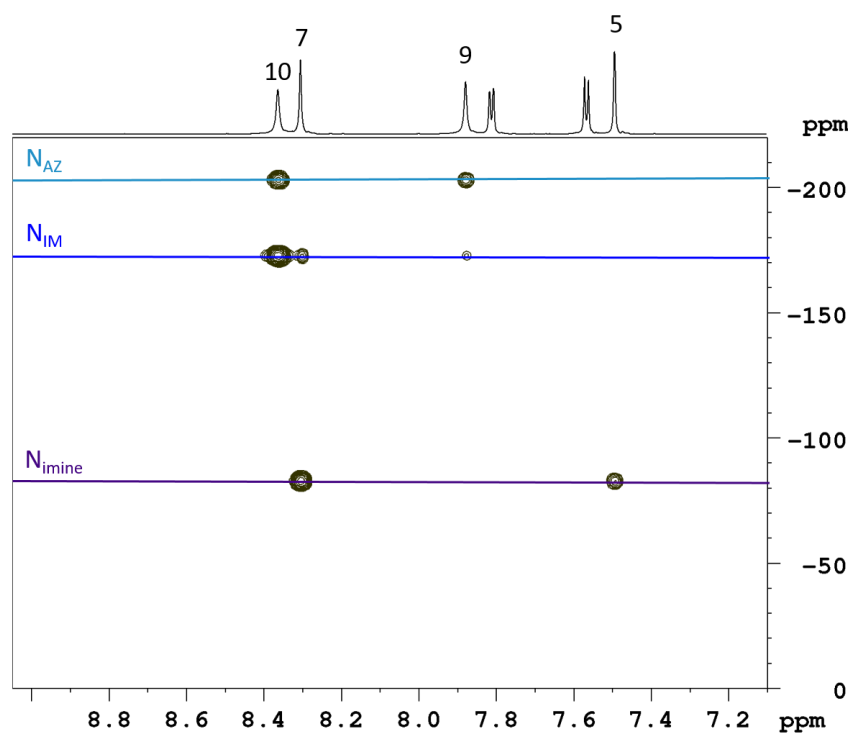


Figure S46. ^1H - ^{15}N HMBC (800 MHz, d_6 -DMSO) of **1**.

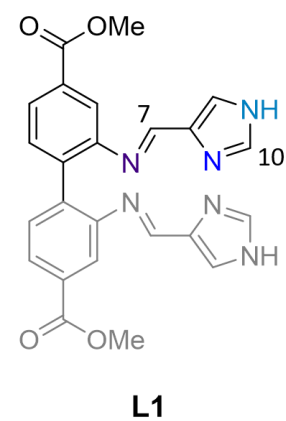
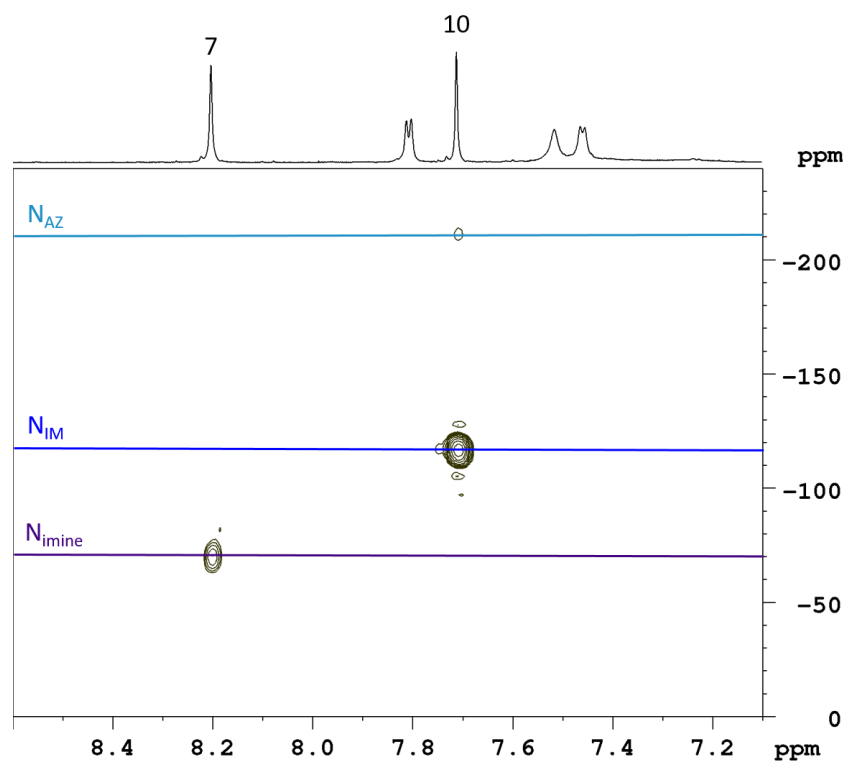


Figure S47. ^1H - ^{15}N HMBC (800 MHz, d_6 -DMSO) of **L1**.

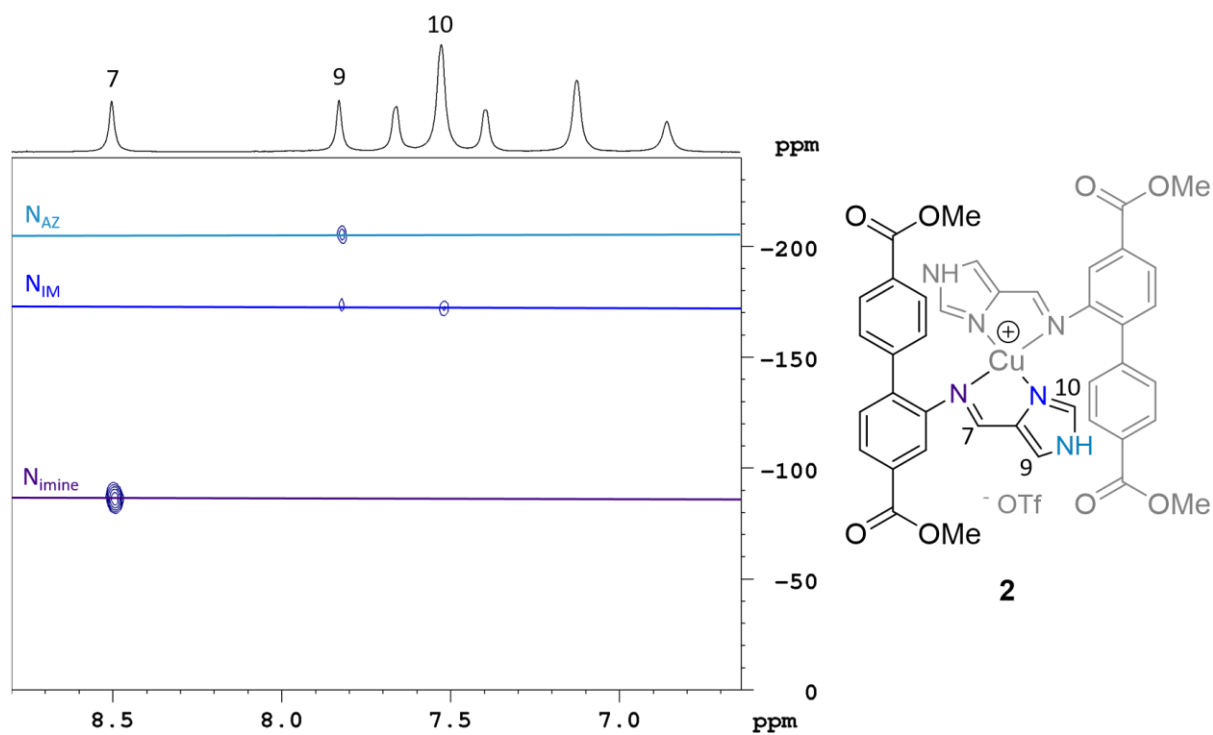


Figure S48. ^1H - ^{15}N HMBC (800 MHz, d_6 -DMSO) of **2**.

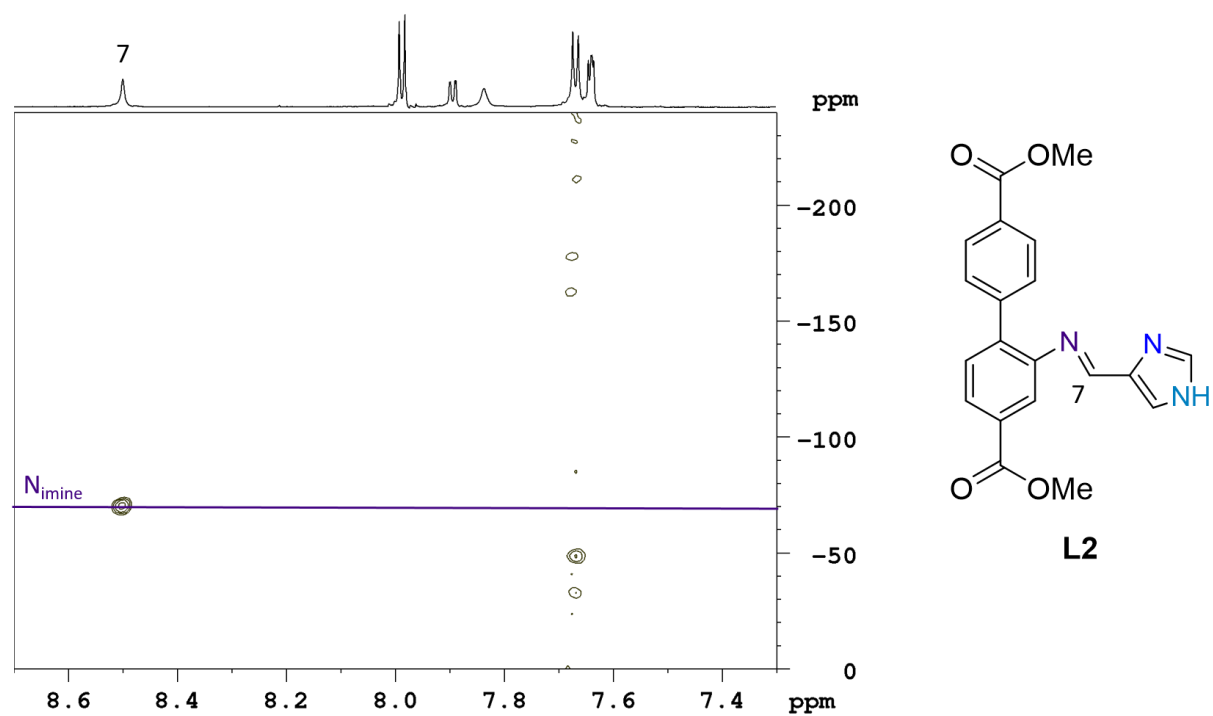


Figure S49. ^1H - ^{15}N HMBC (800 MHz, d_6 -DMSO) of **L2** (~0.5 mg of sample).

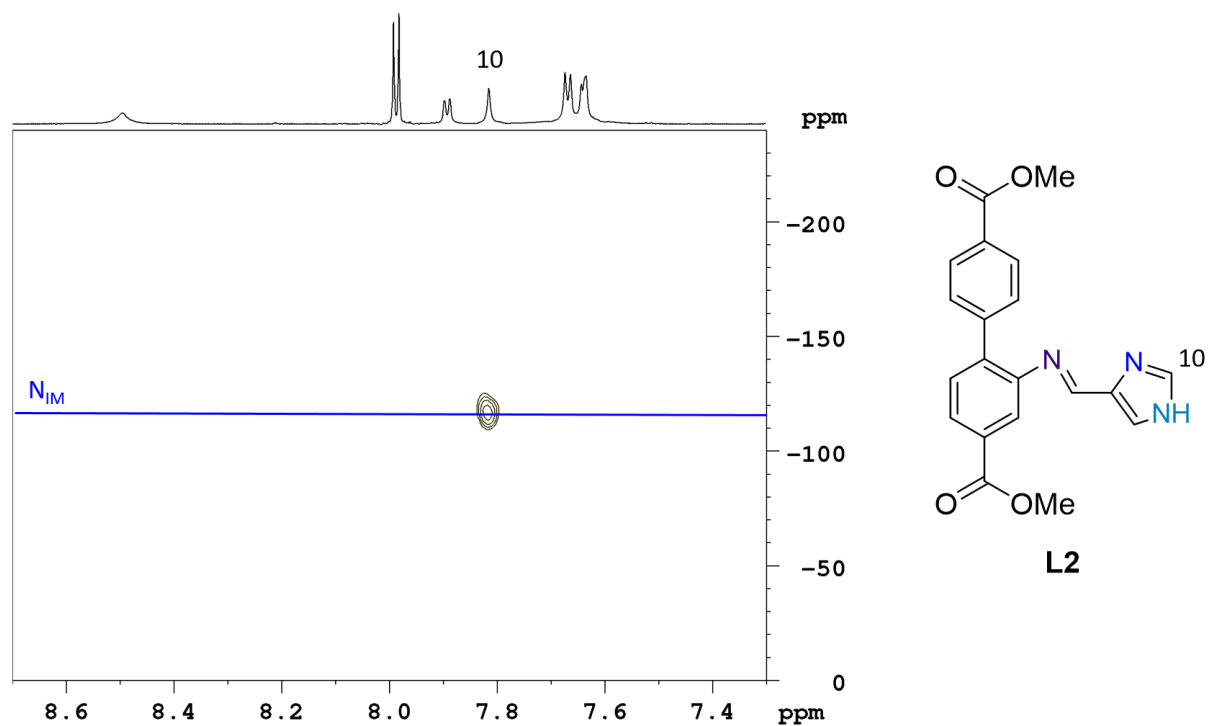


Figure S50. ^1H - ^{15}N HMBC (800 MHz, d_6 -DMSO) of L2 (~1 mg of sample).

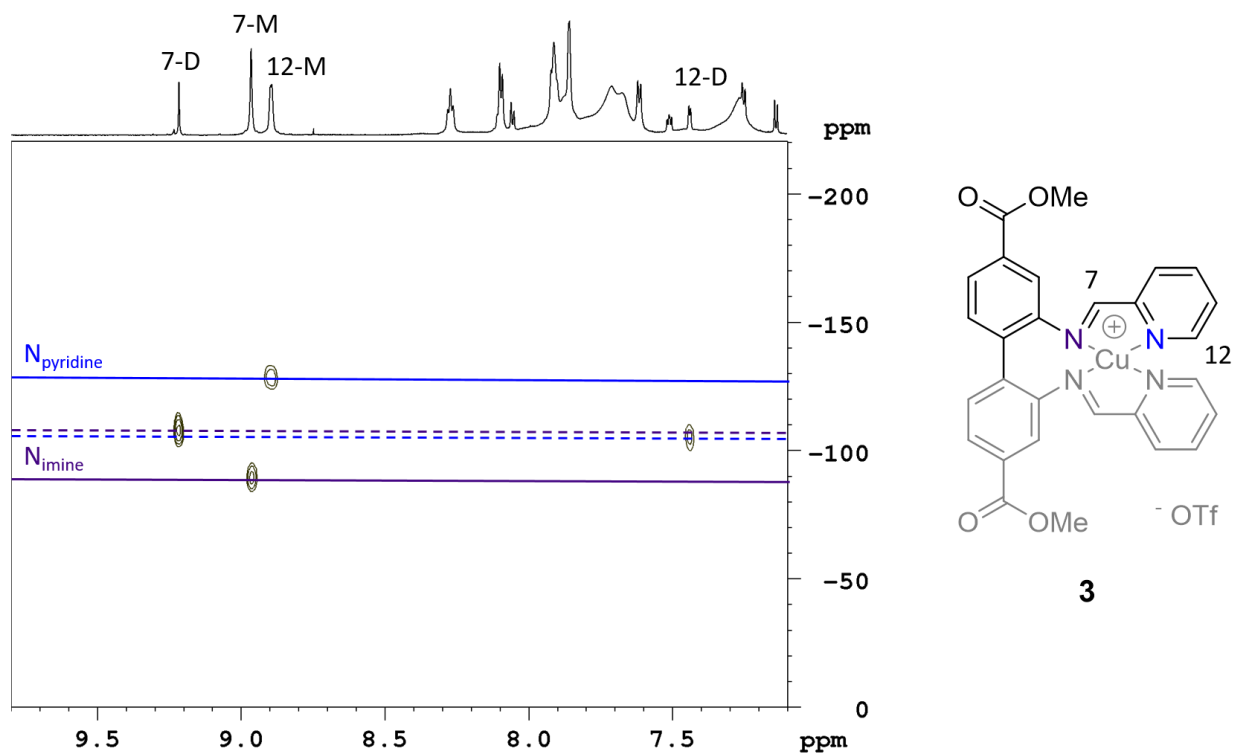


Figure S51. ^1H - ^{15}N HMBC (800 MHz, d_6 -DMSO) of **3**. Solid lines designate the ^{15}N shifts belonging to **3-M**, while dotted lines designate the ^{15}N shifts of **3-D**.

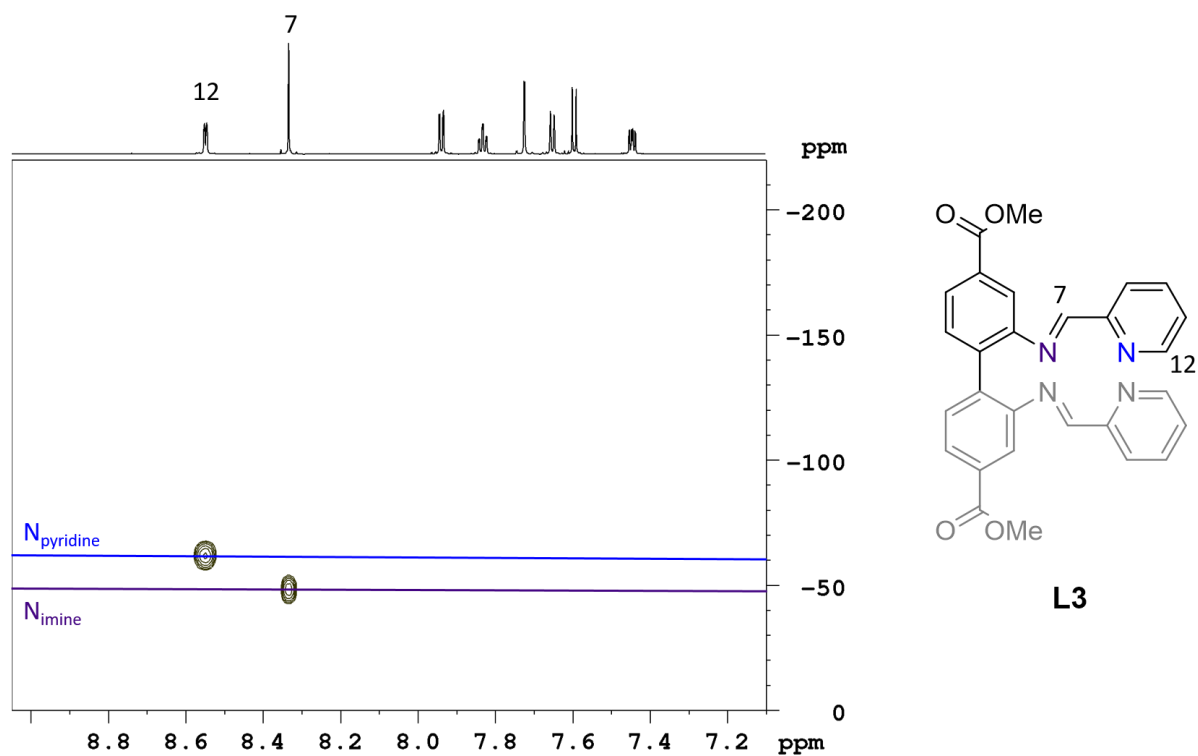


Figure S52. ^1H - ^{15}N HMBC (800 MHz, d_6 -DMSO) of **L3**.

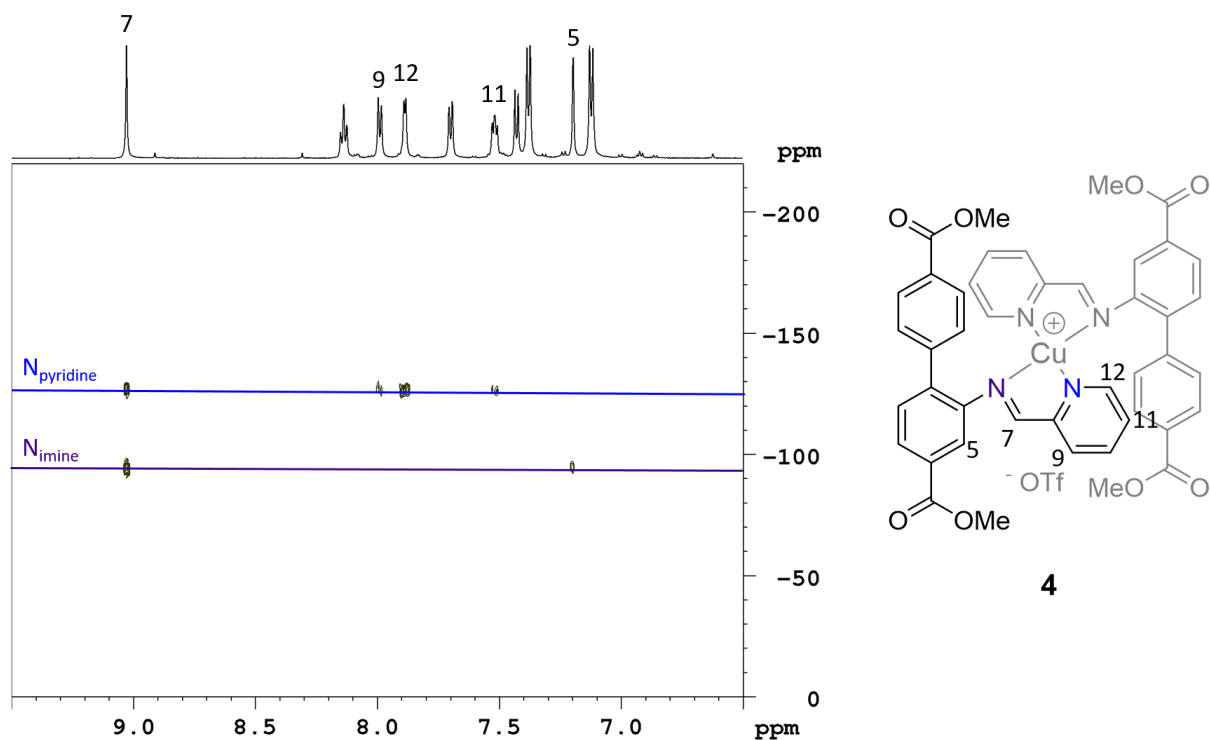


Figure S53. ^1H - ^{15}N HMBC (600 MHz, d_6 -DMSO) of **4**.

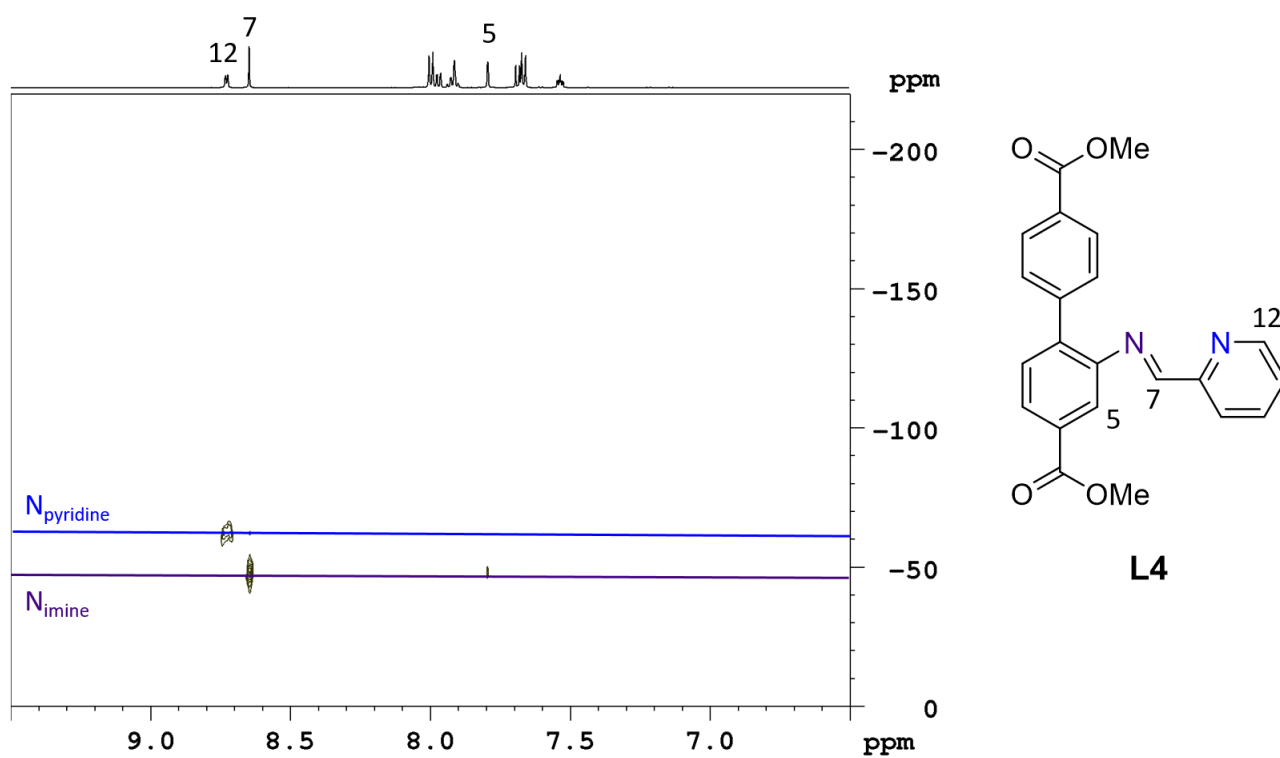


Figure S54. ^1H - ^{15}N HMBC (600 MHz, d_6 -DMSO) of **L4**.

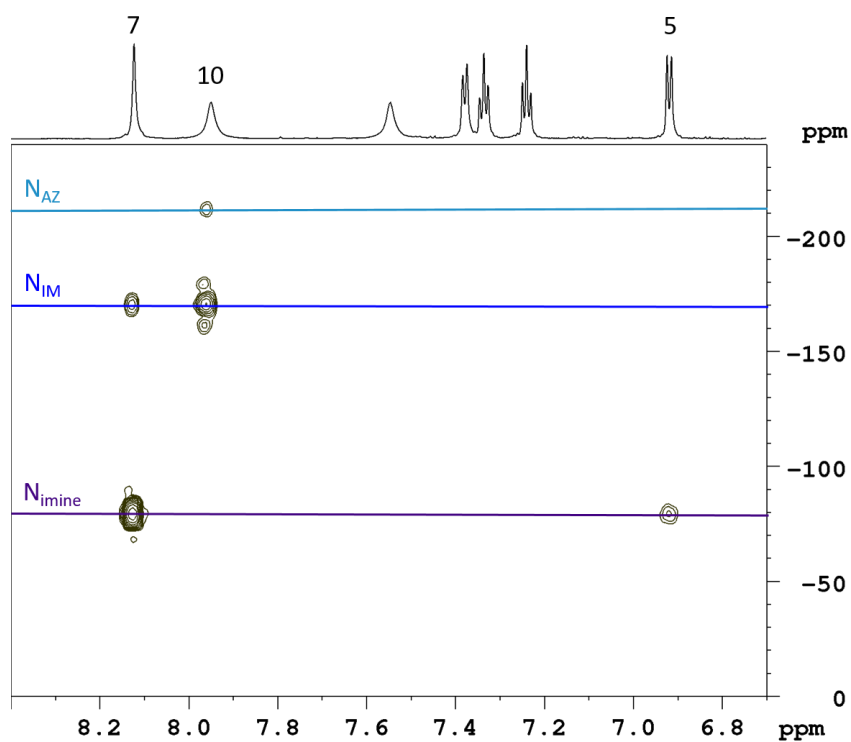


Figure S55. ^1H - ^{15}N HMBC (800 MHz, CD_3CN) of **5**.

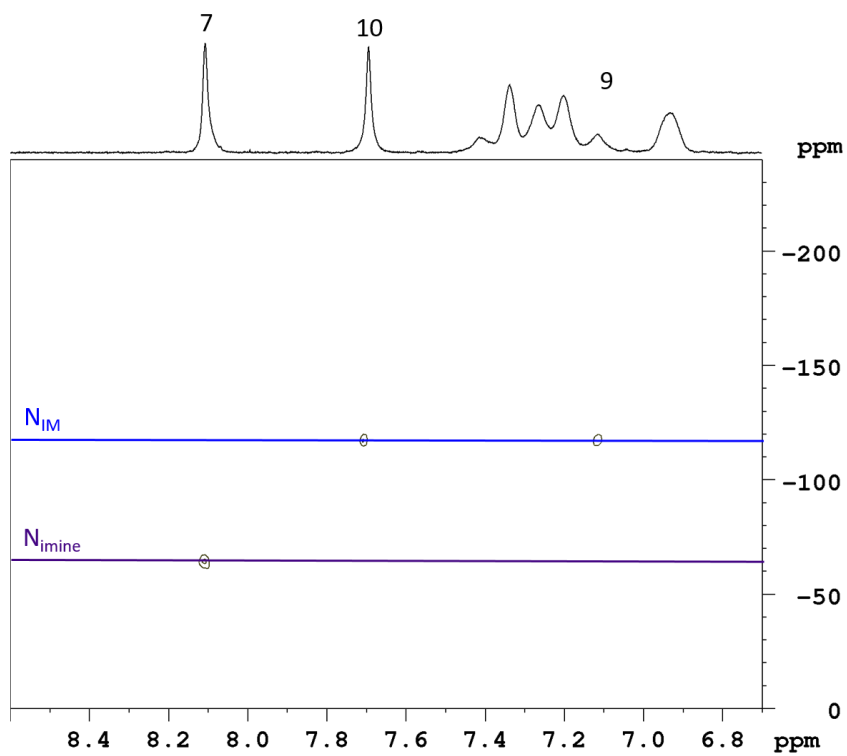
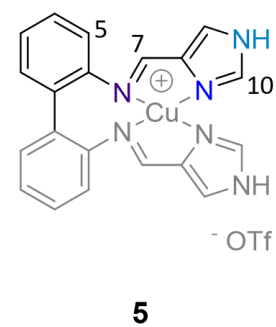
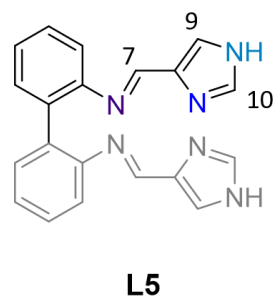


Figure S56. ^1H - ^{15}N HMBC (800 MHz, d_6 -DMSO) of **L5**.



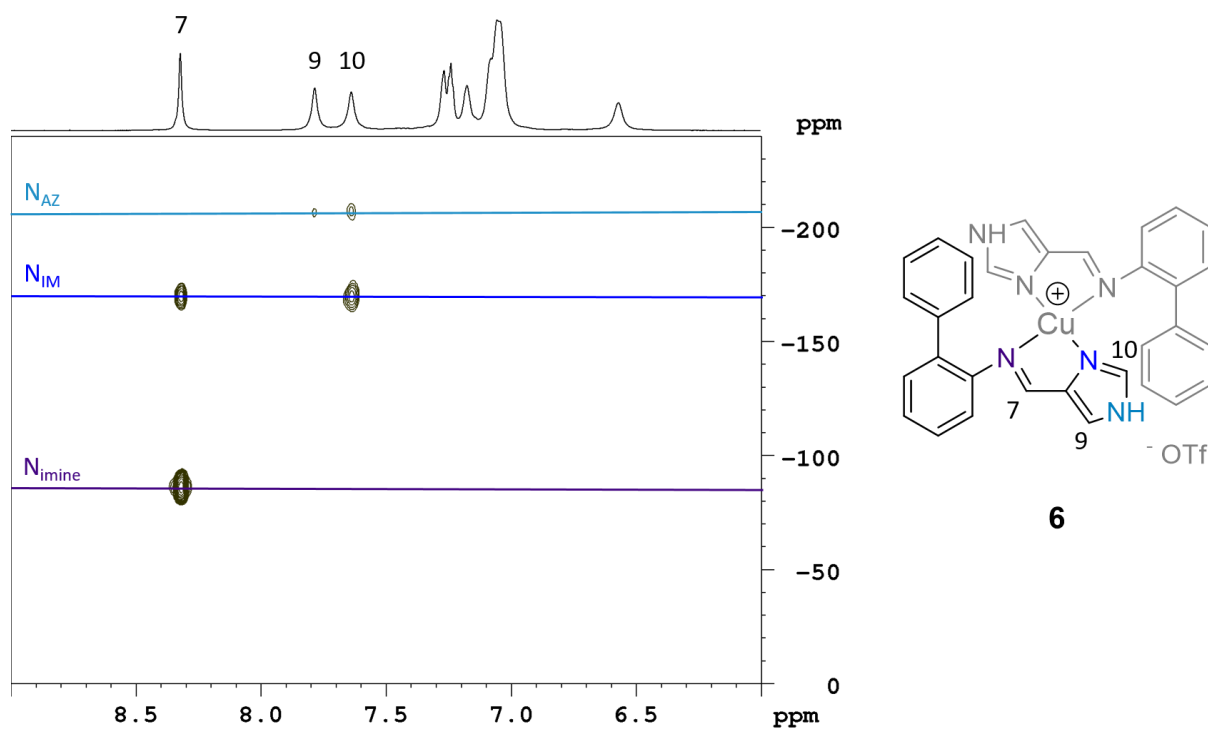


Figure S57. ^1H - ^{15}N HMBC (800 MHz, d_6 -DMSO) of **6**.

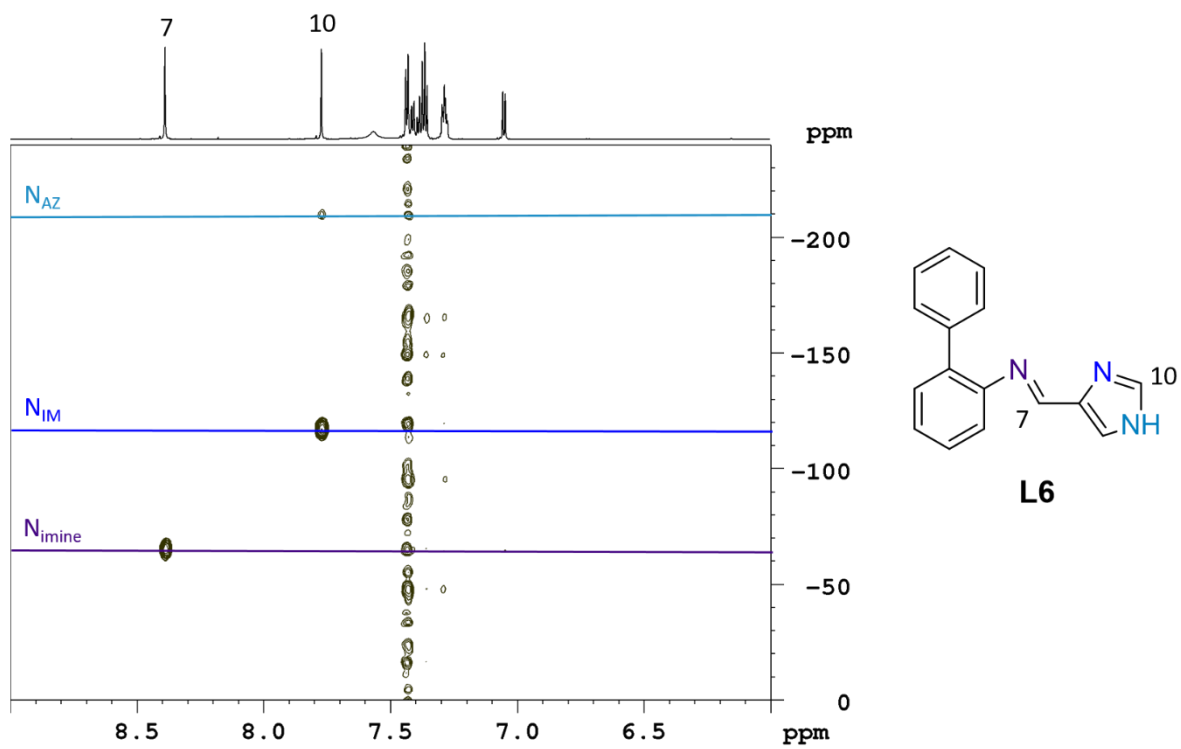


Figure S58. ^1H - ^{15}N HMBC (800 MHz, d_6 -DMSO) of **L6**.

Variable Temperature NMR Experiments

All variable temperature NMR experiments were measured on a Bruker DRX500 instrument. The reversibility of the observed processes was assessed by comparison of the room temperature spectrum (black spectrum) before and after the temperature experiments (grey spectrum on top). The temperature of the variable temperature NMR experiments was measured indirectly by correction of the displayed probe temperature to independently measured temperatures (or extrapolated temperatures for the temperatures above the boiling point of methanol) using a Delta OHM HD9214 thermometer fitted into a NMR tube containing CD₃OD/CH₃OH. Because of this, small deviations from the exact temperature cannot be excluded.

Compound 1

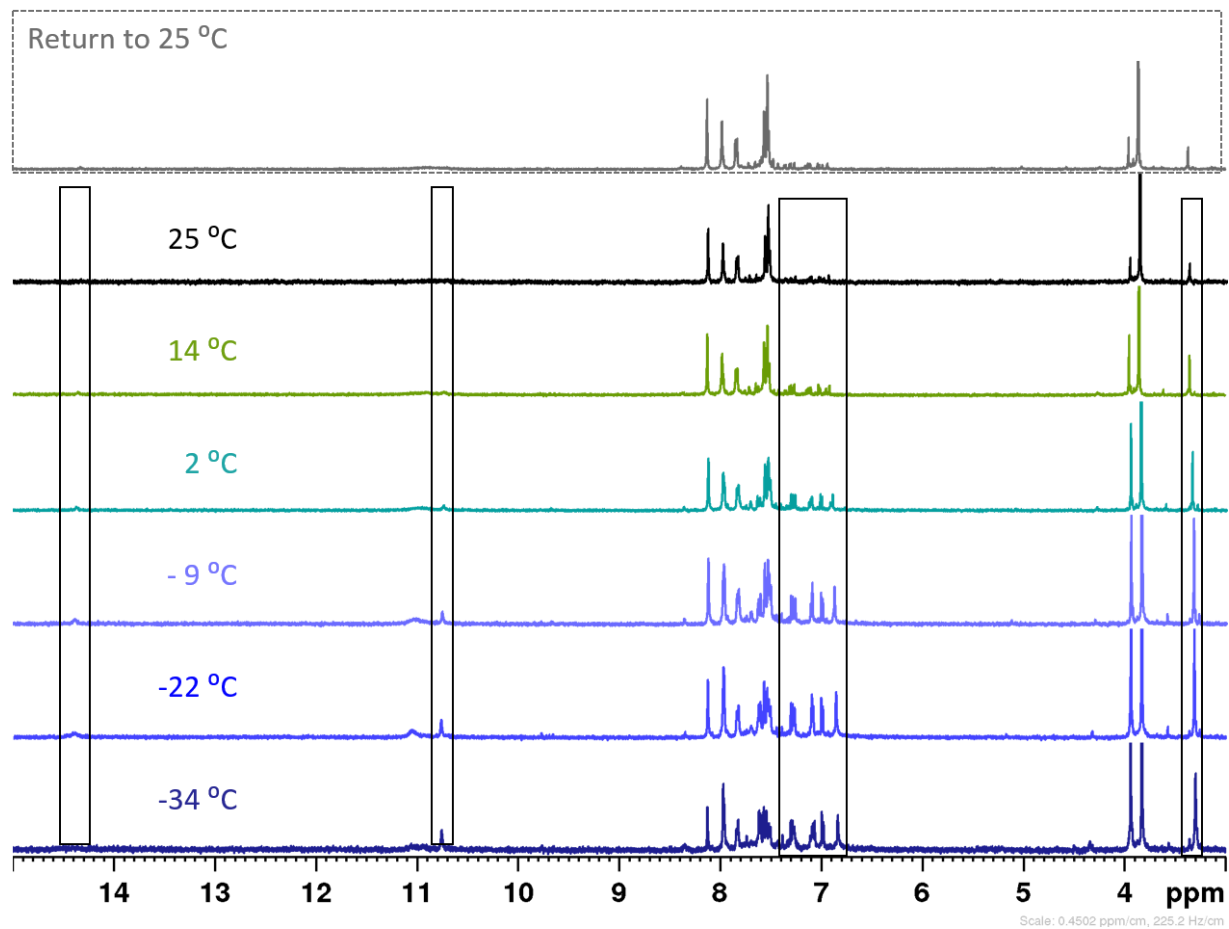


Figure S59. ¹H NMR (CD₃CN, 500 MHz) spectra of **1** at different temperatures. Boxes highlight the minor species rising at lower temperatures.

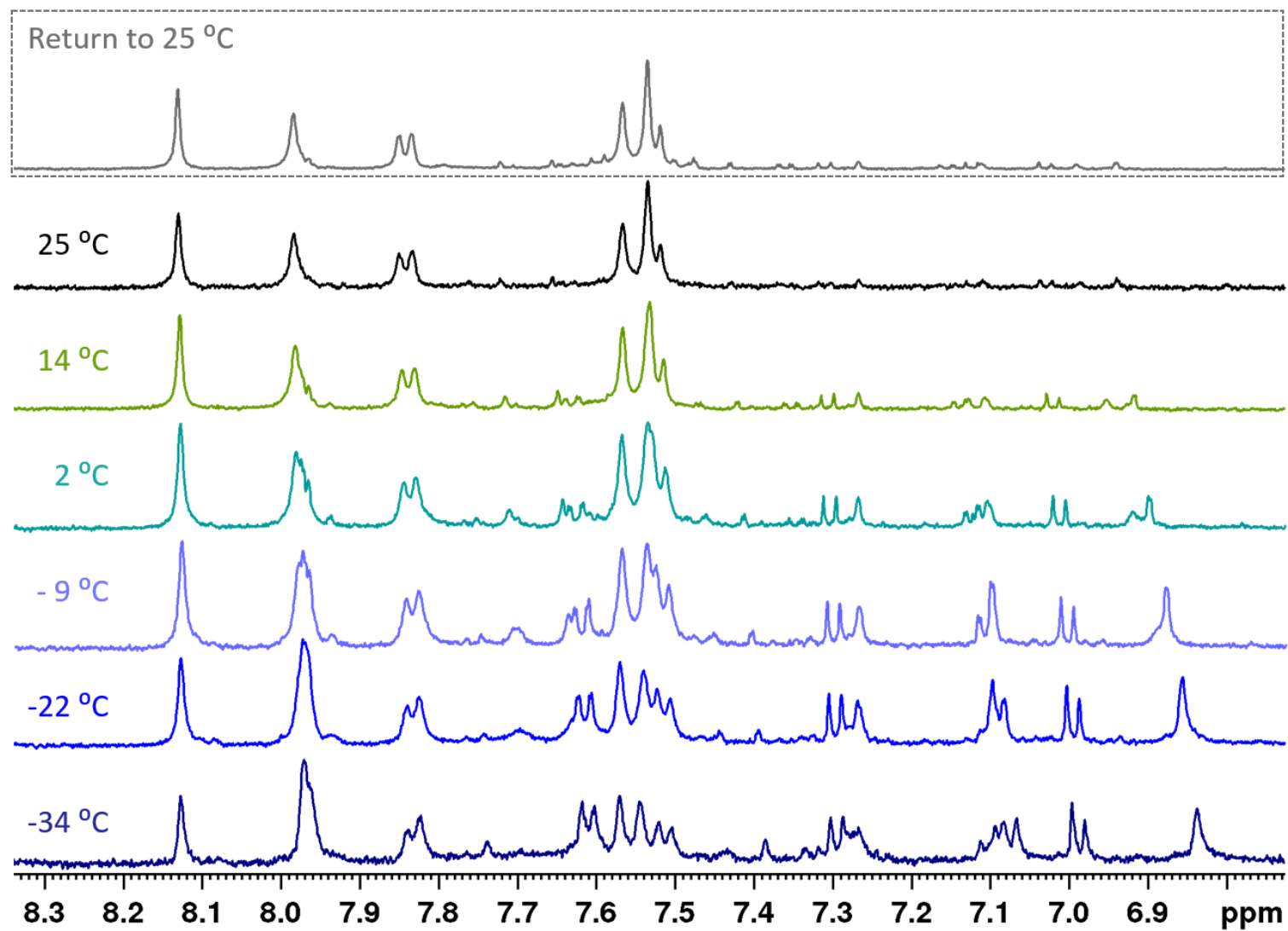


Figure S60. Aromatic region of the ¹H NMR (CD₃CN, 500 MHz) spectra of **1** at different temperatures.

Compound 3

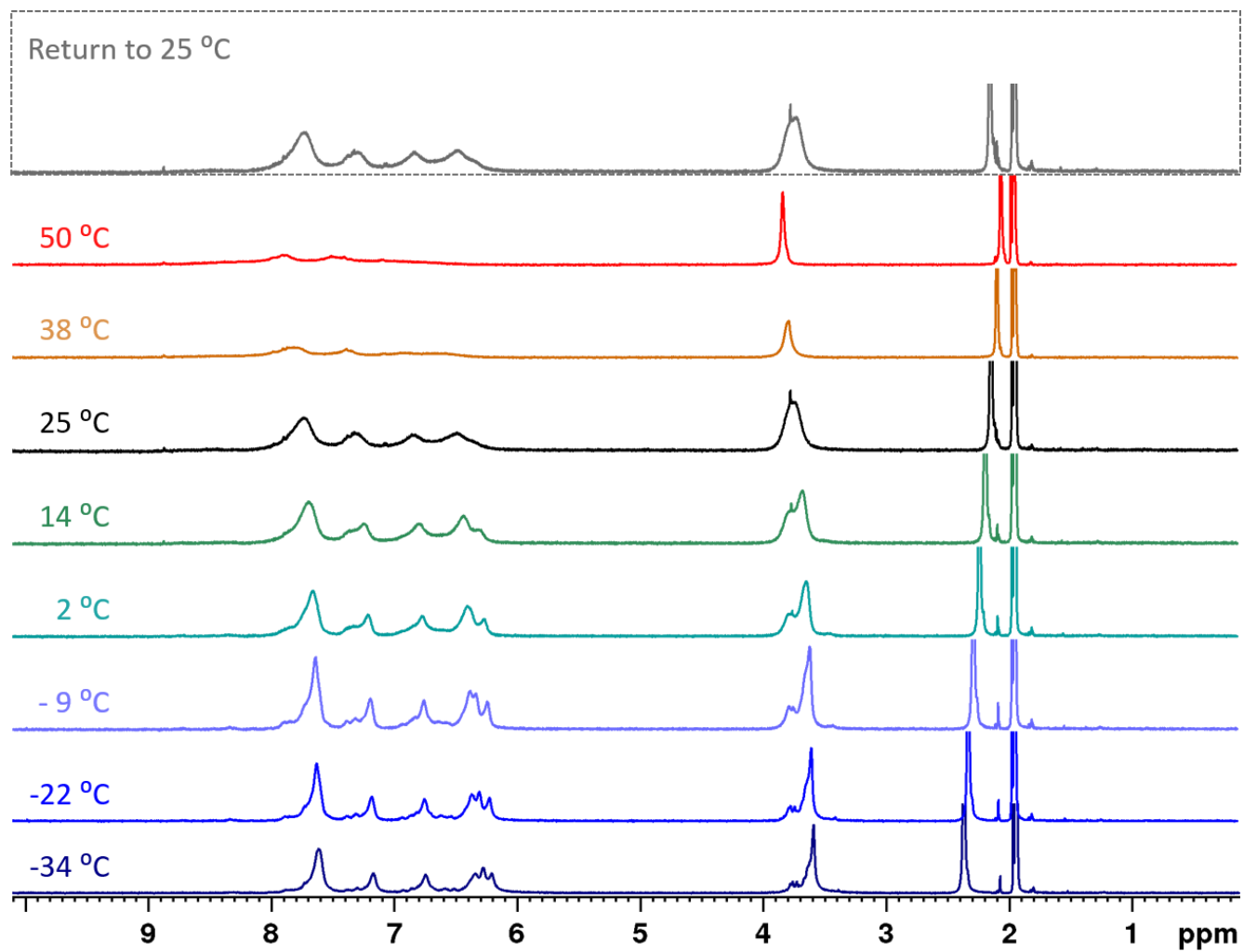


Figure S61. ¹H NMR (CD₃CN, 500 MHz) spectra of **3** at different temperatures.

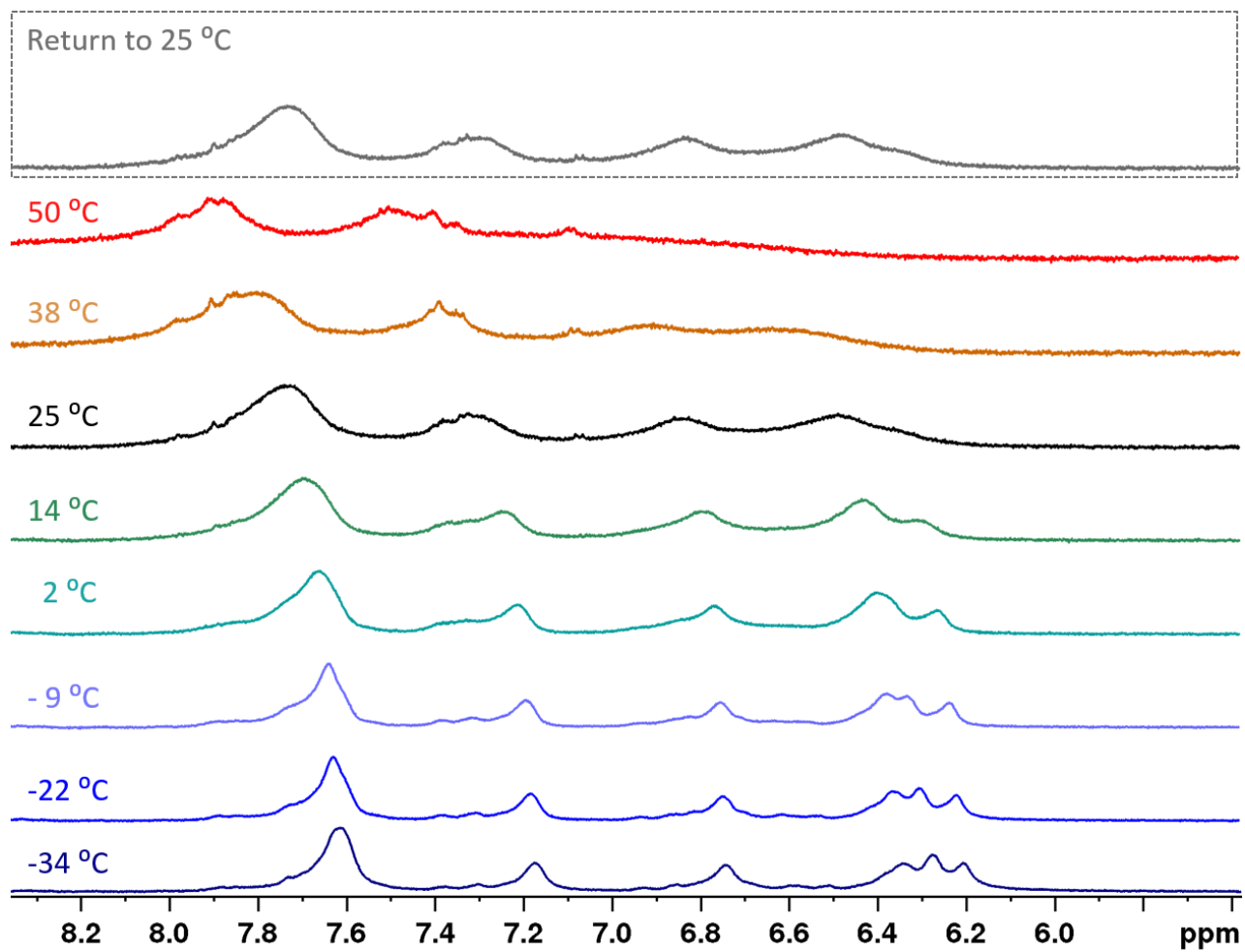


Figure S62. Aromatic region of the ^1H NMR (CD_3CN , 500 MHz) spectra of **3** at different temperatures. The peaks merge into the baseline at higher temperatures.

Compound 5

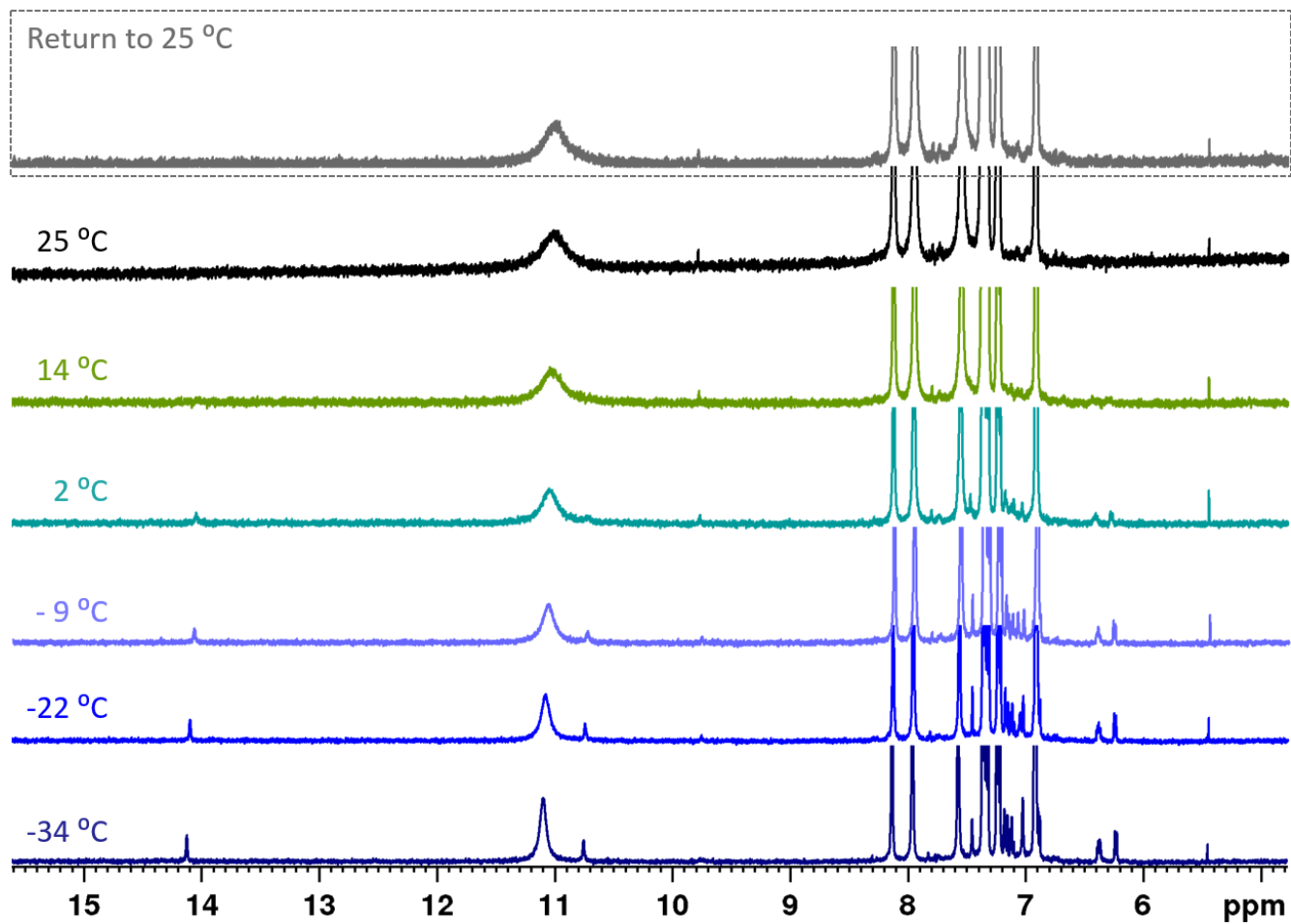


Figure S63. ¹H NMR (CD₃CN, 500 MHz) spectra of 5 at different temperatures.

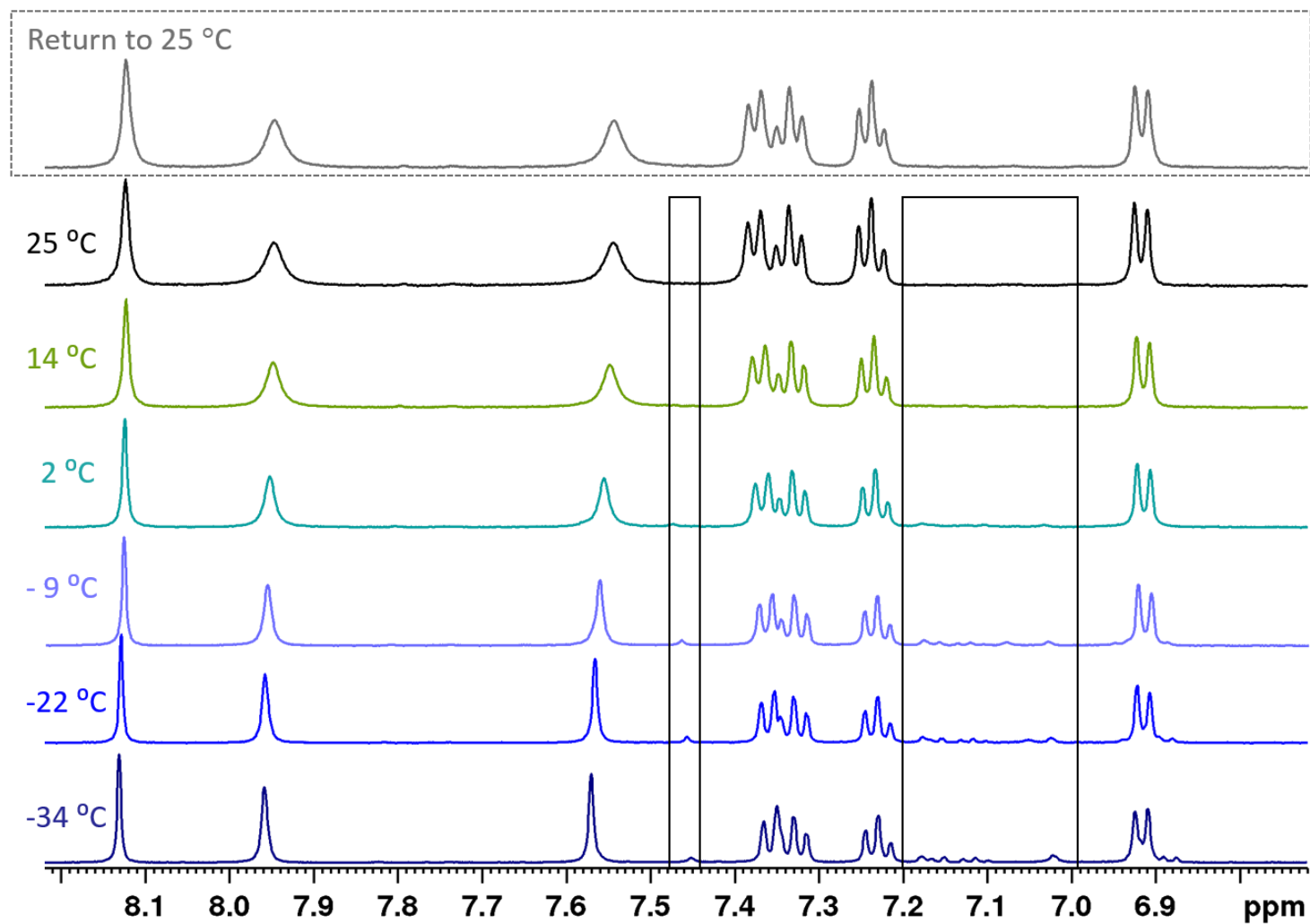


Figure S64. Aromatic region of the ¹H NMR (CD₃CN, 500 MHz) spectra of **5** at different temperatures. Boxes highlight the minor species rising at lower temperatures.

Decomposition During Longer NMR Experiments

We observed that complexes with considerable line broadening decomposed during NMR analysis. A sealed NMR sample of **1** remained unchanged even after months, while **2**, **4**, **5**, and **6** partially showed traces of the starting materials during NMR experiments longer than a day. A juxtaposition of the ^1H NMR spectra of the complexes after prolonged NMR experiments and the amines they were synthesized from shows good agreement between the decomposition peaks and the amine for all four complexes (Figure S65). In combination with the simultaneous rise of an aldehyde peak, it is evident that the decomposition can be attributed to hydrolysis of the imine bond. The hydrolysis of the complexes could have been prevented by use of dry NMR solvents. However, the stability of the complexes was of interest and the decomposition was minor enough to not impede full NMR characterisation.

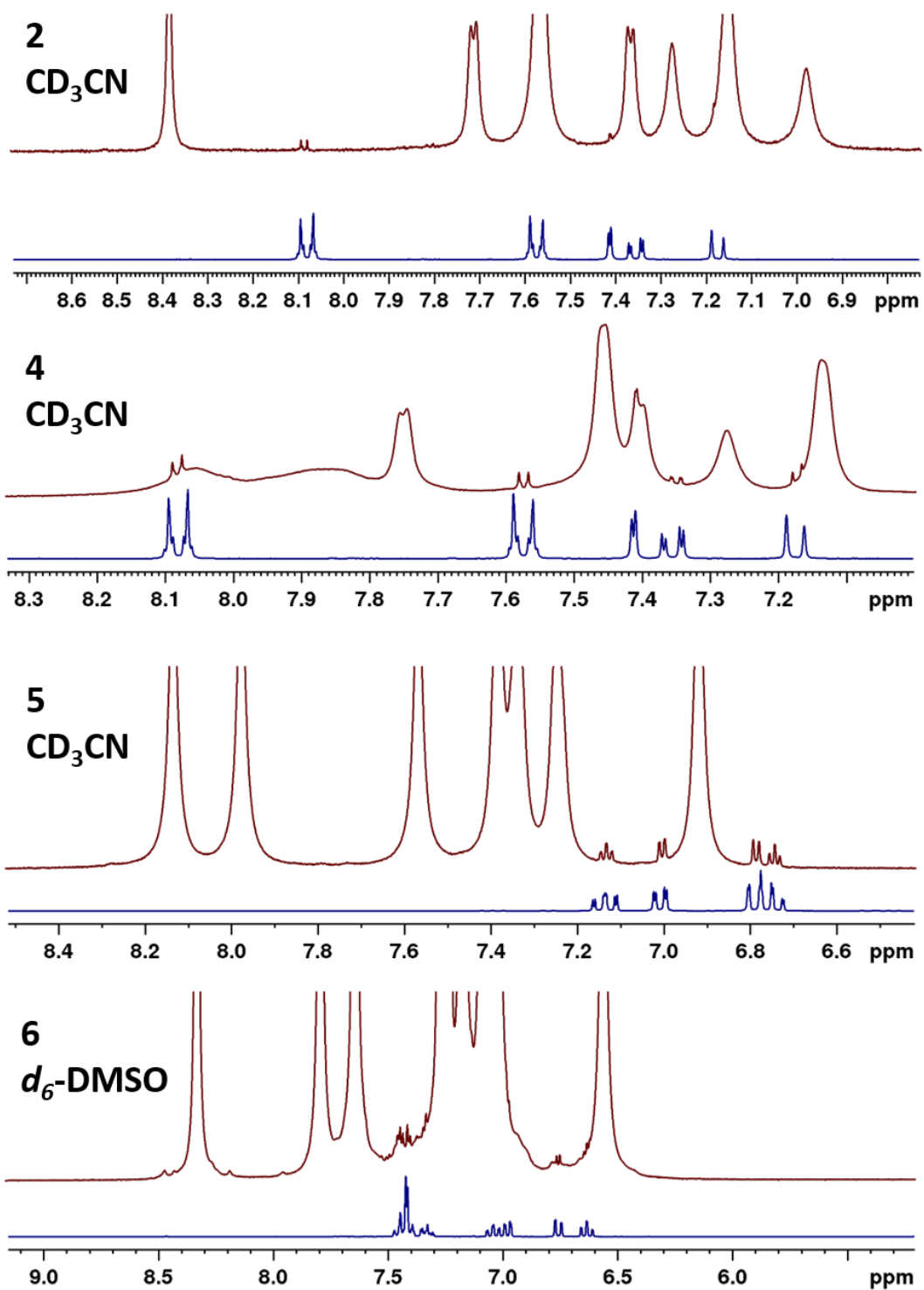


Figure S65. ^1H NMR (600 MHz) spectra of compounds **2**, **4**, **5** and **6** after full NMR analysis (ca. 1 $\frac{1}{2}$ days, in brown) stacked over the spectrum of the amine they were synthesized from (in blue). The decomposition can therefore be attributed to hydrolysis of the imine.

Reduction of complex **1b** with ascorbic acid to form complex **1**

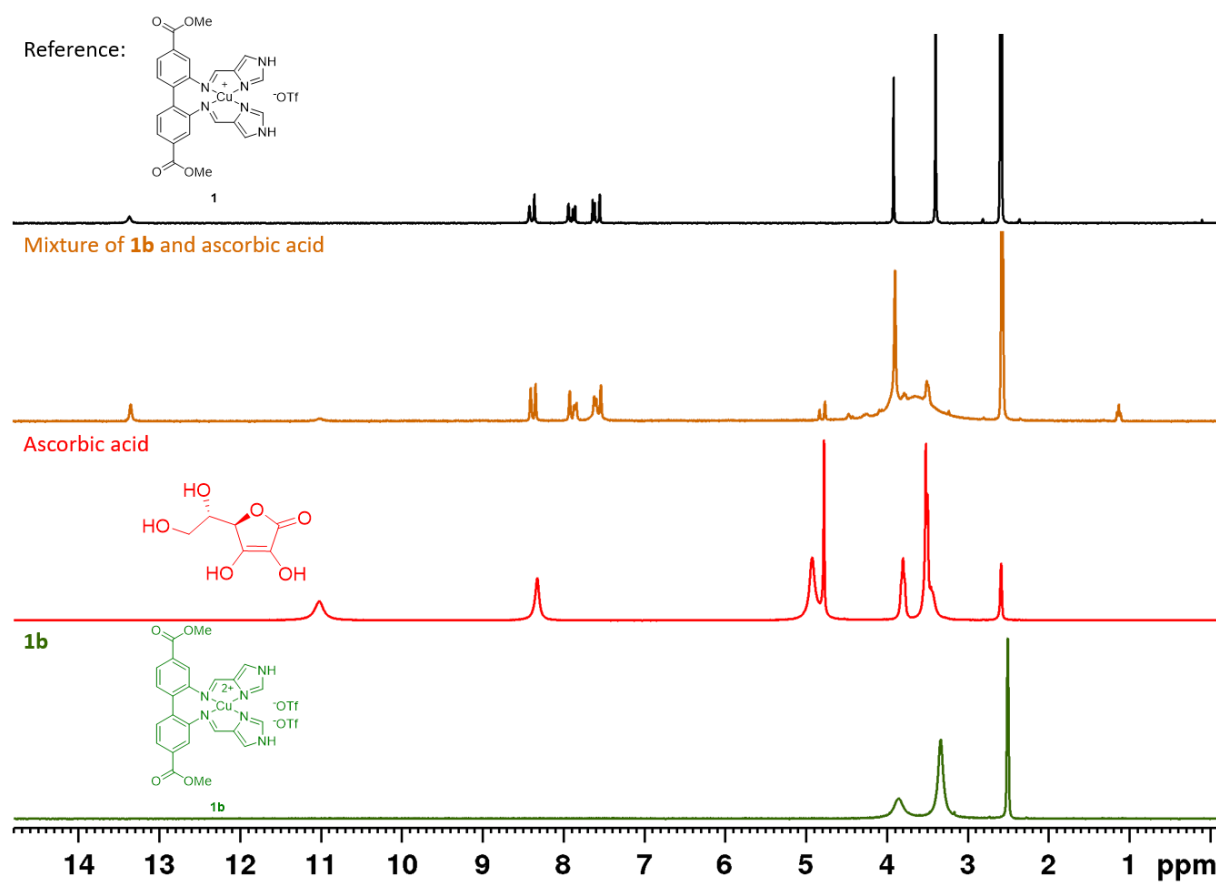
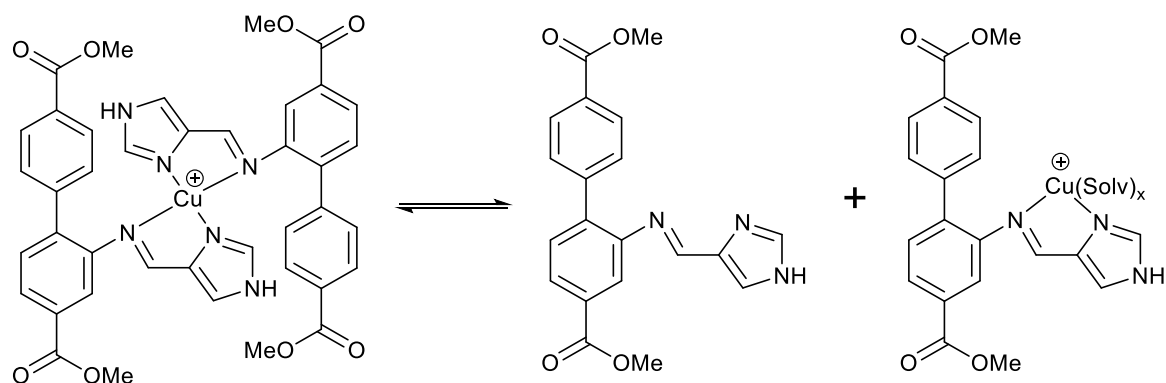


Figure S66. NMR experiment (d_6 -DMSO, 300 MHz) showing the relation between complex **1b** and complex **1**. A solution of complex **1b** (green solution, bottom spectrum) was mixed with an ascorbic acid solution (colorless solution, 2nd spectrum from the bottom), giving rise to sharp peaks and causing a color change (yellow solution, 3rd spectrum from the bottom). The newly formed peaks are in good agreement with the peaks observed for the corresponding copper(I) complex **1** (top spectrum).

Ligand exchange NMR experiments

It is likely that the ML_2 complexes are in equilibrium with the corresponding ML complex and the free ligand. This is exemplified in Scheme S1 for complex **2**.



Scheme S1. Equilibrium of ML_2 complex **2** with the free ligand and the resulting ML complex.

The ML complex might have x solvent molecules as additional ligand(s).

In order to probe if ligands can exchange from one complex to the other, a mixture of **2** and **4** was measured in d_6 -DMSO. The mixture showed peaks that could not be attributed to either species or the free ligands. The spectral appearance of the mixture did not change from the first measurement (ca. 5 min after mixing) to the last measurement (next day).

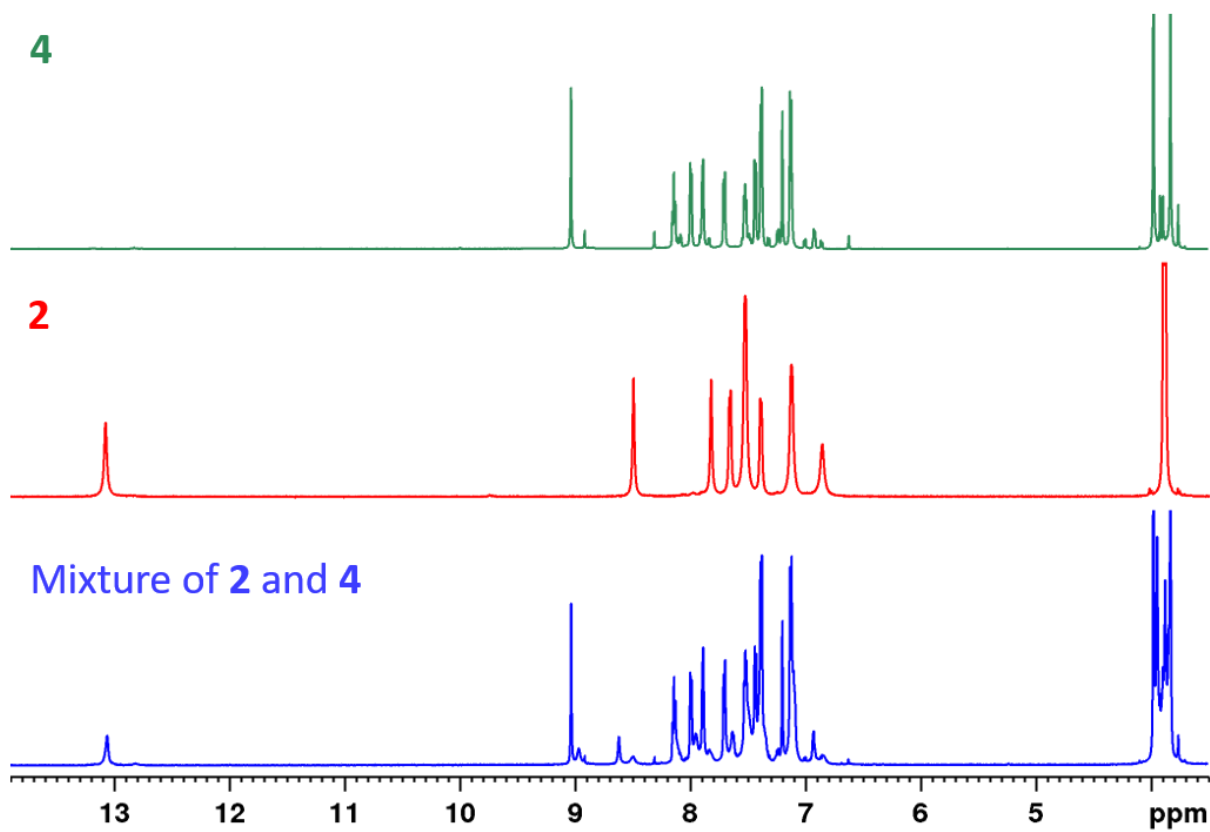


Figure S67. Overlay of the ^1H NMR (d_6 -DMSO, 600 MHz) spectra of complexes **2** (middle) and **4** (top) and a mixture of both (bottom).

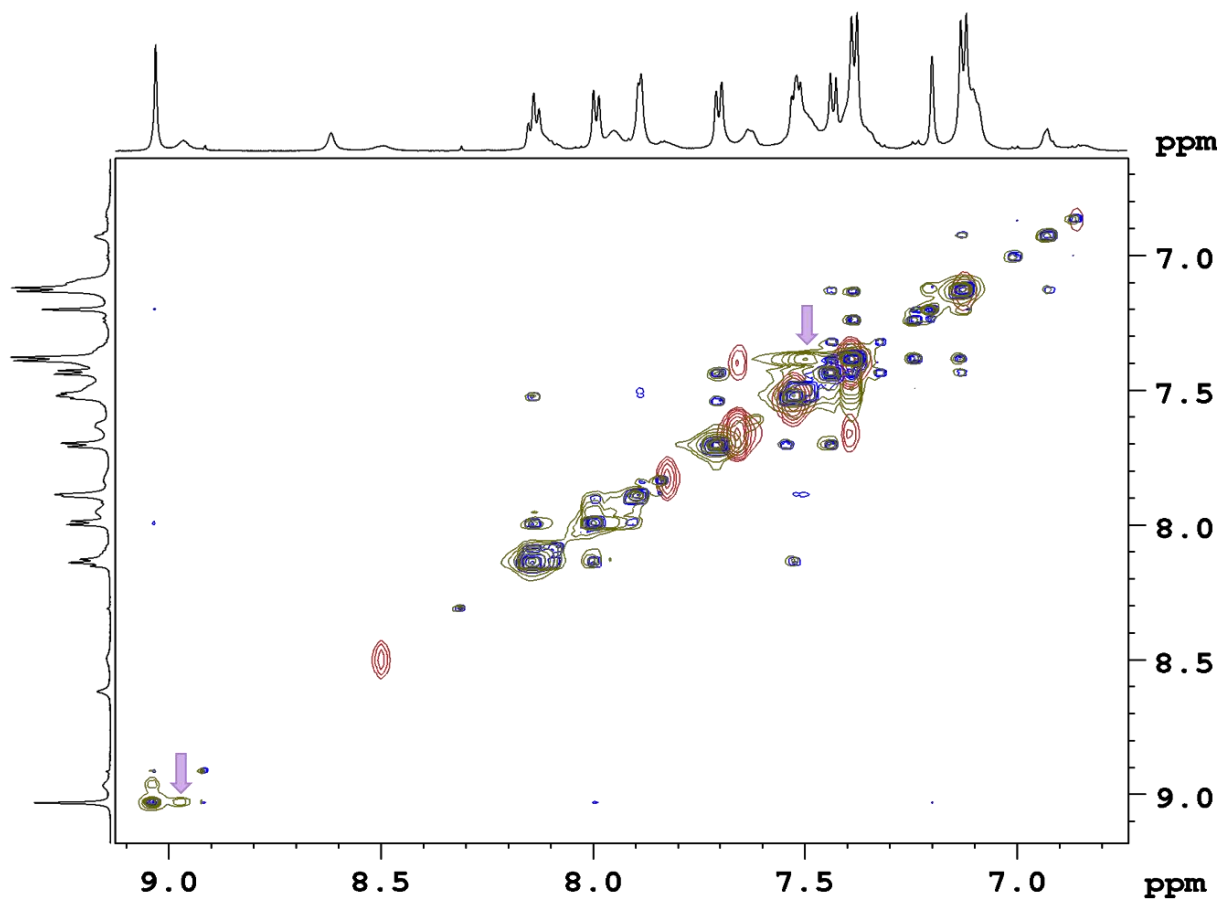


Figure S68. Overlay of the NOESY/EXSY (d_6 -DMSO, 600 MHz) spectra of complexes **2** (red) and **4** (blue) and a mixture of both (dark green). Two of the peaks that stem from neither complex and are only observed in the mixture are highlighted with a lavender arrow.

Diffusion Ordered Spectroscopy (DOSY)

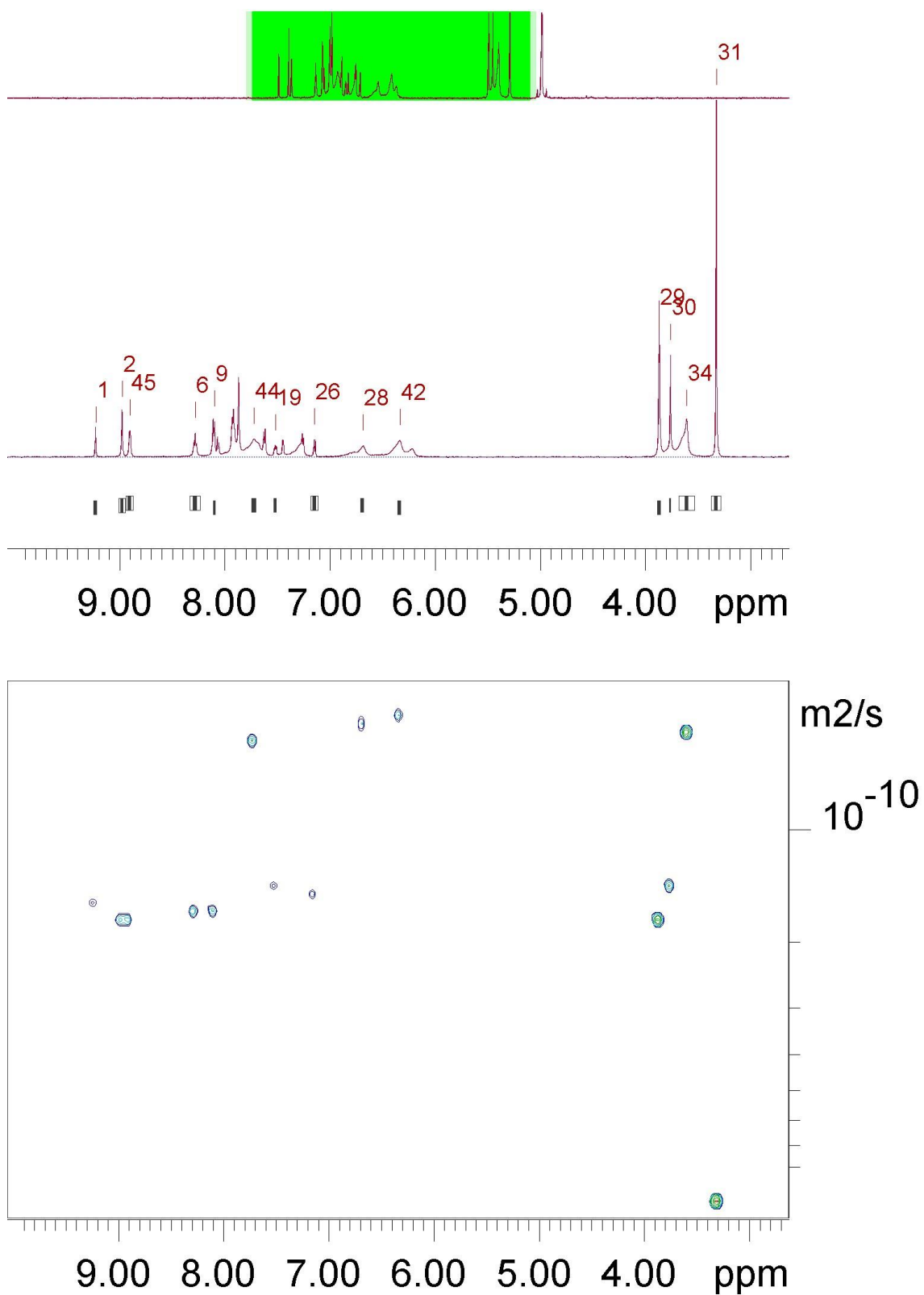


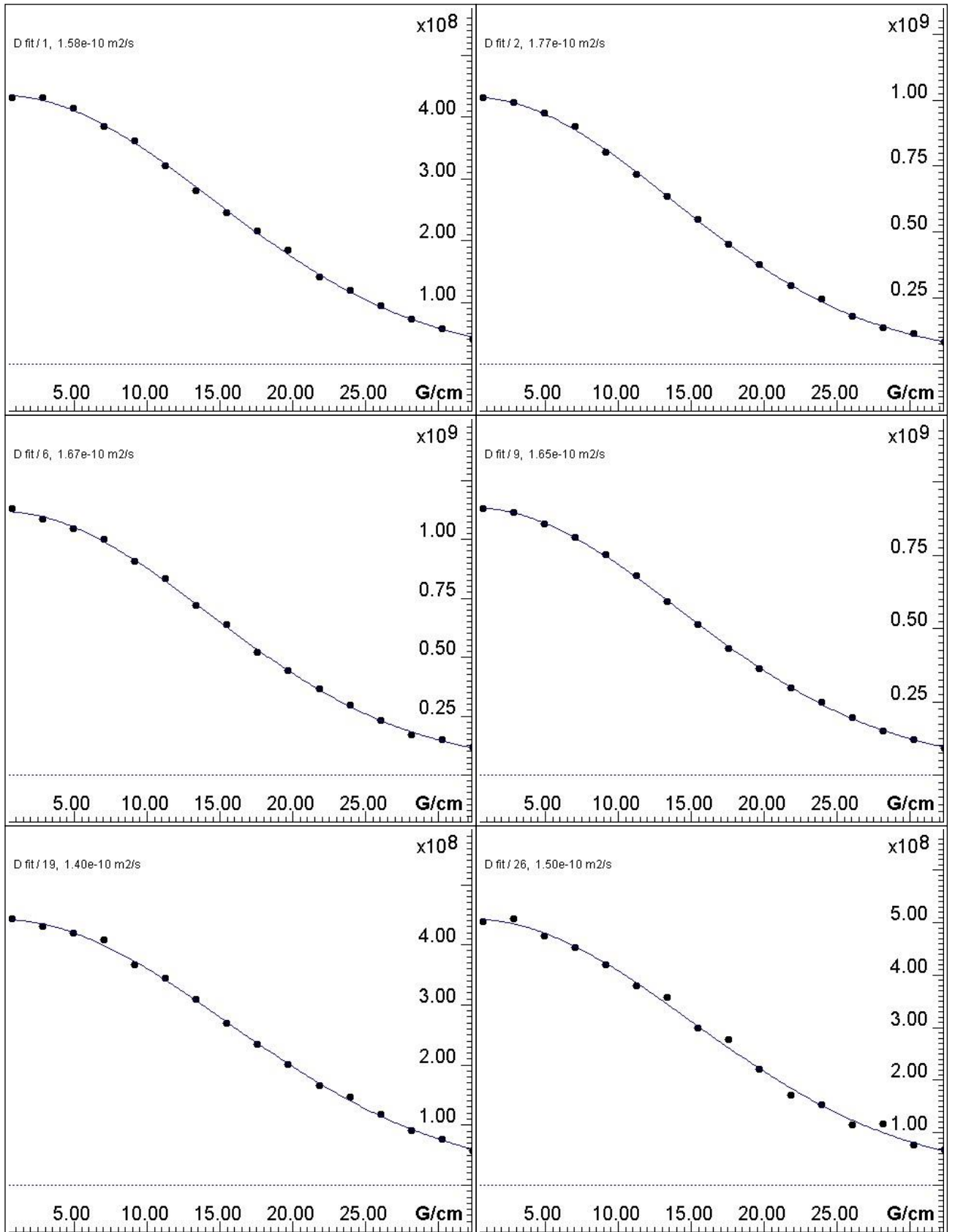
Figure S69. User-defined integration areas to calculate the DOSY spectrum of 3.

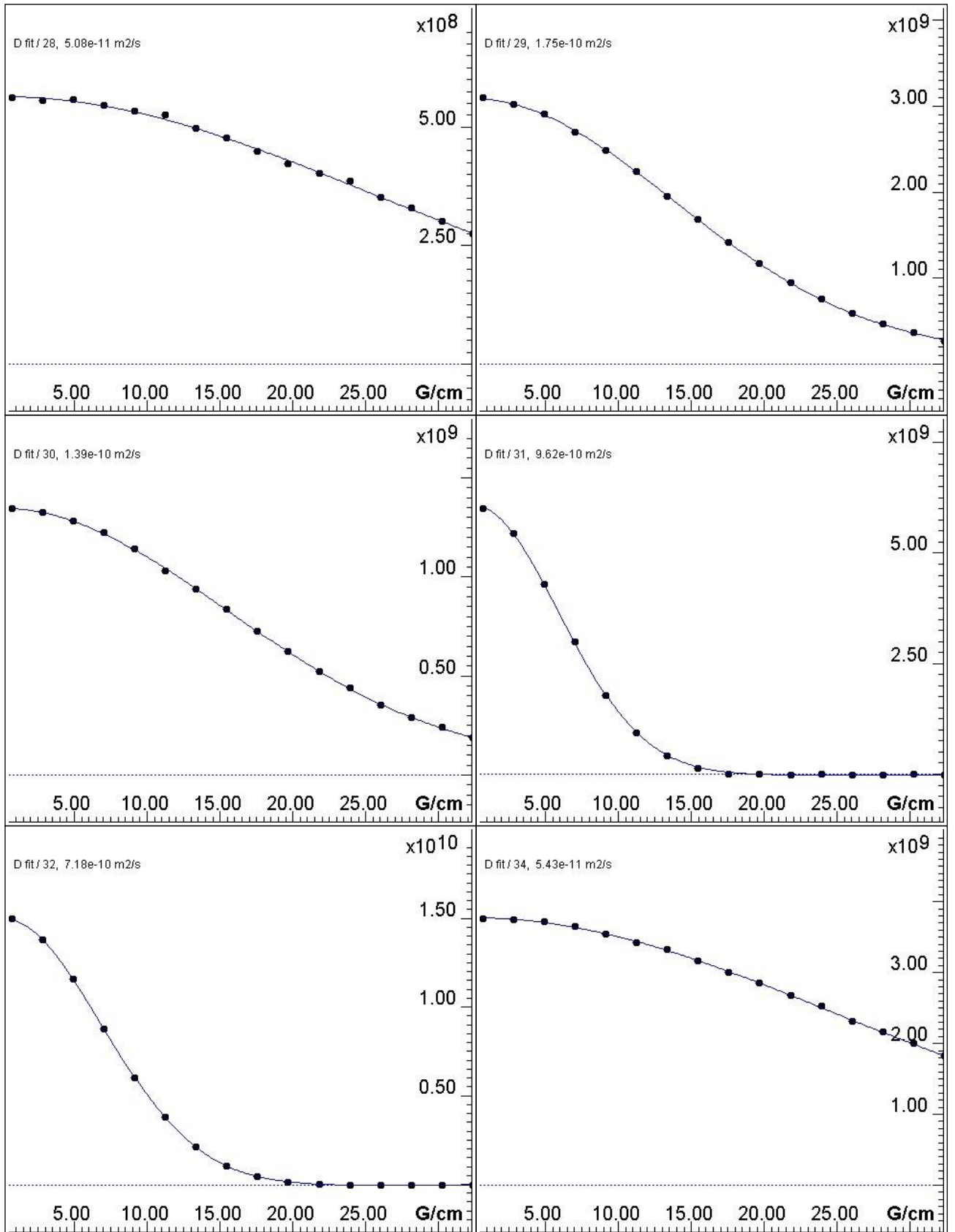
Table S1. DOSY parameters used in the Bruker Dynamics Center.

Fitted function:	$f(x) = I_0 * \exp(-D * x^2 * \gamma^2 * \text{littleDelta}^2 / (\text{bigDelta} - \text{littleDelta}/3) * 10^4)$
used gamma:	26752 rad/(s*Gauss)
used little delta:	0.0049000 s
used big delta:	0.089900 s
used gradient strength:	variable
Random error estimation of data:	RMS per spectrum (or trace/plane)
Systematic error estimation of data:	worst case per peak scenario
Fit parameter Error estimation method:	from fit using calculated y uncertainties
Confidence level:	95%
Used Gradient strength:	all values (including replicates) used

Table S2. Peak list as generated by the Diffusion function in the Bruker Dynamics Center.¹⁰

Peak name	F2 [ppm]	D [m ² /s]	error
1	9.228	1.58e-10	2.290e-12
2	8.976	1.77e-10	1.472e-12
6	8.281	1.67e-10	1.610e-12
9	8.097	1.65e-10	9.936e-13
19	7.520	1.40e-10	2.264e-12
26	7.146	1.50e-10	2.952e-12
28	6.688	5.08e-11	2.771e-12
29	3.867	1.75e-10	3.513e-13
30	3.760	1.39e-10	5.457e-13
31	3.325	9.62e-10	1.126e-12
32	2.508	7.18e-10	3.764e-13
34	3.606	5.43e-11	8.708e-13
42	6.336	5.05e-11	1.876e-12
44	7.720	5.84e-11	1.331e-12
45	8.902	1.76e-10	1.500e-12





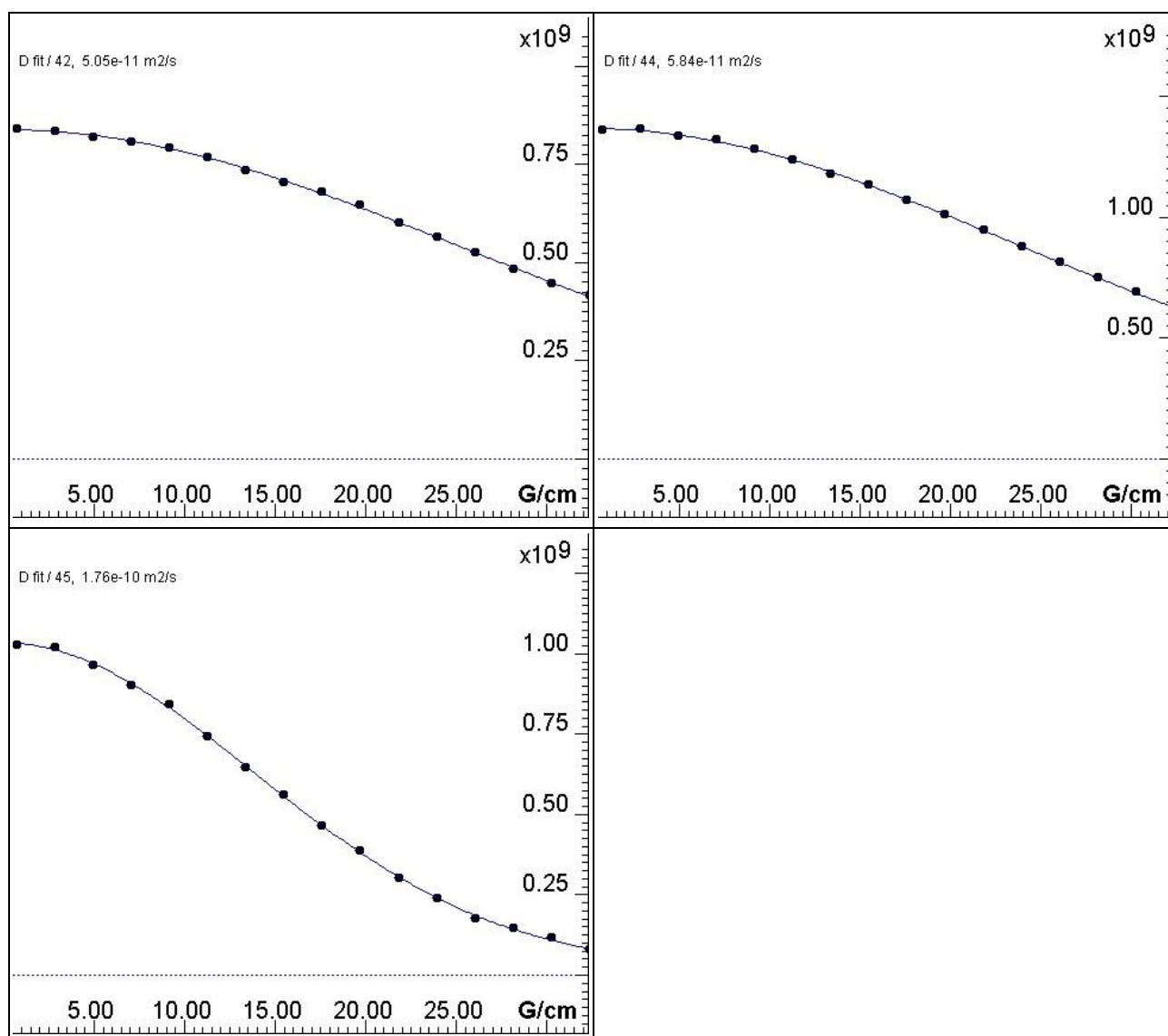


Figure S70. The integrals for selected integration areas at different gradient strength (dots) and their fits (lines). For peak numbering, see **Table S2**.

Crystallographic Data

Compound 2

We made several attempts to crystallize **2**, using different solvent combinations. The only measurable crystals were obtained by vapour diffusion of diethyl ether into a solution of **2** in acetonitrile. The crystals were very thin plates that diffracted poorly. Every crystal we checked was twinned with two diffracting domains, related by a two-fold rotation about the reciprocal c-axis (normal to the ab plane). The diffraction signals were too weak to allow twin integration, so the twin law was applied during structure refinement. The structure contains a solvent accessible void, and attempts to model a solvent molecule (e.g. a linear hydrocarbon) resulted in solvate species with unphysical bond lengths. The location of the inversion centre in this void made accurate solvate structure determination impossible. PLATON/SQUEEZE solvent mask was applied instead.¹¹ The somewhat high R-factor is attributed to the twinning and poor diffraction ability of the crystal.

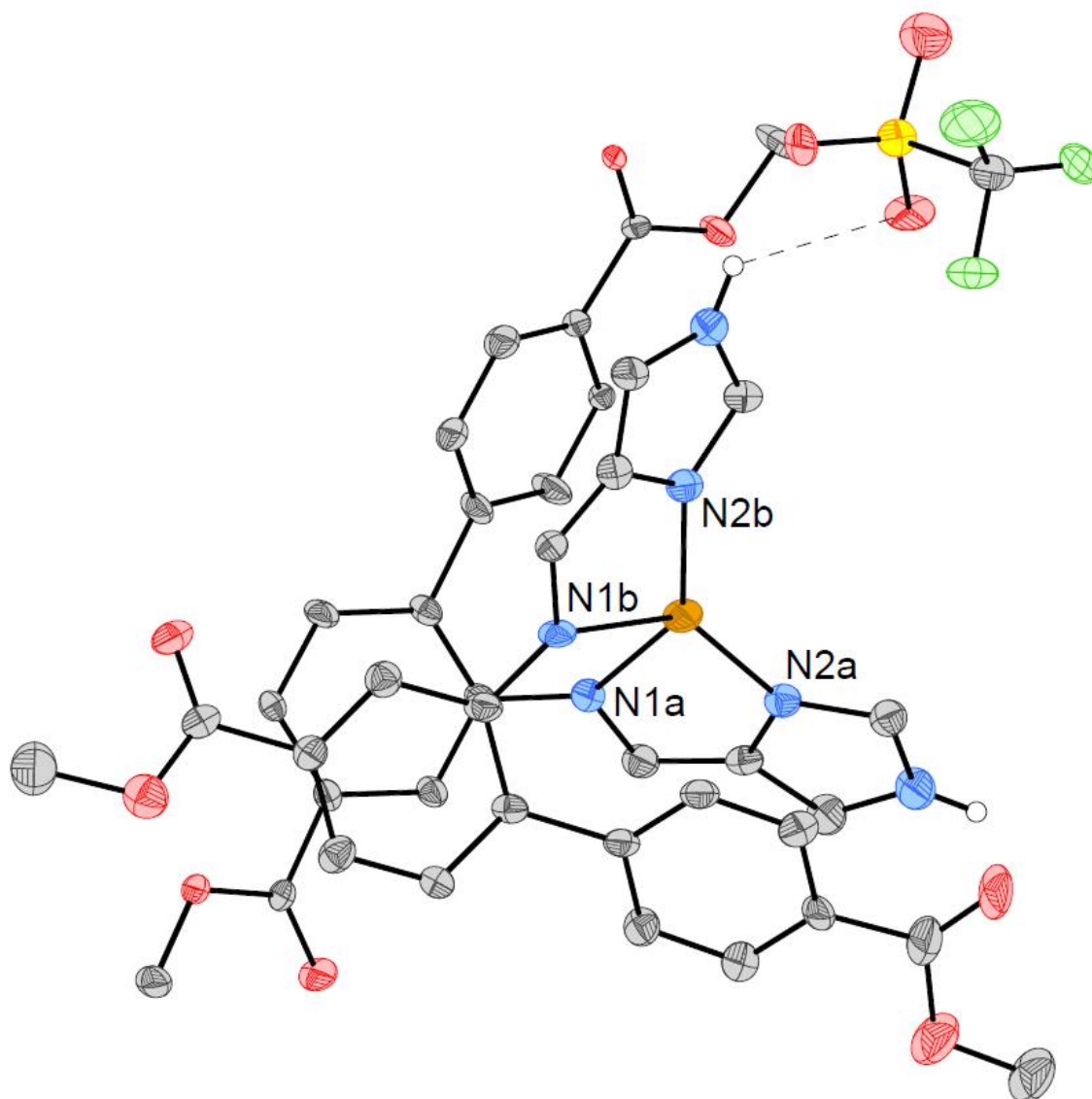


Figure S71. ORTEP plot of compound **2** with 50% probability ellipsoids [ig-62-(2048292)]. Selected bond lengths: N1a-Cu: 2.21(2) Å; N1b-Cu: 2.32(2) Å; N2a-Cu: 1.929(12) Å; N2b-Cu: 1.915(12) Å. Averaged $\tau_4 = 0.60 \pm 0.02$.^{12,13} The hydrogen bond between the imidazole-NH and the triflate anion has a length of 2.76 Å and a NHO angle of 118 °.

Compound 4

Single crystals suitable for single crystal X-Ray diffraction were obtained by vapour diffusion of toluene into a solution of **4** in a toluene/acetonitrile mixture.

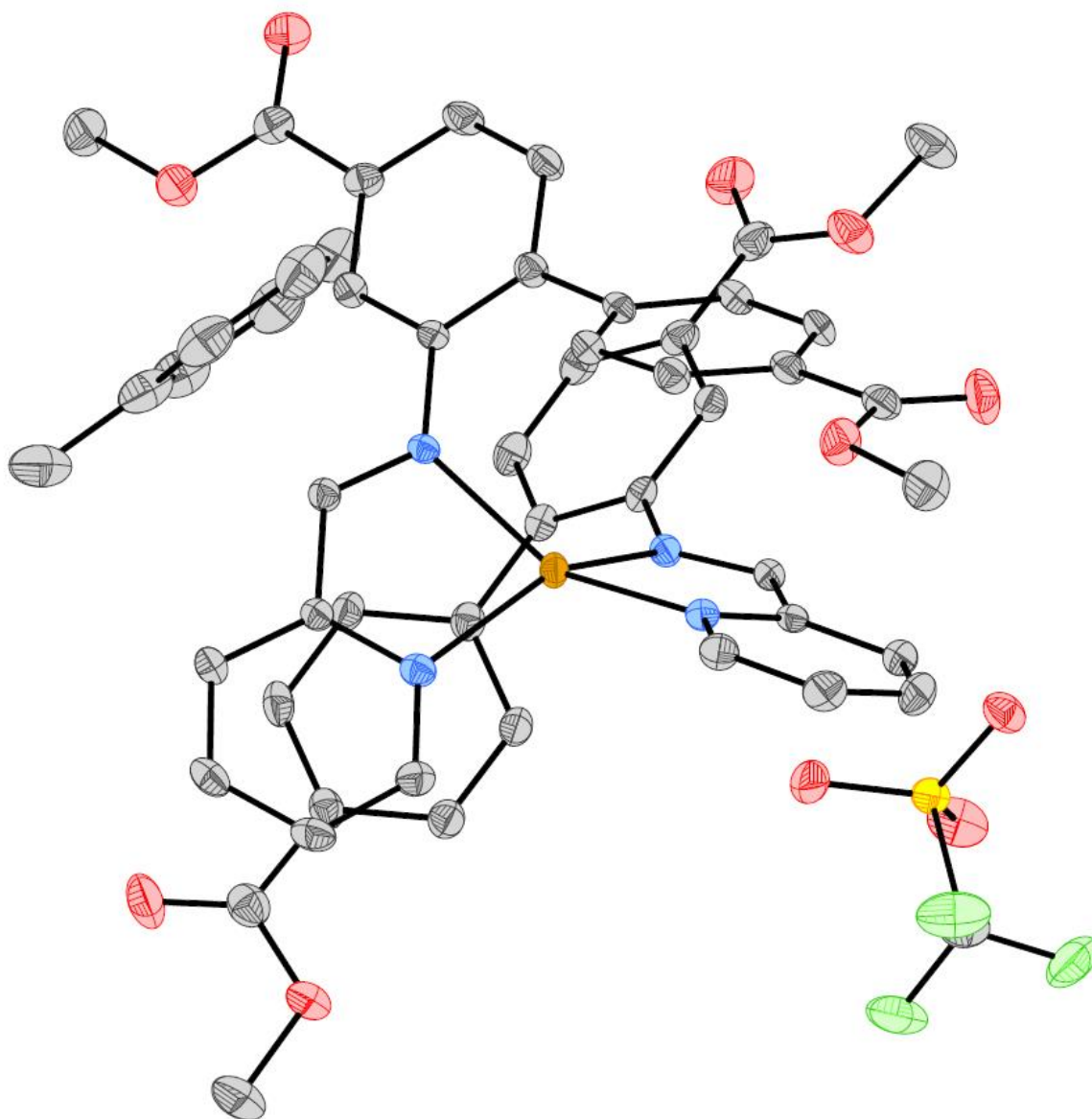
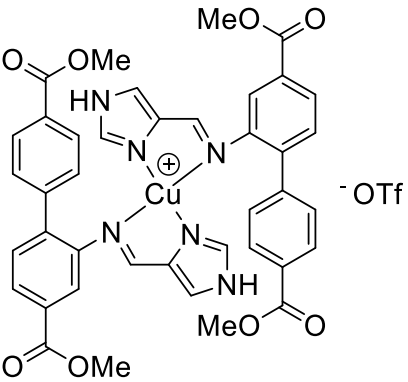
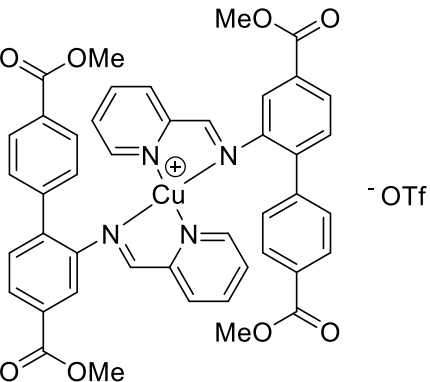


Figure S72. ORTEP plot of compound **4** with a co-crystallized solvent molecule (toluene) with 50% probability ellipsoids [ig-0124-(2048291)].

Table S3. Crystal and refinement data for compounds **2** and **4**.

	ig-62-(2048292)	ig-0124-(2048291)
	 <p style="text-align: center;">2</p>	 <p style="text-align: center;">4</p> <p style="text-align: center;">co-crystallized with toluene</p>
Crystal data		
Chemical formula	C ₄₀ H ₃₄ CuN ₆ O ₈ ·CF ₃ O ₃ S	C ₄₄ H ₃₆ CuN ₄ O ₈ ·CF ₃ O ₃ S·C ₇ H ₈
M_r	939.34	1053.51
Crystal system, space group	Triclinic, <i>P</i> -1	Monoclinic, <i>Cc</i>
Temperature (K)	100	105
<i>a</i>, <i>b</i>, <i>c</i> (Å)	11.839 (7), 12.740 (8), 15.296 (9)	18.2548 (13), 17.2687 (12), 15.2341 (11)
<i>α</i>, <i>β</i>, <i>γ</i> (°)	76.222 (13), 88.825 (13), 81.925 (13)	90, 92.665 (2), 90
<i>V</i> (Å³)	2218 (2)	4797.2 (6)
<i>Z</i>	2	4
Radiation type	Mo <i>Kα</i>	Mo <i>Kα</i>
<i>μ</i> (mm⁻¹)	0.62	0.58
Crystal size (mm)	0.27 × 0.05 × 0.01	1.5 × 0.25 × 0.25
Data collection		

Diffractometer	Bruker D8 Venture/Photon100 detector	Bruker D8 Venture/Photon100 detector
Absorption correction	Multi-scan	Multi-scan
	SADABS2016/2 (Bruker,2016/2) was used for absorption correction. wR2(int) was 0.1273 before and 0.0870 after correction. The Ratio of minimum to maximum transmission is 0.8092. The $\lambda/2$ correction factor is Not present.	SADABS2016/2 (Bruker,2016/2) was used for absorption correction. wR2(int) was 0.1372 before and 0.0401 after correction. The Ratio of minimum to maximum transmission is 0.8463. The $\lambda/2$ correction factor is Not present.
T_{\min}, T_{\max}	0.602, 0.744	0.631, 0.746
No. of measured, independent and observed [$I > 2\sigma(I)$] reflections	16219, 3434, 2826	36839, 14513, 12732
R_{int}	0.107	0.035
θ_{max} (°)	19	30.6
$(\sin \theta/\lambda)_{\text{max}}$ (Å ⁻¹)	0.457	0.716
Refinement		
$R[F^2 > 2\sigma(F^2)], wR(F^2), S$	0.145, 0.408, 1.87	0.041, 0.097, 1.02
No. of reflections	3434	14513
No. of parameters	507	654
No. of restraints	738	2
H-atom treatment	H-atom parameters constrained	H-atom parameters constrained
$\Delta\rho_{\text{max}}, \Delta\rho_{\text{min}}$ (e Å ⁻³)	1.33, -0.97	0.42, -0.32
Absolute structure	–	Flack x determined using 5408 quotients $[(I+)-(I-)]/[(I+)+(I-)]$ (Parsons, Flack and Wagner, Acta Cryst. B69 (2013) 249-259).
Absolute structure parameter	–	-0.003 (7)

XAS

Two-coordinate linear arrangement destabilizes 4pz with respect to the doubly-degenerate 4px,y set. As 4px,y remain non-bonding, they retain high p character, which raises the intensity of the 1s-4px,y transition through the electric dipole mechanism, at energies below that of the 1s-4pz transition. In contrast, as one approaches the tetrahedral limit, the 4p set comes close to triply degeneracy and is allowed to mix with 3dxy,xz,yz set as they all transform as T2. As t2 orbitals in Td complexes are antibonding, 1s-4p transitions are shifted to higher energies relative to 1s-4px,y in D ∞ h.¹⁴

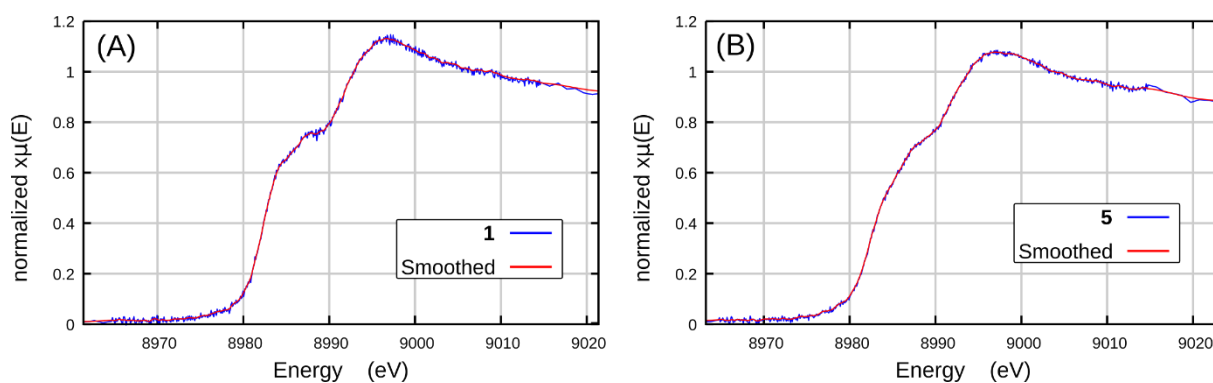


Figure S73. Average of 10 Cu K-edge XAS scans of **1** (A) and **5** (B) in blue overlaid with the respective smoothed spectra in red, as produced by three-point smoothing algorithm with 9 repetitions in Athena software of the Demeter package.¹⁵

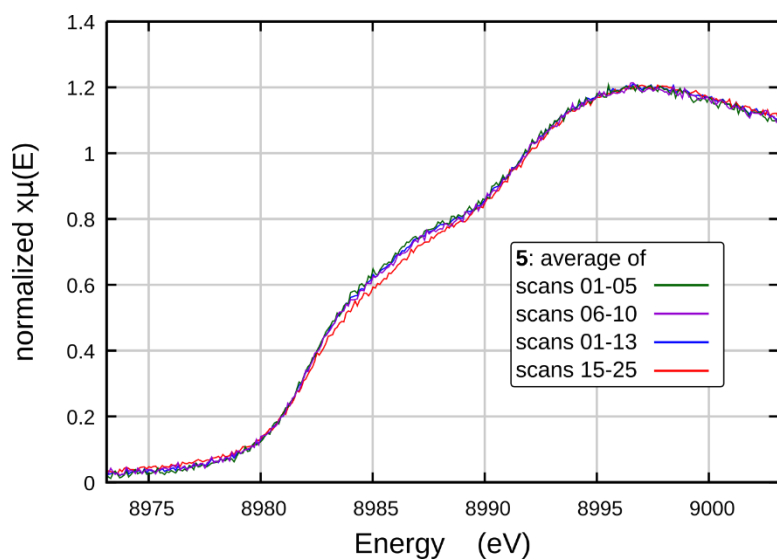


Figure S74. Damage study of **5** in Cu K-edge XAS region. Averages of scans 1 to 5 (green trace) overlaps with the averages of scans 6 to 10 (purple) and 1 to 13 (blue), while scans beyond 15th start to show noticeable decrease in the intensity, as evidenced by the average of scans 15 to 25 in red. Such changes were attributed to decomposition most probably due to slow air permeation into the cell.

XES

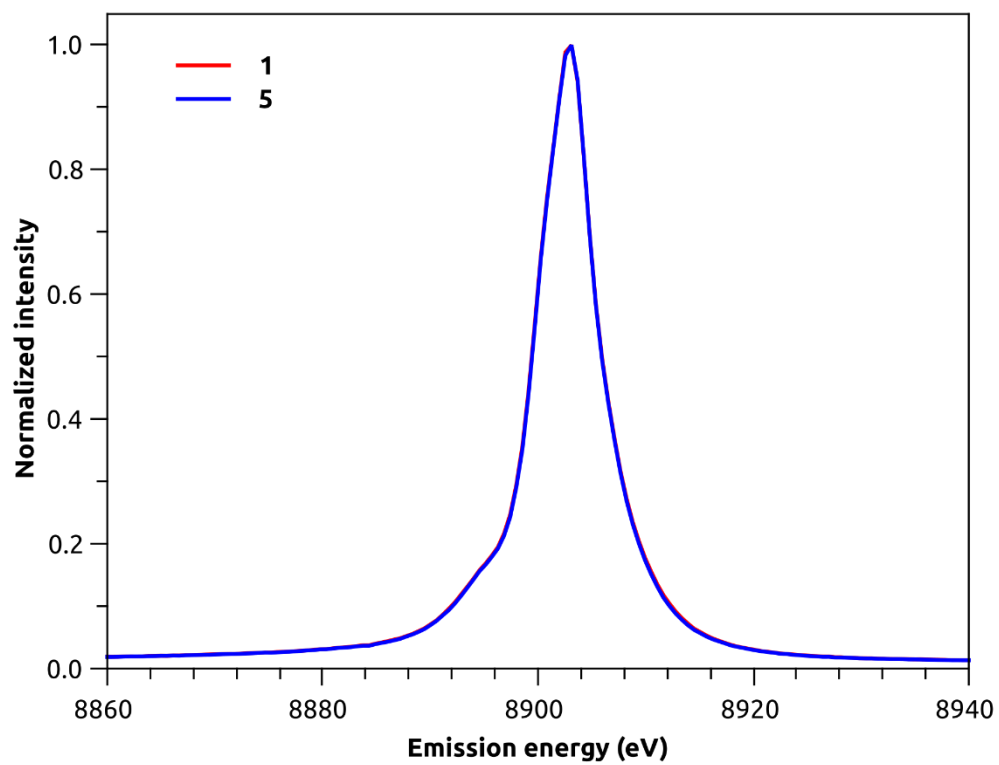


Figure S75. Non-resonant X-ray emission spectra of **1** and **5** in the mainline region.

DFT

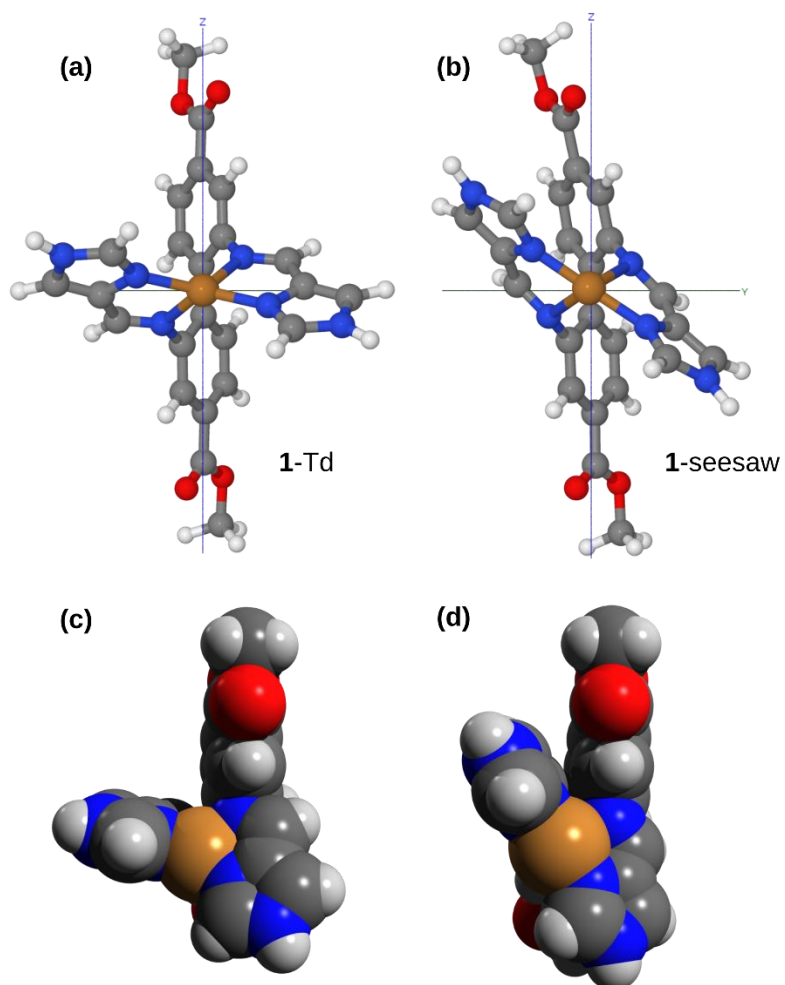


Figure S76. View along the C_2 axis (x) of the DFT optimized structures of (a) **1-T_d** and (b) **1-seesaw**. The vertical axis (z) is biphenyl C-C bond. Space-filling models showing the van der Waals radii of the atoms in (c) **1-T_d** and (d) **1-seesaw**.

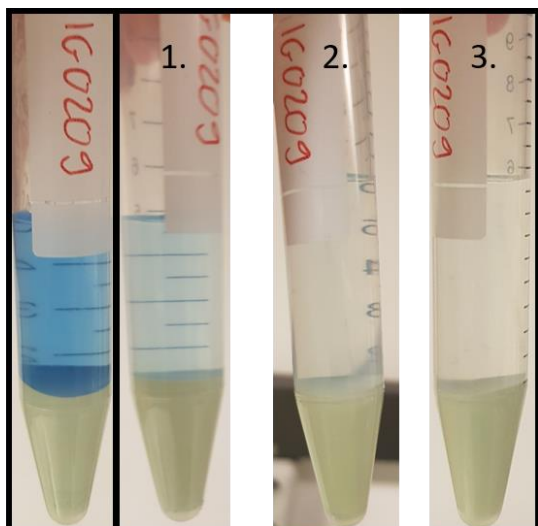
MOF Incorporation

Synthetic procedure for UiO-67-(NH₂)₂-10%

2,2'-diaminobiphenyl 4,4'-dicarboxylic acid was synthesized according to literature.¹⁶ ZrCl₄ (1.00 g, 4.29 mmol, 1 equiv.) was carefully dissolved in a beaker containing DMF (ca. 100 mL) and distilled water (230 μL). The solution was heated and benzoic acid (4.72 g, 38.7 mmol, 9 equiv.) was dissolved under stirring. Thereafter, 2,2'-diaminobiphenyl-4,4'-dicarboxylic acid (0.12 g, 0.44 mmol, 0.1 equiv.) was added to the DMF solution. The mixture was transferred to a round bottom flask containing biphenyl-4,4'-dicarboxylic acid (0.94 g, 3.88 mmol, 0.9 equiv.). It was stirred overnight at 138 °C with a fitted condenser. The solids were collected through filtration and washed with hot DMF (200 mL) and acetone (150 mL). After drying in an oven at 150 °C overnight, the product was obtained as a pale yellow solid (1.31 g).

Synthetic procedure for UiO-67-1b

A 10 mL centrifuge tube with UiO-67-(NH₂)₂-10% (500 mg, ~0.14 mmol diamino-functionalisation), Cu(OTf)₂ (50 mg, 0.14 mmol), 1*H*-imidazole-4-carbaldehyde (30 mg, 31 mmol) and acetonitrile (5 mL) was shaken at 500 rpm over night. The resulting mixture was centrifuged and the supernatant removed. The solid was washed three times with acetonitrile (addition of 5 mL acetonitrile, resuspension of the solid, shaken for 30 min at 500 rpm, centrifugation and removal of the supernatant). The last two washing steps were not coloured (see Figure S77). The pristine MOF was dried for 24 h in a vacuum oven at 80 °C, yielding 488 mg of UiO-67-**1b**.



Reaction mixture Washing steps

Figure S77. Centrifuge tube with the synthesized MOF. Left: Reaction mixture after centrifugation with blue supernatant. Right: Centrifugation after each washing step; while the first washing step still has a faint blue supernatant, the second and third washing step yielded colourless supernatants.

NMR

Ca. 25 mg of sample were digested in 1 mL of 0.1 M NaOD in D₂O overnight. For **1b** and UiO-67-1b, an excess of ascorbic acid was added, resulting in a colour change from green to yellow.

The proof of the incorporation of **1b** by so-called digestion NMR could not be made, as the complex does not tolerate the strongly basic digestion conditions (bottom spectrum in Figure S78) and hydrolyses into aldehyde and amine. However, digested UiO-67-1b contained aldehyde and diamine in similar quantities (Figure S78), supporting incorporation of the complex. The digestion NMR was also useful to estimate the actual percentage of bpdc-(NH₂)₂ in UiO-67-(NH₂)₂-10%. The quantification of the linkers in the NMR spectra is complicated by the presence of multiple species that can be attributed to bpdc-(NH₂)₂. This is likely due to reactions with e.g. formate (that is generated during MOF synthesis from DMF).¹⁷ The estimation of the amount of bpdc-(NH₂)₂ incorporated was therefore attempted on a group of signals that can be attributed to the proton located next to the amino groups (Figure S78, blue box). Its integral was 3-4% of that of the signals belonging to bpdc in the spectra of the digested MOFs (Figure S78), suggesting an incorporation of 6-8% (the bpdc signals account for four protons each). This is consistent with the reported values.¹⁸

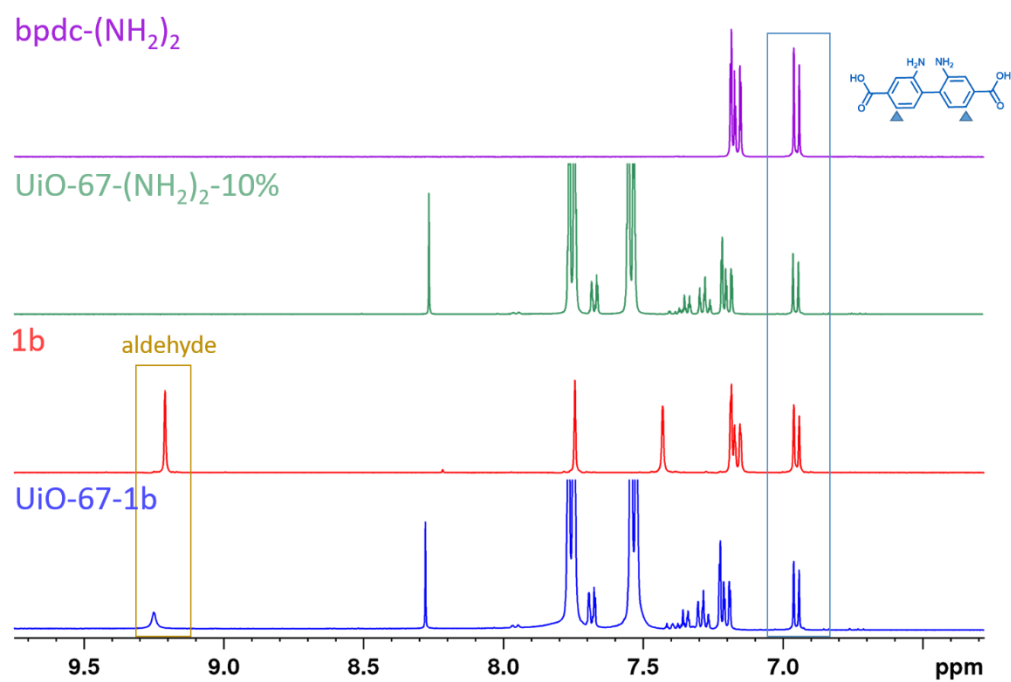


Figure S78. ‘Digestion NMR’ of UiO-67-(NH₂)₂-10% and UiO-67-**1b** (top two spectra) and the diamino linker (bpdc-(NH₂)₂) and complex **1b** after the digestion treatment.’

Elemental Mapping

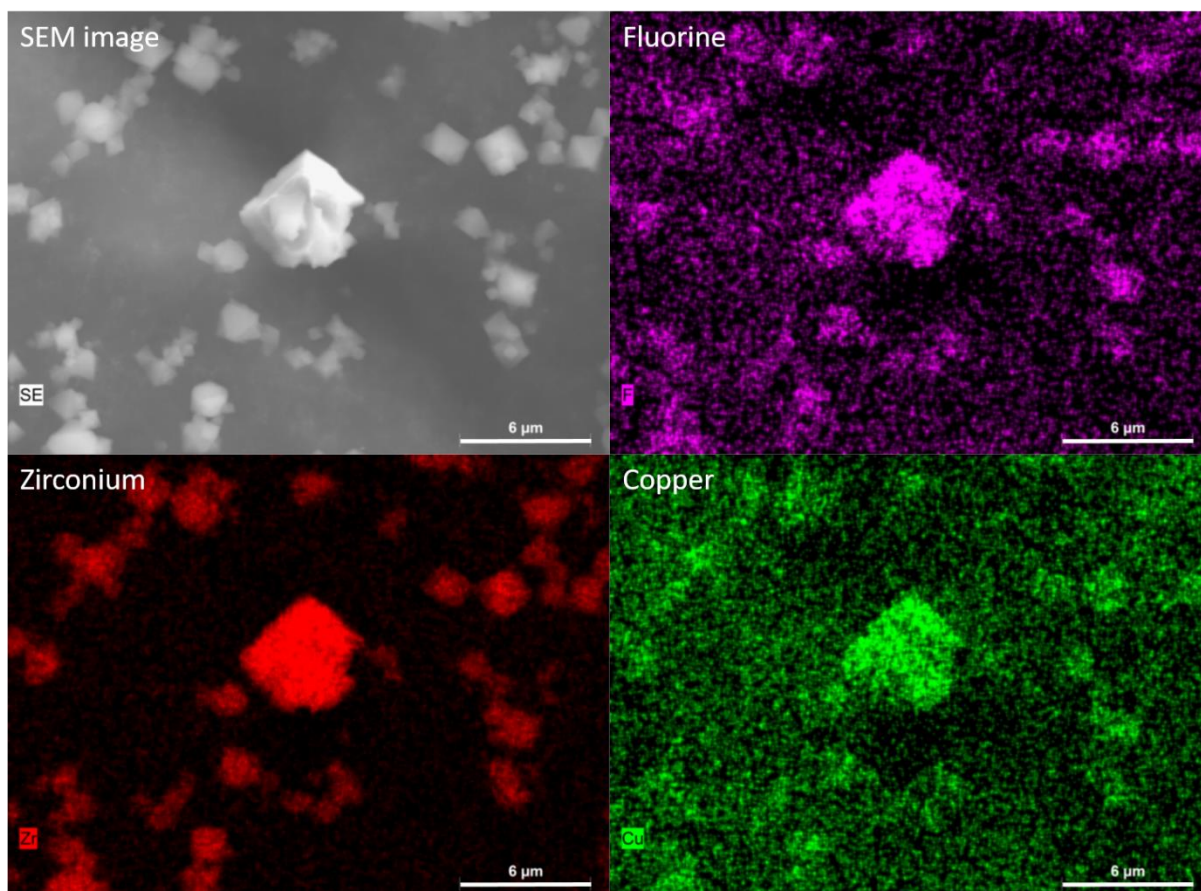


Figure S79. Elemental Mapping showing the distribution of F, Zr and Cu in UiO-67-1b.

EDX

Due to the low copper loading, the error of for the percentage of copper in the functionalised MOF is similar to the percentage itself. By taking the average of three spots, a ratio of copper to zirconium of 1: (0.060 ± 0.003) was obtained. Considering the 1:1 ratio between linker and zirconium in an ideal (defect-free) UiO-67, this value is consistent with the bpdc-(NH₂)₂ incorporation found by NMR.

Elemental Analysis

The zirconium copper ratio was verified by elemental analysis and UiO-67-1b was found to contain 22.49 % zirconium and 0.93 % copper. Adjusted for the relative atomic masses, this gives a ratio of zirconium to copper of 1:0.059, which is in excellent agreement with the value obtained from EDX.

TGA

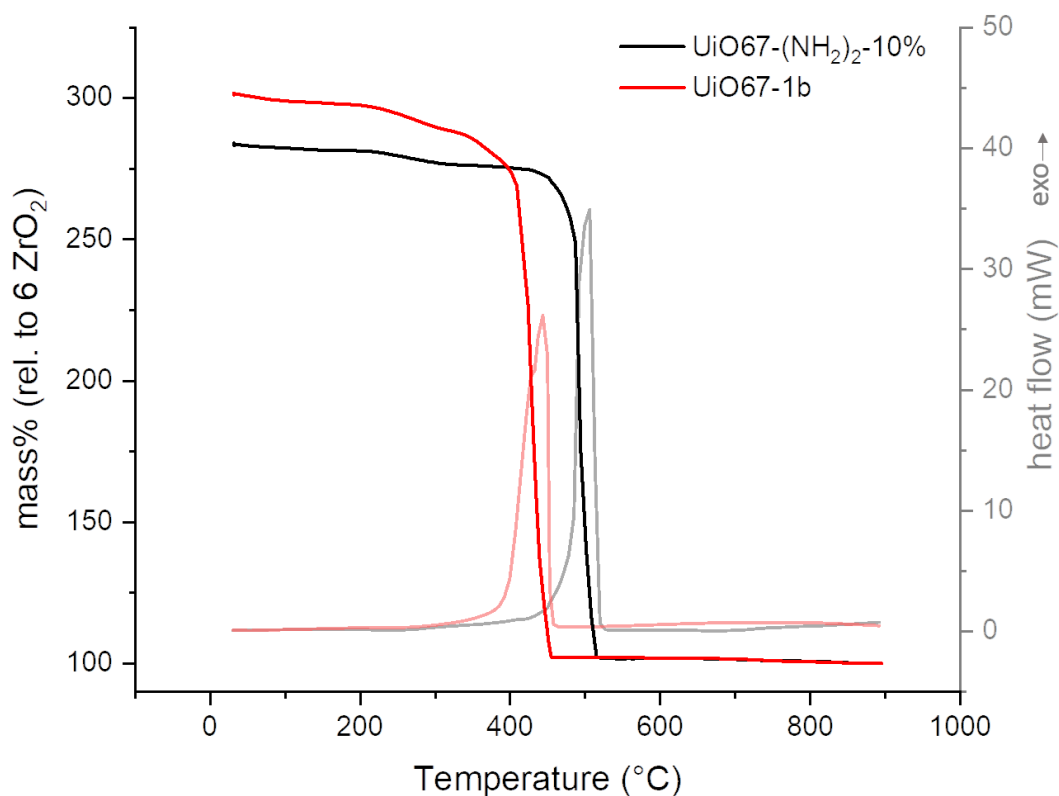


Figure S80. TGA and DSC of the diamino-functionalised MOF (UiO-67-(NH₂)₂-10%) and the MOF after incorporation of complex **1b** (UiO-67-1b).

Sources

- 1 K. T. Hylland, S. Øien-Ødegaard and M. Tilset, *Eur. J. Org. Chem.*, 2020, 4208–4226.
- 2 K. T. Hylland, S. Øien-Ødegaard, R. H. Heyn and M. Tilset, *Eur. J. Inorg. Chem.*, 2020, 3627–3643.
- 3 G. M. Sheldrick, *Acta Cryst.*, 2015, **C71**, 3–8.
- 4 G. M. Sheldrick, *Acta Cryst.*, 2015, **A71**, 3–8.
- 5 O. V. Dolomanov, L. J. Bourhis, R. J. Gildea, J. a. K. Howard and H. Puschmann, *J. Appl. Crystallogr.*, 2009, **42**, 339–341.
- 6 F. H. Allen, O. Johnson, G. P. Shields, B. R. Smith and M. Towler, *J. Appl. Crystallogr.*, 2004, **37**, 335–338.
- 7 A. R. Craze, N. F. Sciortino, M. M. Badbhade, C. J. Kepert, C. E. Marjo and F. Li, *Inorganics*, 2017, **5**, 62.
- 8 S. Mishra, B. Paital, H. S. Sahoo, S. G. Pati, D. Tripathy and N. B. Debata, *Dalton Trans.*, 2020, **49**, 8850–8854.
- 9 T. M. Tallon, PhD Thesis, National University of Ireland Maynooth, 2010.
- 10 Non-Frequency Dimension NMR Analysis Software, <https://www.bruker.com/en/products-and-solutions/mr/nmr-software/dynamics-center.html>, (accessed July 28, 2021).
- 11 A. L. Spek, *Acta Cryst.*, 2015, **C71**, 9–18.
- 12 D. Rosiak, A. Okuniewski and J. Chojnacki, *Polyhedron*, 2018, **146**, 35–41.
- 13 A. Okuniewski, D. Rosiak, J. Chojnacki and B. Becker, *Polyhedron*, 2015, **90**, 47–57.
- 14 L. S. Kau, D. J. Spira-Solomon, J. E. Penner-Hahn, K. O. Hodgson and E. I. Solomon, *J. Am. Chem. Soc.*, 1987, **109**, 6433–6442.
- 15 B. Ravel and M. Newville, *J. Synchrotron Rad.*, 2005, **12**, 537–541.
- 16 N. Ko, J. Hong, S. Sung, K. E. Cordova, H. J. Park, J. K. Yang and J. Kim, *Dalton Trans.*, 2015, **44**, 2047–2051.
- 17 K. M. Zwoliński, P. Nowak and M. J. Chmielewski, *Chem. Commun.*, 2015, **51**, 10030–10033.
- 18 G. Kaur, PhD Thesis, Oslo University, 2020.